T H E U N I V E R S I T Y O F M I C H I G A N

COLLEGE OF LITERATURE, SCIENCE, AND THE ARTS
Department of Astronomy

Final Report

SOLAR SOFT X-RADIATION

Roger J. Thomas

ORA Project 05567

under contract with:

NATIONAL AERONAUTICS AND SPACE ADMINISTRATION
GODDARD SPACE FLIGHT CENTER
CONTRACT NO. NAS5-3176
GREENBELT, MARYLAND

administered through:

OFFICE OF RESEARCH ADMINISTRATION ANN ARBOR

April 1970

This report was also a dissertation submitted in partial fulfillment of the requirements for the degree of Doctor of Philosophy in The University of Michigan, 1970.

TABLE OF CONTENTS

TABLE OF CONTENTS (Concluded)

LIST OF TABLES

LIST OF TABLES (Concluded)

LIST OF FIGURES

LIST OF FIGURES (Concluded)

ABSTRACT

Data from The University of Michigan's ion chamber photometer aboard the earth-orbiting satellite OSO-III are used to investigate relationships between solar soft X-radiation and phenomena observed at other wavelengths. The Michigan 8-12 Å X-ray data are exceptionally well suited for such studies because they cover an interval of more than a year on a nearly continuous basis with excellent time resolution, sensitivity, dynamic range, and stability. X-ray fluxes are determined using the assumption of a 2×10^6 K gray-body spectrum which remains constant with time. Uncertainties in derived fluxes that are caused by this assumption are shown to be small even during X-ray bursts.

We find that the slowly varying component of solar soft X-radiation is closely related to both the area and intensity of the Ca^+ emission of chromospheric plages. The X-radiation associated with each plage apparently originates from a condensation which is significantly above the chromosphere and whose thickness does not depend strongly on its area. There is some evidence that these condensations are not isothermal and that their temperatures and/or densities decrease with age. In addition, the data suggest that the temperature of the X-ray emitting source is influenced by variations in the general level of solar activity.

The burst component of solar soft X-radiation is examined for 283 events that are associated with well verified Hα flares of importance ≥ 1. Of these flares, 282 are accompanied by a significant enhancement in X-radiation. The peak amplitude of this X-ray enhancement correlates with the area and intensity

of the Hα flare. For a flare of a given area and intensity, the peak amplitude of the associated X-ray burst is found to be a function of its distance from the solar limb, an effect attributed to the Hα observations. The peak amplitude also depends on the general level of solar activity at the time of the burst and on the age and "flare-richness" of the associated plage. The latter effects are most likely due to density variations in the X-ray emitting region itself.

The properties of the general time-profiles for flare-associated bursts, as well as their frequency of occurrence from center to limb, imply that such bursts are predominantly thermal in nature. It is shown that thermal bremsstrahlung radiation is negligible at 8-12 Å for these bursts, so that the dominant mechanisms are recombination and line emission. However, some cases are observed of a relatively weak, impulsive component in 8-12 Å bursts which may be due to nonthermal processes.

We find that the start of the soft X-ray burst typically, but not always, precedes the onset of the Hα enhancement by a few minutes. In general, the Hα intensity of the flare's brightest point and the associated soft X-ray flux have roughly similar time-profiles. Isophotometry of three selected flares shows that in two cases the similarity is even more striking when the X-ray flux curve is compared to that of the flare's total Hα flux. This suggests that the time variation of each emission process is governed by the energy source term rather than the decay term as is usually assumed.

In addition, we find that the peak enhancements in the soft X-ray and Hα emission rates are nearly identical for these flares. Furthermore, it is shown that the total energies emitted by these flares in the forms of 8-12 Å X-radia-

tion and Hα emission are the same within observational errors. Finally, it is estimated that energy radiated between 8-12 Å may account for almost one-tenth of a flare's total electromagnetic emission.

CHAPTER I

INTRODUCTION

The University of Michigan's ion chamber photometer aboard the National Aeronautics and Space Administration satellite OSO-III was one of the first to monitor the soft X-radiation of the sun for more than a year on a nearly continuous basis. The data it provided are exceptionally well suited for the investigation of many aspects of various solar phenomena. The present study takes advantage of these fine observations to examine the properties of the solar X-ray "slowly varying" and "burst" components, as well as to infer some of the physical characteristics of those regions in the solar atmosphere which are responsible for this radiation.

The first suggestion that the sun might emit X-radiation was made independently by Hulburt (1938) and Vegard (1938) as a possible mechanism for the maintenance of the earth's ionosphere. The fact that sudden ionospheric disturbances (SID's) seemed to be closely related to solar flares (Martyn et al., 1937; Newton and Barton, 1937) then implied that the sun's "ionizing radiation" was appreciably enhanced during these chromospheric eruptions and that this enhanced emission originated from the same general region as the optical flare (Giovanelli, 1938). Therefore, the ionosphere can be considered as being a very broad-band detector of short wavelength solar radiation, and by monitoring distant radio signals using certain standard techniques (see for example Aarons ed., 1963), data can be easily obtained for the study of XUV solar radiation (roughly 1-1500 Å).

Until recently, this technique had provided a major source of information about the "slowly varying" and "burst" components of radiation in this spectral region (e.g., Kundu, 1965). These ionospheric studies are continuing (e.g., Donnelly, 1968a, 1969a; Reid, 1969), and have even advanced to the point where emitting region sizes can be estimated from observations during a solar eclipse (Meisel, 1968). Unfortunately, the interpretation of ionospheric disturbances in terms of the incident solar radiation is quite uncertain, requiring detailed knowledge of the temperature, density, and composition of the earth's upper atmosphere, as well as the appropriate dissociation and recombination rates, among other parameters. In addition, some early investigators naturally assumed that most of the enhanced ionizing radiation during a solar flare was due to hydrogen Lyman-alpha emission (C. S. Warwick, 1963), an assumption which is now known to be incorrect (Hallam, 1964). Furthermore, it appears that hard X-radiation (< 1 Å) does not contribute to SID's (Donnelly, 1968a) or to the maintenance of the ionosphere (Allen, 1965), so that ionospheric studies provide no direct information about this spectral region. For these reasons and because many X-ray bursts of only moderate amplitude do not produce any observable ionospheric effects (Dickerman and Thornton, 1966), data from ground-based detectors are insufficient to support a complete and quantitative investigation of solar X-radiation. Direct observations made above the earth's atmosphere are essential for this program.

The U. S. Naval Research Laboratory pioneered in obtaining such observations, the first of which utilized a captured V-2 rocket to carry a photographic plate shielded by a thin beryllium filter to an altitude greater than

100 km on 6 August 1948. Upon recovery, the plate was found to be darkened, thus providing the first direct evidence for solar soft X-radiation (Burnight, 1949). This observation was followed by a series of flights which allowed the NRL group to develop and refine their instrumentation in order to expand the spectral region covered, improve spectral resolution, and put the measurements on a quantitative basis. Friedman (1962, 1963a) reviews the work of the NRL solar X-ray group from 1948 to 1961, a period when they were virtually the only observational researchers in the entire field.

By 1961, these rocket-borne X-ray detectors were providing data of sufficient quality to reveal the main characteristics of solar X-radiation and to allow a better determination of the ionospheric parameters mentioned earlier. However, a major limitation of this technique is the fact that the detector is above the earth's atmosphere for only a few minutes of the flight. Although such brief observations do not seriously compromise studies of the quiet sun, they are inadequate to follow the total development of X-ray bursts, since these may last more than an hour. Furthermore, the occurrence of a burst is unpredictable (at least at this time) so that there is very little chance for a rocket flight to bracket the initial rise of an event, which in many respects is the most interesting phase of the entire burst.

These difficulties may be overcome to some extent by means of detectors aboard a very high altitude balloon. On 20 March 1958, the first complete profile of a directly observed X-ray burst was recorded with this technique (Peterson and Winckler, 1958). Many such balloon observations were made by the University of Minnesota group, and their work through 1962 has been summarized by

Winckler (1964). Unfortunately these studies also have severe limitations in that only the most energetic X-rays can penetrate the earth's atmosphere to balloon altitudes. In addition, a relatively large and somewhat uncertain correction must still be applied to account for the atmospheric absorption above the balloon (Peterson and Winckler, 1959). Therefore, even this method is not completely satisfactory.

Since ionospheric observations and suborbital and balloon flights are relatively inexpensive and simple, much valuable information about solar X-radiation has been and will be obtained by these means. But some other observing technique is obviously required in order to conduct an "ideal" X-ray experiment. In addition to high stability, accurate absolute calibration, and high signal-to-noise ratio, the characteristics of such an ideal experiment should include:

1. Time resolution better than 1 second.

   Unlike the slowly varying background component which changes on a time scale of several hours, the time scale of solar X-ray bursts is less than a minute and in some cases is as small as a second (e.g., Kane, 1969).

2. Spectral resolution ($\lambda/\Delta\lambda$) better than 1000 at 10 Å.

   Since X-ray emission lines have widths of about 0.1 Å, a spectral resolution better than 1000 at 10 Å will be necessary to observe these line profiles properly (J. W. Evans et al., 1969).

3. Spatial resolution better than 1 arc-second.

   Several lines of evidence, including direct photographs (e.g., Vaiana

et al., 1968), all suggest that X-ray emitting regions have significant structure at 1 arc-second, and that perhaps 0.1 arc-second resolution is necessary to resolve them adequately (J. W. Evans et al., 1969).

4. High dynamic sensitivity.

The initial, very gradual rise often associated with soft X-ray bursts can normally be observed only with a detector which has a high dynamic sensitivity (Teske and Thomas, 1969).

5. Adequate absolute sensitivity.

Longward of 2 Å, a sensitivity of 10^{-8} erg/(cm^2 sec Å) is sufficient even during solar minimum. For shorter wavelengths, only upper limits to the minimum solar flux are known, so that the necessary absolute sensitivity levels in this interval cannot yet be established. However, an unambiguous observation of quiet sun hard X-radiation and gamma radiation is of extreme importance in determining to what extent nonthermal electromagnetic or nuclear processes occur in the nonactive solar atmosphere (Neupert, 1969).

6. Dynamic range better than 4 orders of magnitude.

Soft X-ray flux variations of nearly 3 orders of magnitude have been observed (Van Allen, 1968), while in the hard X-ray region, the variations may be greater than 4 orders of magnitude (Kane and Winckler, 1969). Therefore, a dynamic range at least this large is needed to avoid detector saturation.

7. Coverage of the entire X-ray spectrum.

An X-ray emitting region cannot be characterized by a single temperature

and density (Blake et al., 1963a; Mandel'shtam, 1965a; Cline et al., 1968). Therefore, each interval of the X-ray spectrum gives information about a different portion of the emitting region, so that the entire spectrum must be observed in order to develop a realistic emission model.

8. Continuous operation for more than 10 years.

Investigations into possible variations of X-ray emission characteristics during the entire solar cycle require observations over at least a 10-year period. However, in order to include the unpredictable starting phase of the X-ray burst component, these observations must be of a continuous monitoring type.

Although present technology is not sufficiently advanced to conceive of a single instrument combining all these characteristics, all but the last can be approached by observing the sun with several instruments simultaneously, each of which provides some part of the total desired properties. However, the long-term, continuous monitoring capability can only be achieved by detectors aboard space satellites (short of building at least three observatories on the surface of Mercury or the Moon). With the advent of such X-ray instrumented satellites, the amount of information concerning the sun's X-radiation has increased at a tremendous rate.

After Vanguard 3 and Explorer 7 failed to return useful data, the first successful solar X-ray satellite, Solar Radiation I, was launched in June 1960, and once again it was the U. S. Naval Research Laboratory that pioneered this new field (Kreplin et al., 1962). Following this initial success, a great num-

ber of satellites with solar X-ray detectors were put into orbit by Great Britain and the Soviet Union, as well as the United States. Although the vast majority of these X-ray satellites orbit the earth, there are some which are orbiting the moon (Explorer 35) or the sun (Mariner 5). The great amount of effort being expended in this field can be seen by noting that in the interval March 1967 to March 1968, the period of special concern to this dissertation, at least 12 different satellites were monitoring the sun's X-radiation (Cosmos 166, Explorers 30, 33, 35, and 37, Mariner 5, OGO's 4 and 5, OSO's 3 and 4, and Velas 7 and 8), some of which had several solar X-ray experiments aboard! These satellite experiments were in addition to rocket and balloon flights during this period, along with the continuing indirect studies using ionospheric effects.

The question naturally arises: why is there so very much effort over a mere 100 Å spectral band from a single, ordinary star? Of course, the reasons usually cited for studying the sun are appropriate here:

(a) since the sun is about 250,000 times closer than the next nearest star, requirements on instrumental absolute sensitivity are less stringent by a factor of more than 10^{10};

(b) also because of its proximity, the sun is the only star whose surface features can presently be resolved;

(c) the fact that the sun is near the middle of the Hertzsprung-Russell main sequence means that knowledge about the sun may be extrapolated to the greatest number of other stars with a minimum amount of uncertainty;

(d) since the sun's particle and radiation emission affects every object in the solar system to some extent, knowledge of solar emissions is essential to a complete understanding of these objects;

(e) and naturally, such a study is intrinsically interesting.

The X-radiation of the sun is of particular importance for other reasons as well:

(a) X-ray emitting regions in the corona can be observed during their entire disk passage, while these coronal condensations can be seen in visible light only at the limb;

(b) since these regions consist of very hot plasma confined by a magnetic field and since bursts seem to be related to instabilities in this field, solar X-ray observations touch on several problems associated with controlled thermonuclear fusion;

(c) solar X-radiation gives information about plasma under conditions unobtainable in the laboratory;

(d) some hard X-ray bursts seem to be caused by very energetic nonthermal acceleration processes and thus may provide information in this area of great current interest;

(e) knowledge of the sun's X-ray flux and its variations is essential for a proper understanding of the earth's ionosphere;

(f) such knowledge is also necessary to assess correctly the possibility of X-ray induced changes in the structural characteristics of materials considered for space applications;

(g) through its effect on the ionosphere, solar X-radiation strongly in-

fluences the quality of long-distance radio communication, which can be completely disrupted during a large X-ray burst;

(h) X-ray bursts are usually associated with solar flares and so give additional information on these complex phenomena;

(i) there is evidence that a soft X-ray enhancement is the very first manifestation of a solar flare, a possibility of obvious consequence for a flare early-warning system;

(j) since high-altitude nuclear explosions produce large bursts of X-radiation, it is important for national defense to be able to distinguish them from solar X-ray bursts;

(k) in addition, it may be possible to utilize solar bursts to estimate the effects of nuclear explosion X-radiation on defense systems such as anti-missile tracking, guidance, and communications.

Clearly, the X-ray region of the solar spectrum is exceptionally rich in information content and well worth intensive investigation, even though it accounts for only one-millionth of one percent of the sun's total luminosity! Many excellent reviews of previous solar X-ray studies are already available and so will not be duplicated here. In addition to references cited earlier, these reviews include, in chronological order, Friedman (1963b), Kundu (1963), Lindsay et al. (1965), Mandel'shtam (1965a, 1967), Goldberg (1967), Underwood (1968), and most recently Neupert (1969). However, a summary of present ideas concerning solar X-radiation, including those derived from this study, will be given in Chapter VI.

CHAPTER II

THE SOLAR SOFT X-RAY EXPERIMENT

1. INTRODUCTION

On 8 March 1967, NASA's Third Orbiting Solar Observatory (OSO-III) was launched from Cape Kennedy, Florida, and successfully attained earth orbit. A brief description of this satellite and the seven scientific experiments aboard is given by Brandt (1969). The present study is primarily concerned with The University of Michigan's soft X-ray ion chamber photometer which is located in the rotating wheel section of OSO-III.

The original design of this ion chamber was due to Dr. Robert W. Kreplin of NRL. The associated electronics were developed by the Consolidated Systems Corporation of Monrovia, California, which also constructed the entire instrument. The designs of both the electronics subsystem and the ion chamber were modified somewhat for this experiment by The University of Michigan Space Physics Research Laboratory, which was also responsible for the final testing and calibration of the complete system. Dr. Richard G. Teske heads The University of Michigan's solar X-ray project and is the principal investigator in this OSO-III experiment.

2. GENERAL CHARACTERISTICS

Basically, an ion chamber photometer is a gas-filled container with a window made of some very thin material. Incident photons, which pass through this window and are absorbed in the filler gas, produce free electrons by the process

of photoionization. The energy of each photo-ejected electron is quickly converted into secondary ionizations of the gas, producing many more free electrons. These are collected by a low-voltage anode in the chamber and the resulting current is then measured by an electrometer.

Such measurements can be treated quantitatively because of the following properties of X-ray photoionization (Hinteregger, 1965):

(a) the average number of ion-electron pairs formed per unit number of photons absorbed in a gas is directly proportional to the photon energy;

(b) the value of this proportionality factor, called the gas ionization efficiency, is known reliably from numerous experiments;

(c) the fractional number of photon absorption events not leading to any ion formation is practically negligible.

Since the operating voltage across the chamber is low, no electron multiplication occurs in the filler gas. Therefore, only those free electrons produced by the radiation entering the detector are collected. Because the number of these electrons is proportional to the energy of the absorbed photons, an ion chamber photometer functions as a total energy detector.

With this type of detector some spectral information is obtained in the sense that it responds effectively only to radiation in certain wavelength intervals. These intervals are determined by the transmission properties of the window material, the window's thickness, the absorption characteristics of the filler gas, the gas pressure, and the effective length of the chamber. By an appropriate combination of these parameters, the detector's response can be re-

stricted to a particular spectral band of only a few Ångstroms. This procedure is limited, however, by the relatively small number of suitable filler gases and window materials.

A more complete discussion of X-ray detector instrumentation in general and the ion chamber photometer in particular can be found in the excellent review articles by Boyd (1965) and Giacconi et al. (1968).

3. CORRECTION FOR THE BACKGROUND SIGNAL

The above description of an ion chamber's operation refers to an ideal observing situation. In reality, the orbiting satellite is passing continuously and at a high relative velocity through a medium of charged particles which exists at this altitude. Some of these charged particles penetrate into the detector and cause ionizations in the filler gas. Because the resulting free electrons are in addition to those caused by solar X-radiation, this background signal must be subtracted from the total response in order to obtain a value which is due solely to the sun.

Since the Michigan experiment is located in the rotating wheel section of OSO-III, the background signal is measured directly during those intervals when the detector is pointed away from the sun. The encoded voltage of the ion chamber's electrometer is recorded every 0.64 second, while the satellite's wheel section rotates with a period of 1.7 seconds. Therefore, each wheel rotation results in roughly one word of solar soft X-ray data and two words of particle background data. It is easy to distinguish between them since the total response is always larger than the background alone. However, as a check, a sun-sensing

photocell mounted next to the ion chamber puts a "tag" on each solar word to insure its proper identification.

In the remainder of this paper, the term "ion chamber response" will refer to only that part which is due to the sun's X-radiation.

4. THE EFFECTIVE BANDPASS

The Michigan experiment has an aluminum window 5×10^{-4} cm thick and a nitrogen gas filling at about one atmosphere pressure. This combination gives rise to the spectral efficiency response, $\epsilon(\lambda)$, shown in Figure 2-1. Here spectral efficiency is defined as the ratio of the radiation flux absorbed within the filling gas to that incident upon the detector window. It can be shown (e. g., Acton, 1964a) that this ratio is given by the expression:

$$\epsilon(\lambda) = [1 - e^{-(\mu_m \rho x)_G}] e^{-(\mu_m \rho x)_W} \qquad (2.1)$$

where μ_m is the mass absorption coefficient, ρ the density, x the thickness of the material in question, and the subscripts G and W refer to the gas filling and window material, respectively. The relation shown in Figure 2-1 was first calculated from this expression using parameters appropriate for the Michigan detector and then checked by illuminating the instrument with a calibrated iron-55 source in air.

Clearly, the definition of an effective bandpass is somewhat arbitrary for a detector with such a spectral efficiency response. One possibility is to choose those wavelength intervals in which the ion chamber has at least 10% of its maximum response efficiency. By this definition, the effective bandpass of

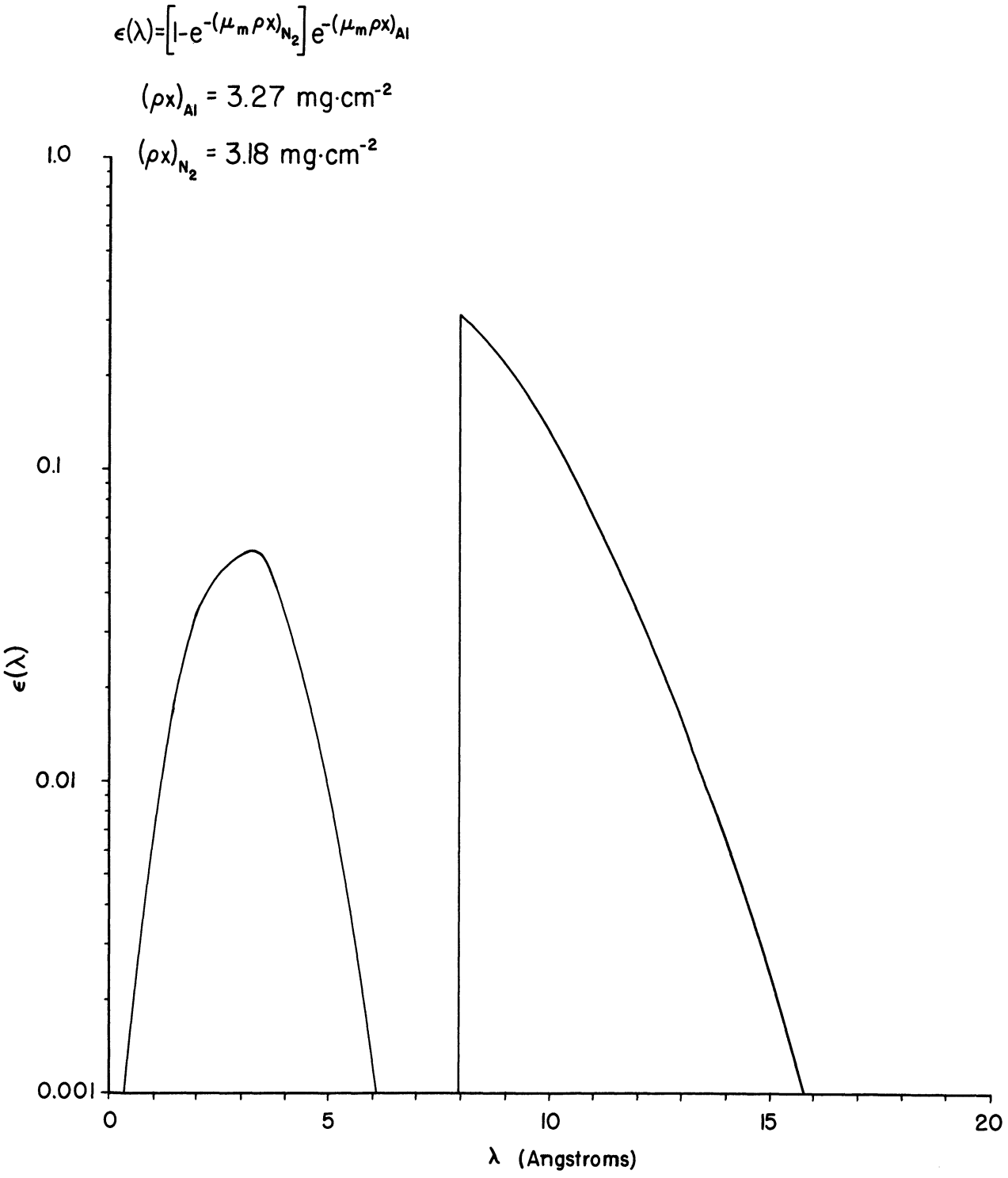

Figure 2-1. Spectral efficiency of the Michigan ion chamber. The mass absorption coefficients as a function of wavelength were taken from Victoreen (1949) and Cooke et al. (1962). The nitrogen surface density of the instrument actually flown was 0.00331 gm/cm^2. This change alters the above curve by less than 5%.

the Michigan instrument is 8.0 to 12.1 Å and 2.0 to 4.0 Å.

However, it would be more convenient to consider a bandpass which consists of a single wavelength interval. Therefore, one may choose that spectral band in which the detector efficiency is always larger than the peak of the short wavelength lobe. This definition results in an effective bandpass of 8.0 to 11.5 Å. Moreover, it seems justifiable to ignore the short wavelength lobe since solar radiation is always observed to be at least a factor of five stronger at 10 Å than at 3 Å (for example, see the flare spectra published by Culhane et al., 1969; Pounds, 1970). This means that radiation in the interval 2-4 Å contributes less than 2% of the Michigan detector's response.

Yet another method is to select that interval which minimizes the effect on the detector's response due to changes in the spectral distribution of the incident radiation. This procedure was first described by Van Allen (1967a) and further developed by Wende (1969). It is described in more detail in Section II-9 of this chapter. For The University of Michigan instrument, this method implies a bandpass of 8.0 to 11.9 Å.

Since all three methods give approximately the same result, the response function shown in Figure 2-1 can be adequately characterized by an effective bandpass of 8 to 12 Å, and measurements made by the Michigan ion chamber photometer will be considered as referring only to this wavelength interval.

5. THE SOLAR ASPECT CORRECTION

Actually, the spectral efficiency relation shown in Figure 2-1 is correct only when the sun is in the direction normal to the detector window. In the

general case where the sun is at some angle β to this direction, the surface densities ρx of the window material and filler gas become larger than the values indicated in Figure 2-1 by a factor of sec β. The detector response is further altered by the fact that the ion chamber's effective aperture is proportional to cos β.

However, this aspect effect is negligible for the Michigan experiment because of two characteristics of the OSO-III system. First, the ion chamber is designed to telemeter the value of the highest response which occurred during the 0.64-second interval since the previous transmission. This means that one of the three data words recorded in each wheel rotation will always refer to a measurement made at the smallest aspect angle attained during that rotation. Second, the attitude of the satellite is maintained so that the angle between the wheel section's rotation plane and the direction to the sun never exceeds 2-1/2°, which is therefore the largest possible angle for a recorded solar measurement. Since the change in Michigan's ion chamber response at a 2-1/2° aspect angle amounts to less than 0.2%, a correction for this effect has not been applied.

It should also be noted that because the ion chamber window is recessed in a physical collimator, it is fully illuminated only when the sun is within 9° of the normal direction. Therefore, the 2-1/2° limit on the angle of the rotation plane with respect to the sun is completely adequate to insure that the sun does pass through the "view cone" of the Michigan detector. However, since the sun's diameter is just 1/2°, this 9° view cone does not allow any resolution of the solar disk, so that all measurements refer to the total X-ray flux

emitted by the sun's entire visible hemisphere.

6. TIME RESOLUTION, ACCURACY, AND COVERAGE

Since a measurement is made each time the sun passes through the detector's cone of view, the time resolution of the original data is 1.7 seconds, i.e., the rotation period of the satellite. However, for economy of presentation, the final output was determined by averaging sets of four consecutive data points, so that the effective time resolution is actually 6.8 seconds. There appears to be no significant loss of information due to this reduction procedure (Teske, 1969a).

The absolute time at which a measurement was made can be assigned within 1 second of the correct value in all cases, although the timing usually is much more accurate than this. The differences in accuracy are caused by a peculiarity of the satellite's internal timing system, but are of little concern to the present study.

The Michigan experiment began returning data on 9 March 1967 with an expected lifetime of only six months; but it continued to transmit useful information until 17 August 1969, when the experiment was finally terminated by ground command. This remarkable longevity of nearly 2-1/2 years speaks well indeed for the design and construction quality of this sturdy device. Unfortunately, the second of the two tape recorders aboard OSO-III failed on 28 June 1968. After that date, only real-time data could be acquired during the ten-minute intervals when the satellite passed over a tracking station, thus severely limiting the utility of these observations.

However, even while the satellite's tape recorders were operating properly, the data coverage is not continuous. The major loss occurs during "satellite night" when the satellite's orbit carries it into the earth's shadow. In the case of OSO-III, there is approximately one hour of solar observation for every thirty minutes of satellite night. But this coverage is further interrupted by two other causes. One of these is due to the fact that nothing can be recorded while the satellite's tape recorder is "playing back" previously made observations to a ground station, a procedure which normally takes about five minutes. The other type of interruption occurs whenever the satellite passes through the enhanced density of charged particles in the region called the South Atlantic Anomaly. The background response caused by these particles becomes so large that it is not possible to determine accurately the component due to solar X-radiation. Therefore, all time intervals with high background rates have been carefully identified and eliminated from the following analysis.

7. THE DYNAMIC RANGE AND SENSITIVITY

The length of the data word which describes the response of the Michigan instrument is limited to seven bits by the OSO-III telemetry system. Therefore, just 128 different values of the ion chamber current can be distinguished. This means that any attempt to increase the experiment's dynamic range can be accomplished only by degrading its dynamic resolution, or sensitivity.

In order to overcome this difficulty to some degree, the Michigan ion chamber's response can be encoded according to one of two operating modes, whose characteristics are listed in Table 2.1.

TABLE 2.1

DYNAMIC CHARACTERISTICS OF THE MICHIGAN INSTRUMENT

Mode	E(8,12) erg/cm^{2}sec	
	Range	Resolution
High sensitivity	0 - 0.0044	0.000035
Low sensitivity	0 - 0.12	0.00095

The flux values in this table were derived from the ion chamber's response by a method described in Section II-9. Note that the high sensitivity mode has excellent flux resolution but covers only a rather small dynamic range. On the other hand, the low sensitivity mode has a much larger dynamic range but with poorer flux resolution. The instrument is designed to switch automatically between these two modes depending on whether the inferred 8-12 Å solar flux is above or below the value of 0.0044 erg/cm^{2}sec. This permits a total range (0.12 erg/cm^{2}sec) which is adequate for all but the very largest X-ray bursts, and yet allows the detection of subtle changes (0.000035 erg/cm^{2}sec) in the quiet sun level.

Unfortunately, it was not possible to take full advantage of this strategy, since the quiet sun level exceeded 0.0044 erg/cm^{2}sec more than one-half of the time, thus causing the ion chamber to operate in its low sensitivity mode even during the majority of nonburst periods. On the other hand, although the available high sensitivity coverage is somewhat limited, it is of great importance to many of the investigations described in Chapters III and IV.

8. INSTRUMENTAL STABILITY

There are several possible sources for both short-term and long-term varia-

tions in the operation of the Michigan ion chamber photometer. In the first place, the response of the instrument is partially a function of its temperature. This is due to the temperature-dependent values of the resistors, across which the electrometer measures its voltage. The temperature of these resistors varies during a given orbit, since the satellite is heated while exposed to the sun and cools when in the earth's shadow. However, this effect is negligible because the range in temperature which is encountered, 18 to 32°C, gives rise to only a 1% difference in the detector's output. Therefore, a constant temperature (20°C) is assumed for the instrument in the actual data reduction procedure.

Another possibility is a deterioration of the experiment's electronic subsystem which amplifies, encodes, and then transmits the reading of the ion chamber. In order to check for this, a known current is applied to the electrometer's input terminals about every six minutes. This calibration technique shows that the electronics have remained stable within around 1% during the experiment's lifetime.

However, there is no internal calibration system to monitor the nitrogen gas pressure in the ion chamber. Gas leakage is a particularly worrisome problem with this type of instrument because an ultra-thin foil window accounts for a large portion of the chamber wall. Any significant loss of filler gas would alter the spectral efficiency curve of Figure 2-1 in such a way as to lower the detector's response to a given flux of solar X-radiation.

The permeability of the foil window in the Michigan experiment was measured by a helium leak detector before launch. This measurement implied that the cham-

ber would retain its filler gas for more than six months, but only if the foil window did not become punctured. Careful fabrication and handling might protect against such an accident on the ground, but once the instrument is in orbit the foil window is completely exposed to the possibility of micrometeoroid impacts. An attempt to estimate the frequency of impact by particles energetic enough to damage the foil led to contradictory results (Teske, personal communication). Depending on which observation of micrometeoroid density was considered, the expected lifetime of Michigan's aluminum window ranged from 23 days to well over a year.

Fortunately, there is an external calibration source which can be used to overcome this difficulty: the sun itself. The excellent relation between the daily 2800 MHz solar flux and the soft X-ray base-level is well known (e.g., W. A. White, 1964; Pounds, 1965a; Teske, 1969a; Wende, 1969). The fact that all the E(8,12) values obtained between March 1967 and March 1968 followed very nearly the identical relation with the 2800 MHz flux (Teske, 1969b) is a strong indication that the entire Michigan experiment, including the nitrogen gas filling, remained highly stable during this period.

9. CONVERSION OF DETECTOR RESPONSE TO X-RAY FLUX

The ion chamber photometer has a relatively restricted bandpass of effective response, as described in Section II-4, but it cannot give any information whatsoever concerning the spectral distribution of the radiation within that bandpass. The response to a large number of low energy X-ray photons is identical to that caused by a smaller flux of higher energy radiation. There-

fore, the incident X-ray spectrum first must be known in order to convert the measured ion chamber current into the proper energy flux of that radiation. Since the spectrum is in fact not generally known, the results of X-ray studies which use ion chamber detectors have been subject to a great deal of uncertainty. Thus, it is necessary to examine in some detail both the extent of this uncertainty and, in particular, the degree to which the flux values derived from the Michigan experiment can be considered as valid.

Following Kreplin (1961), the ion chamber current as a function of time can be expressed as:

$$i(t) = AGe \cdot \int_0^\infty \epsilon(\lambda) F(\lambda,t) d\lambda \qquad (2.2)$$

where A is the detector's effective aperture, G is the ionization efficiency of the filler gas, e is the electronic charge, $\epsilon(\lambda)$ is the detector's spectral efficiency given by equation (2.1), and F is the specific flux of the incident radiation. For the Michigan instrument, the total window aperture is 3.88 cm^2; but the thin window foil is supported by a wire grid which has a transmission of 83% as determined by optical calibration. Therefore, the effective aperture is actually 3.22 cm^2. Then, with e given as 1.60×10^{-19} coul and G taken to be 1.73×10^{10} ion pairs/erg for nitrogen gas, the Michigan ion chamber is characterized by:

$$AGe = 8.91 \times 10^{-9} \text{ coul cm}^2/\text{erg} \qquad (2.3)$$

In order to approximate the incident specific flux, previous investigators

have always assumed that F can be separated into two components, one of which is just a function of wavelength and another of which varies only with time. That is:

$$F(\lambda,t) = B(\lambda) \cdot D(t) \tag{2.4}$$

However, the quantity of interest in the case of the Michigan experiment is the integrated flux between 8 and 12 Å as a function of time:

$$E(8,12;t) \equiv \int_8^{12} F(\lambda,t)d\lambda = D(t) \cdot \int_8^{12} B(\lambda)d\lambda \tag{2.5}$$

The time dependence of this value will be implicitly understood hereafter, so that this quantity will be called simply E(8,12). The above expressions then imply that E(8,12) can be written in the following form:

$$E(8,12) = \gamma \cdot i(t) \text{ erg/cm}^2\text{sec} \tag{2.6}$$

where:

$$\gamma = \frac{\int_8^{12} B(\lambda)d\lambda}{AGe \cdot \int_0^{\infty} \epsilon(\lambda) \cdot B(\lambda)d\lambda} \text{ erg/(cm}^2\text{sec amp)} \tag{2.7}$$

Note that, for a given detector, this conversion factor γ depends on both the effective bandpass (here 8 to 12 Å) and the assumed form of the spectral distribution $B(\lambda)$.

The most common procedure for the reduction of ion chamber measurements

is to assume that B has the same wavelength dependence as the Planck black-body function:

$$B(\lambda) = \frac{1}{\lambda^5(e^{hc/\lambda kT}-1)} \qquad (2.8)$$

This is often termed the gray-body approximation, since the complete expression for the specific flux (2.4) includes the time-varying "dilution" factor D(t). A great many investigators have used this approximation with a gray-body temperature T of 2×10^6 K for observations near 10 Å (see the reviews by Friedman, 1963a; and Mandel'shtam, 1965a). Therefore, the same procedure was followed for the Michigan experiment in order to compare the present results directly with those already observed. Furthermore, when the Michigan project began, very little was known about the true nature of the solar spectrum at X-ray wavelengths, so the gray-body approximation seemed the best possible choice at that time.

With $T = 2 \times 10^6$ K, equations (2.1), (2.3), (2.7), and (2.8) can be used to calculate the conversion factor γ of equation (2.6). Under the assumptions just described, the conversion factor for the Michigan experiment is:

$$\gamma = 7.71 \times 10^8 \text{ erg}/(\text{cm}^2 \text{ sec amp}) \qquad (2.9)$$

This constant will be used throughout the present study to determine E(8,12).

Values of E(8,12) derived by the above procedure are presented graphically as a function of Universal Time (UT) by a computer-controlled plotter. Figure 2-2 shows examples of two such consecutive plots which display many of the

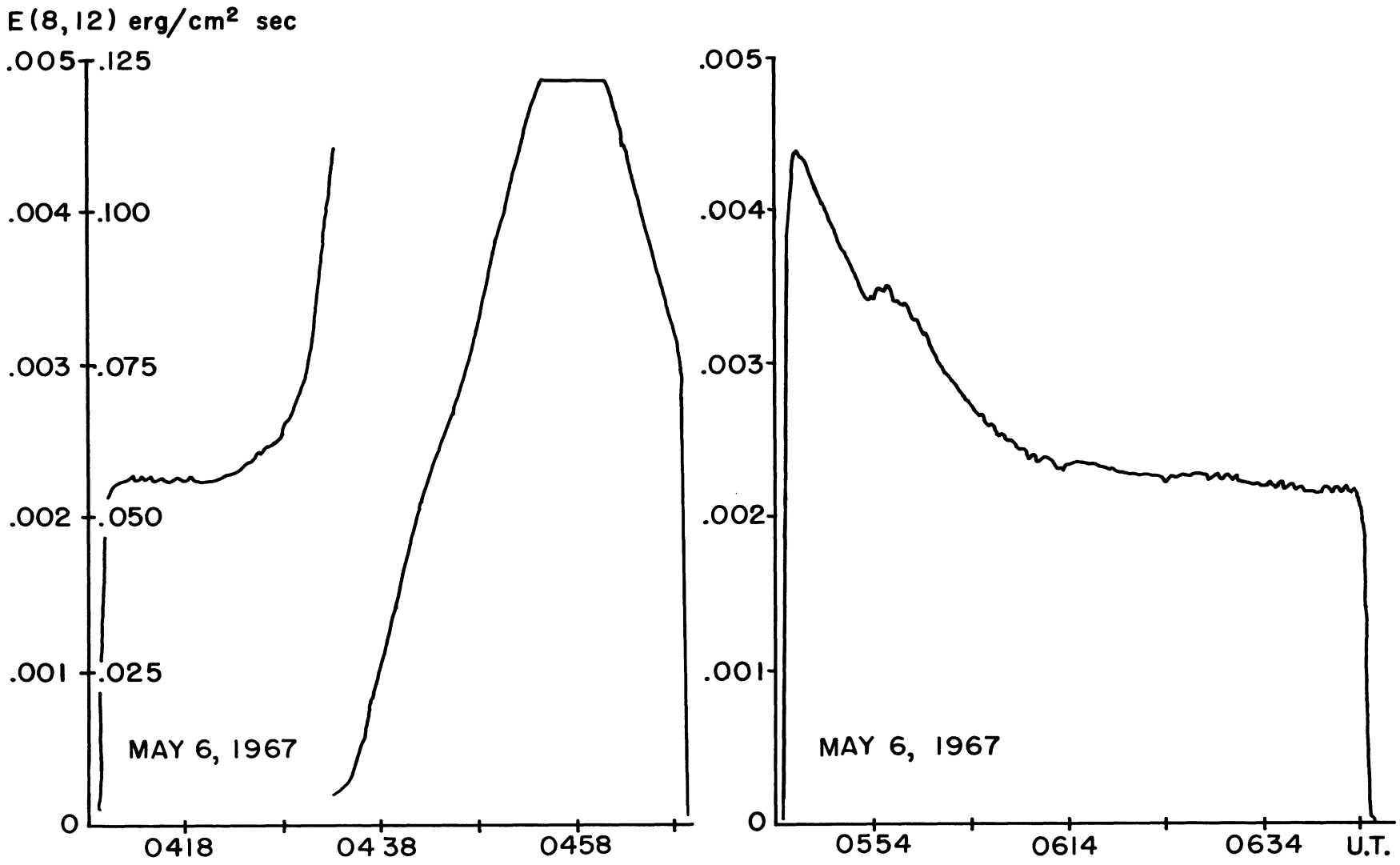

Figure 2-2. Time-profile of the soft X-ray burst on 6 May 1967. Satellite "sunrise" and "sunset" mark the beginning and end of each record. The Michigan detector switches its operating mode from high sensitivity (flux scale on left of axis) to low sensitivity (scale on right) at 0433 UT, and is saturated between 0455 and 0500 UT. The second record shows high sensitivity operation only.

features mentioned earlier for this experiment. "Sunrise" and "sunset" mark the beginning and end of these two records, which are separated by about half an hour of satellite "night." An X-ray burst begins at 0422 UT, when the detector is in its operating mode of high sensitivity. (The flux values are given by the scale on the left side of the ordinate axis.) The detector automatically switches to its low sensitivity mode as the burst exceeds .0044 erg/cm^2 sec, and then becomes saturated for about six minutes during the peak of the burst. (Now the flux scale on the right side of the axis applies.) At the start of the second record, the detector is back in its high sensitivity mode with the X-ray flux gradually decaying to its pre-burst level.

Studies to be presented in the remainder of this paper were all based upon measurements made from plots similar to those just described.

10. ACCURACY OF THE X-RAY FLUX VALUES

How closely do the E(8,12) values derived by the above method approximate the actual integrated fluxes incident on the detector window $E_o(8,12)$? A relation between them can be written in the form:

$$E_o = aE^b \qquad (2.10)$$

where b is, in general, not constant. The factor a is a measure of the absolute error in the reduction procedure and depends in part upon instrumental calibration inaccuracies. The absolute calibration of the Michigan instrument itself is believed to be within 6% of correct (Teske, 1969a). This type of error is relatively harmless in the sense that all final results can be corrected easily

by applying a single constant factor. Furthermore, any statistical relationships derived from such measurements remain qualitatively valid.

On the other hand, the relative error in the data reduction, represented by the exponent b, is a much more serious problem. This error results from the fact that the solar X-ray spectrum does not actually correspond to a two million degree gray body and, more importantly, that the spectrum changes significantly with time. If b differs much from unity and especially if b is not a monotonic function of E_o, ion chamber measurements would be extremely difficult to interpret and any conclusions drawn from them would be highly questionable.

After a careful study of this problem, Acton (1964) concluded that observations from an aluminum window ion chamber and reduced by assuming a constant two million degree gray-body spectrum are probably correct within a factor of four. But many investigators claim that this type of error can exceed an order of magnitude (Pounds and Willmore, 1963; Lindsay et al., 1965; Mandel'shtam, 1965a), while Neupert (1969) points out that the difficulty is enhanced for a detector such as the Michigan instrument, which has a very large dynamic range.

One way to measure this error is to determine the effect on the calculated E(8,12) values due to expected changes in the solar X-ray spectrum. Figure 2-3 shows the result of one such study made by Teske (1969a). If the true spectrum is that of a gray body at a temperature T, this graph gives the correction factor which must be applied to E(8,12). It can be seen that this correction exceeds an order of magnitude whenever the corresponding gray-body temperature is greater than about twenty million degrees.

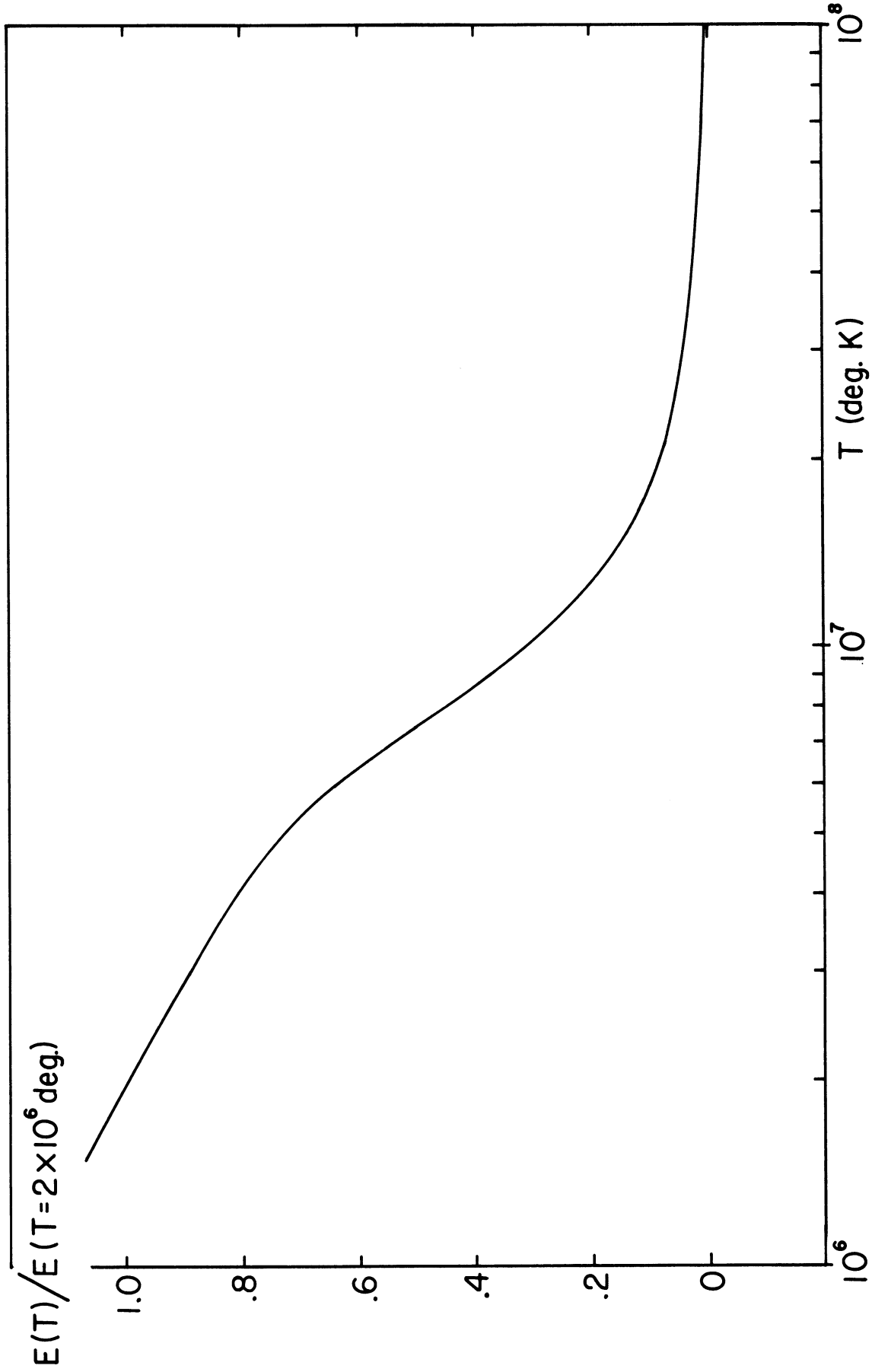

Figure 2-3. Correction for any error due to the adopted gray-body temperature of 2 x 10^6 K. Multiply E(8,12) by the factor given here in order to obtain the correct flux for a spectral slope of gray-body temperature T. (Figure from Teske, 1969a.)

Now it is necessary to discover what range of T is to be expected. In principle, the appropriate gray-body temperature for a given set of observations can be estimated from measurements made by the ion chamber during satellite "sunrise" and "sunset." At these times, the earth's atmosphere differentially extinguishes the solar X-radiation and thus acts as a broad-band spectral analyzer. Such a technique has been used for observations made by moderate altitude rockets (Chubb et al., 1957; Mandel'shtam et al., 1962) and by an orbiting satellite with simultaneous measurements from three detectors of different wavelength intervals (Landini, 1967). The analysis is much more complex in the latter case, since the solar radiation passes into and then out of the earth's atmosphere at a large slant angle. This method therefore appears to be impractical for a single detector experiment, such as Michigan's, because of the great uncertainty due to errors in the atmospheric parameters which must be used (Mount, personal communication). It is interesting to note that this technique is now being inverted in order to determine more accurately these atmospheric parameters using high resolution observations of the solar X-ray spectrum (Rugge, personal communication).

Although individual temperatures cannot be derived from the Michigan experiment itself, it is possible to estimate the expected range of T from values quoted by other investigators. Table 2.2 summarizes many such temperatures determined by a number of techniques which are appropriate for the spectral region around 10 Å. Some caution is necessary in using these values, however, because in general they refer to the electron temperature of the emitting plasma rather than its gray-body temperature, which is needed for expression (2.8). Moreover,

TABLE 2.2

TEMPERATURE DETERMINATIONS OF SOLAR ACTIVE REGIONS

T (10^6 K)	Wavelength Interval (Å)	Solar Activity	Method*	Reference
1.0-1.5	< 10	nonflare	1	Mandel'shtam et al., 1961
1.5-1.9	~ 20	nonflare	2	Zhitnik et al., 1967
1.5-2.1	8-20	nonflare	3	Reidy et al., 1968
1.6-2.6	~ 20	nonflare	2	Jones et al., 1968
1.7	8-11	nonflare	3	Pounds and Sanford, 1963
1.7-2.2	8-12	nonflare	4	Culhane et al., 1963
1.8	7- 9	nonflare	4	Bowen et al., 1964
1.8	8-20	nonflare	3	Reidy and Vaiana, 1966
1.9-6.4	2-18	flare	3	Mandel'shtam, 1965a
2	8-20	nonflare	3	Negus and Glencross, 1968
2 -3	< 10	nonflare	3	Mandel'shtam, 1965b
2.2	8-15	nonflare	2	Blake et al., 1965a
2.3	"soft X-rays"	nonflare	5	Billings, 1959
2.4-2.9	2-18	nonflare	3	Tindo and Surygin, 1965
< 2.5	2-18	nonflare	3	Mandel'shtam, 1965a
2.7	7- 9	flare	4	Bowen et al., 1964
2.8-3.0	< 10	nonflare	3	W. A. White, 1963
3 -4	11-22	nonflare	2	Evans and Pounds, 1965
3	> 11	nonflare	3	Pounds et al., 1968
3	8-20	subflare	3	Landini et al., 1965
3 -8	2-14	flare	3	Beigman et al., 1969
3 -10	"soft X-rays"	flare	6	DeJager, 1965a
< 4 -5	< 14	flare	3	Acton, 1968
4**	8-12	flare	4	Pounds, 1965b
4 -5	< 10	flare	1	Mandel'shtam et al., 1961
4.5	< 10	nonflare	7	Mandel'shtam et al., 1962
< 5	> 8	nonflare	4	Culhane et al., 1968
< 6	2-12	flare	3	Wende, 1969
6	"soft X-rays"	flare	6	Kawabata, 1966a
10	8-20	2^+ flare	3	Elwert, 1964

*Methods:

1 Ionospheric effects
2 Ratio of emission line intensities
3 Ratio of broad-band responses
4 Proportional counter
5 Visible coronal condensation
6 Theoretical model
7 Differential atmospheric extinction

**Temperature revised by Acton (1968).

since the solar atmosphere is optically thin to X-radiation (Allen, 1969), the X-ray spectrum in reality cannot possibly be that of a gray body. Fortunately, this is not a serious problem because Acton (1964) points out that the spectral slopes given by both temperatures are very similar over a limited wavelength interval. According to the conversion scheme given by Mandel'shtam (1965a), the electron temperature extremes of 1 and 10 million degrees shown in Table 2.2 correspond to a gray-body temperature range of roughly 0.7 to 5 million degrees. With these limits, Figure 2-3 then implies that the relative error in E(8,12) is always less than 30%, assuming there is no line emission.

A more comprehensive estimate of this error can be obtained by means of the Van Allen-Wende method mentioned in Section II-4. In this procedure, expression (2.7) is used to calculate γ as a function of effective bandpass for a variety of assumed spectra. Since the short wavelength limit of the Michigan detector's bandpass is clearly the aluminum K-edge at 8 Å, only variations in the long wavelength limit λ_2 are considered here. Figure 2-4 shows the results of such calculations for gray-body and free-free (thermal bremsstrahlung) spectra as well as spectra which are softer than free-free by a factor of λ^2. Furthermore, a curve for each of these spectral types is plotted using temperatures of one, two, four, six, and ten million degrees (except for a gray-body spectrum at ten million degrees, which is unrealistic, as shown above).

The set of curves in Figure 2-4 forms a "bow-tie" and so the combination of γ and λ_2 which defines the narrowest part of this distribution will result in flux values which have the smallest possible relative errors. For example, the optimum point in this plot is:

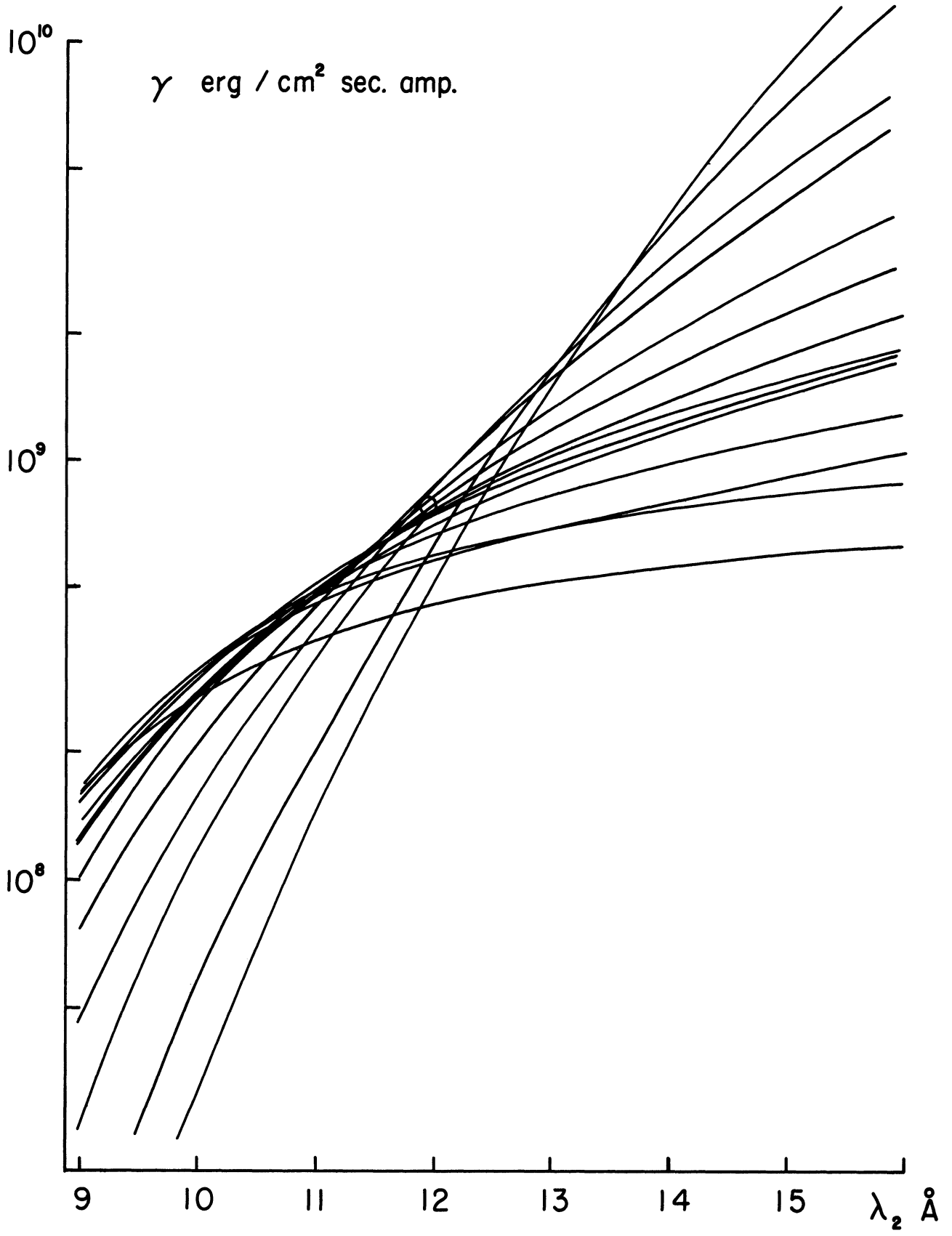

Figure 2-4. Relation of the conversion factor γ to the Michigan experiment's effective bandpass as defined by λ_2. Curves are shown for three types of spectra at five different temperatures between 1 - 10 x 10^6 K. The values of γ and λ_2 adopted for this study are indicated by o.

$$\gamma = 5.9 \times 10^{8} \text{ erg/(cm}^2 \text{ sec amp)}, \lambda_2 = 11.9 \text{ Å}$$

where variations in γ due to changes in the X-ray spectrum lead to relative errors of less than 27%. This is only slightly better than the results obtained by the conversion factors actually used in the Michigan data reduction procedure:

$$\gamma = 7.71 \times 10^{8} \text{ erg/(cm}^2 \text{ sec amp)}, \lambda_2 = 12 \text{ Å} .$$

Although the E(8,12) values calculated by these factors are too large by about 20% in general, the relative error is less than 30% for the wide range of possible spectra considered in Figure 2-4.

In all of the discussion to this point, it has been tacitly assumed that the solar X-ray spectrum near 10 Å, whatever its slope, is predominantly a continuum. This assumption is probably incorrect, at least during major X-ray bursts. With the exception of Fritz et al. (1967), and Meekins et al. (1968), all investigators who have observed solar X-radiation with high spectral resolution find that line emission strongly dominates the continuum around 10 Å (e.g., Blake et al., 1965a, 1965b; Rugge and Walker, 1967; Walker et al., 1967; Evans and Pounds, 1968). The great enhancement of this line emission during an X-ray burst is clearly seen in Figure 2-5 (taken from Neupert et al., 1969). The figure shows a spectrum observed while an importance 2b flare was in progress, as well as one observed prior to the flare. These observations led Underwood (1968) to remark: "It appears necessary to reevaluate much of the earlier work done with broad-band photometers in terms of a spectrum dominated by line radiation."

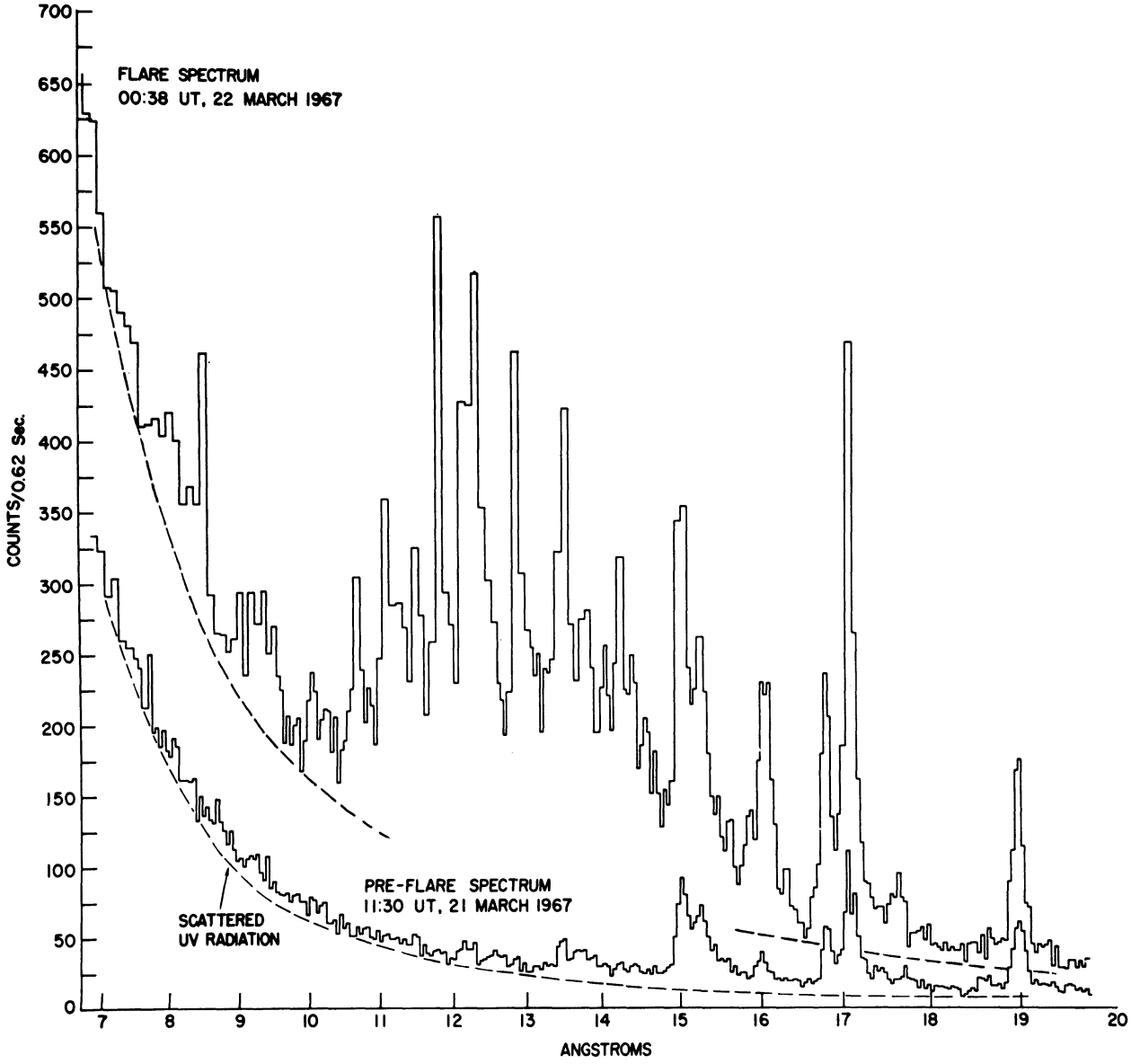

Figure 2-5. High resolution X-ray spectra between 7 and 20 Å obtained by the Goddard Space Flight Center's crystal spectrometer aboard OSO-III. The measured values must be corrected for scattered UV radiation as shown. (Figure from Neupert et al., 1969.)

Such a "reevaluation" was made for the Michigan experiment using the flare spectrum of Figure 2-5. With an instrumental efficiency curve kindly supplied by Dr. Neupert, this spectrum was converted into absolute units, as shown in Figure 2-6, and then planimetered to obtain the "true" flux between 8 and 12 Å:

$$E_o(8,12) = 0.0137 \text{ erg/cm}^2\text{sec} \qquad (2.11)$$

Next, the spectrum of Figure 2-6 was "folded" into the efficiency curve for Michigan's detector to give Figure 2-7. Planimetry of this curve then leads to the value of the ion chamber current which would be measured for such an incident spectrum:

$$i = 1.70 \times 10^{-11} \text{ amp} \qquad (2.12)$$

Finally, this current was multiplied by the conversion factor of expression (2.9) to give the equivalent two million degree gray-body flux:

$$E(8,12) = 0.0131 \text{ erg/cm}^2\text{sec} \qquad (2.13)$$

It may be just coincidental that this value, derived by means of such a poor approximation to the actual X-ray spectrum, should be so close to the "true" solar flux shown in expression (2.11); but it does make those who worried about relative errors greater than an order of magnitude appear overly pessimistic.

However, a good deal of care must still be exercised when interpreting the E(8,12) values measured by the Michigan ion chamber photometer. For example, Figure 2-7 shows that over 20% of the instrument's response is due to the single

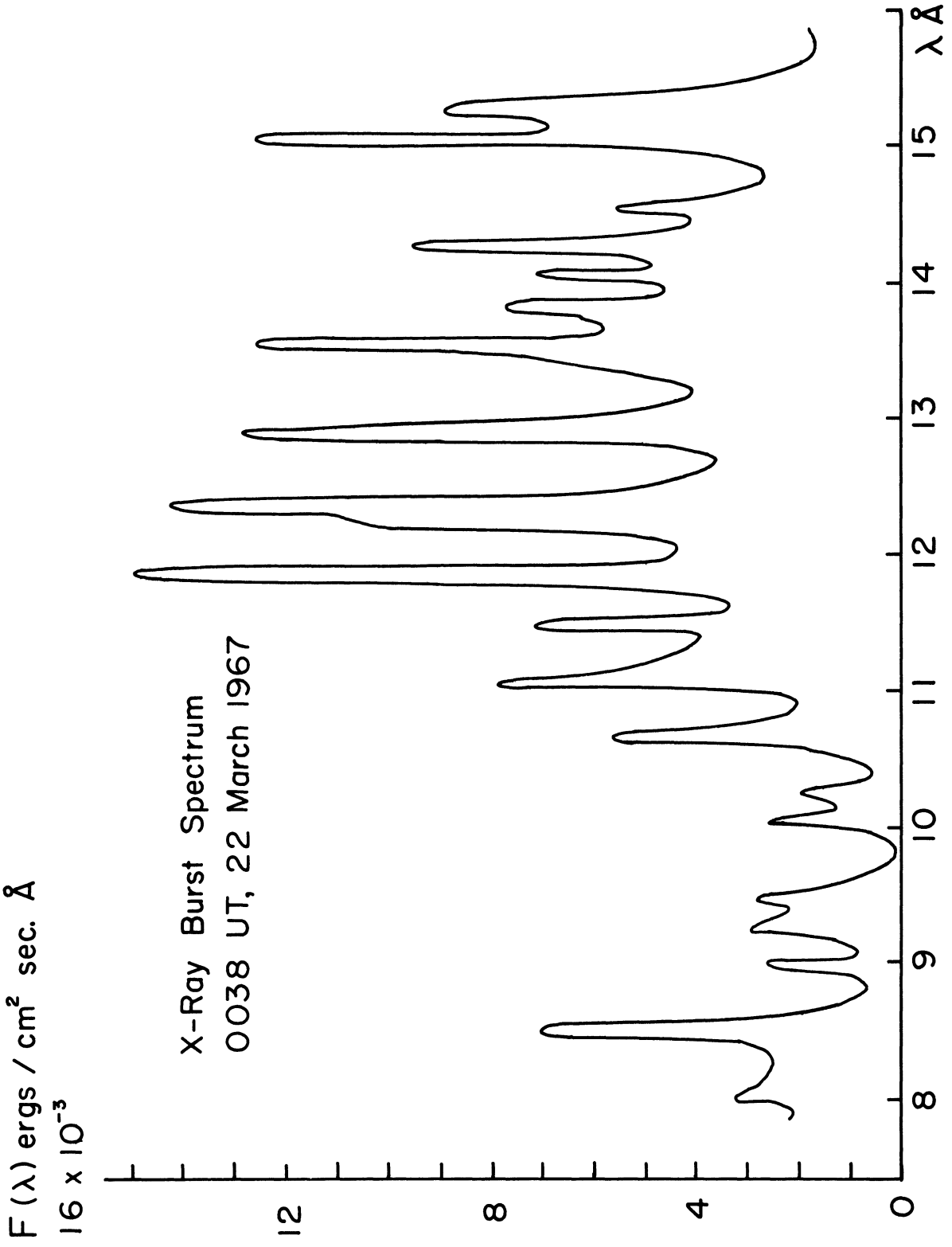

Figure 2-6. Spectrum of a major X-ray burst on 22 March 1967 plotted in absolute units.

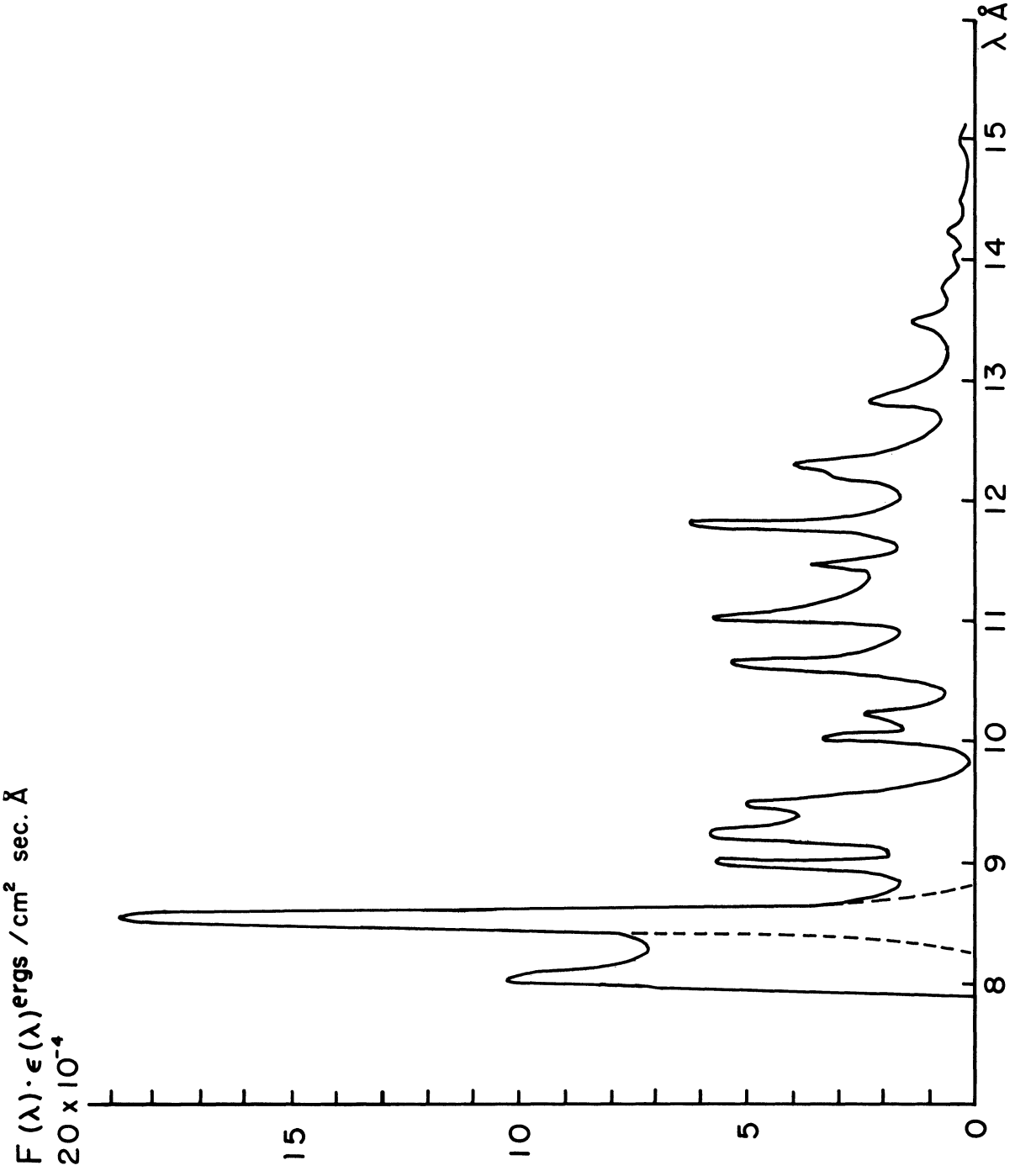

Figure 2-7. Spectral response of the Michigan ion chamber to a major X-ray burst on 22 March 1967. The dashed curve is an estimated extrapolation of the emission line profile for the feature at 8.5 Å.

emission line at 8.5 Å. This feature has been identified as a resonance line of Mg XII by Garcia and Mack (1965), Rugge and Walker (1967), and Beigman and Vainshtein (1969). Therefore, the Michigan experiment can be considered a combination broad-band flux detector and Mg XII line monitor.

In addition, it should be noted that the Michigan detector was observing the sun at the time the spectrum of Figure 2-6 was made. At that time, the ion chamber was saturated, which means that the implied value of E(8,12) was greater than 0.12 erg/cm^{2}sec. This value is, of course, much larger than the one in expression (2.13), which, according to Neupert's observations, should have resulted. But this discrepancy merely points out the uncertainties in the absolute calibration of these two instruments. For instance, Neupert (personal communication) warned that the calibration of his experiment may be in error by more than a factor of three. He also noted another possible explanation for this discrepancy: the scattered UV radiation in his observations might not have been taken properly into account. But whatever the cause of this difficulty, the above analysis shows that relative ion chamber results derived by means of the gray-body approximation may still be valid even during a large X-ray burst when the actual spectrum is as complex as the one in Figure 2-6.

This can be shown in yet another way. If the results of broad-band photometers do depend strongly on the actual shape of the solar X-ray spectrum, one would not expect a simple relation between the measurements made by two detectors with different spectral efficiency characteristics, since this would require the relative errors of the two instruments to match perfectly at all times. Figure 2-8 shows the relation between E(8,12) and the 1-8 Å flux measured by a NRL ion

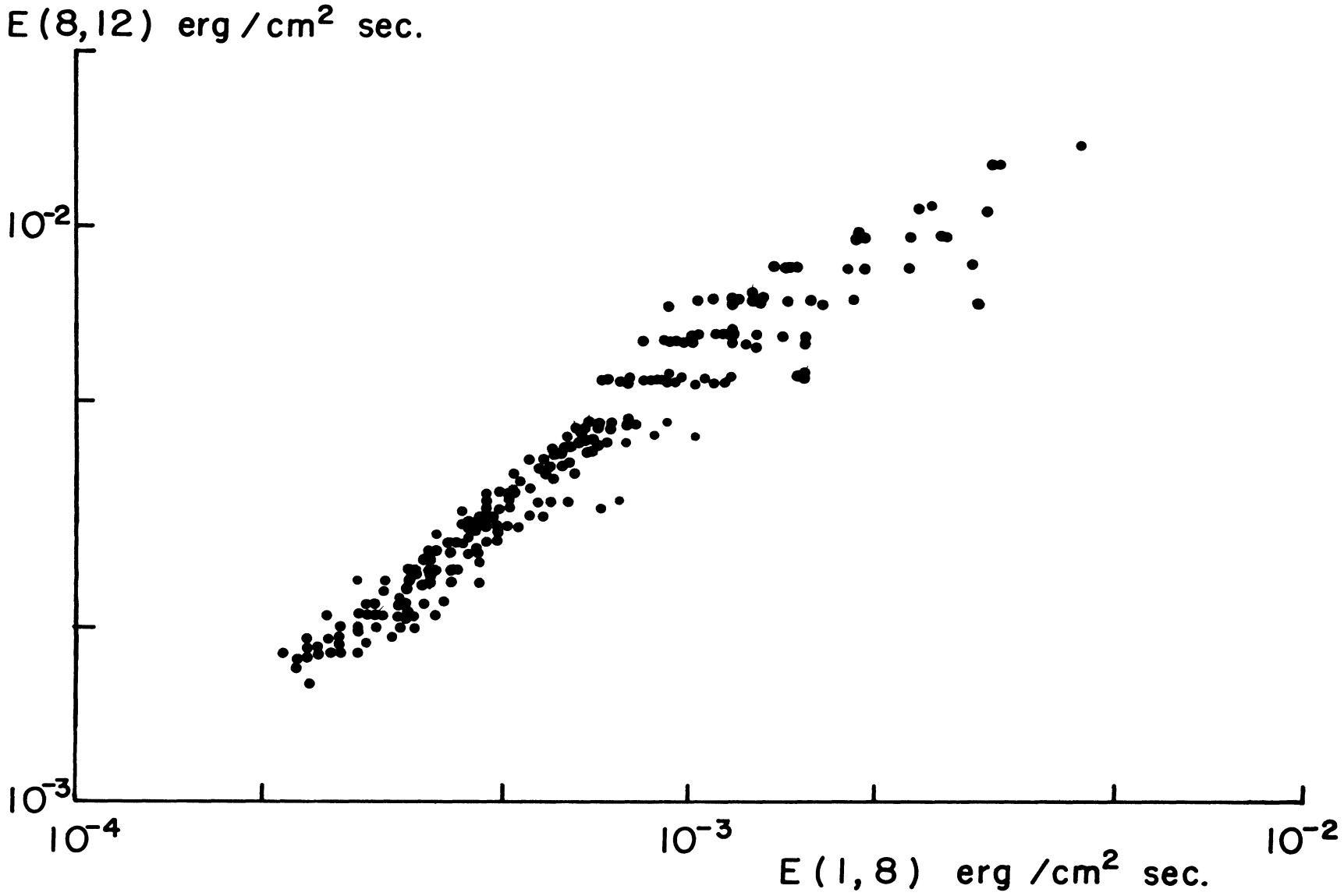

Figure 2-8. Comparison of the daily base-levels of E(8,12) and E(1,8) from 1 August 1967 to 31 March 1968. The E(1,8) values were derived from NRL observations by means of the 2 x 10^6 K gray-body approximation.

chamber photometer aboard OGO-4. (The 1-8 Å measurements were supplied by D. M. Horan of the NRL.) Specifically, the daily X-ray base-levels for both experiments on each day between 1 August 1967 and 31 March 1968 are plotted in this figure. The correlation between these two sets of data is clearly very good and the relation is almost linear. This relation will be discussed further in the next chapter, which will also define the "base-level" values used here.

The X-ray spectrum is relatively simple during quiet sun conditions as in the above study, however. A much more stringent test would involve data from X-ray bursts where the spectrum is extremely complex and changing rapidly. Figure 2-9 shows such a comparison between E(8,12) and the 2-12 Å flux observed by a University of Iowa detector (Drake, personal communication) and reduced on the assumption of a constant spectrum. The values plotted are the respective peak fluxes for every burst in Catalog II (described in Chapter IV) which was observed by both experiments. Again the correlation is excellent, in this case over a range of nearly two orders of magnitude. All six of the points which do not lie directly on the nominal relation were marked as uncertain by one or both investigators.

It therefore seems safe to conclude that order of magnitude relative errors do <u>not</u> occur in properly reduced broad-band observations, even during large X-ray bursts. The actual relative error for the Michigan experiment is perhaps less than 30%.

However, the absolute error may be much greater. For example, note that the E(8,12) values in Figure 2-9 are larger than the corresponding E(2,12) values from the Iowa observations, a situation which cannot possibly be correct.

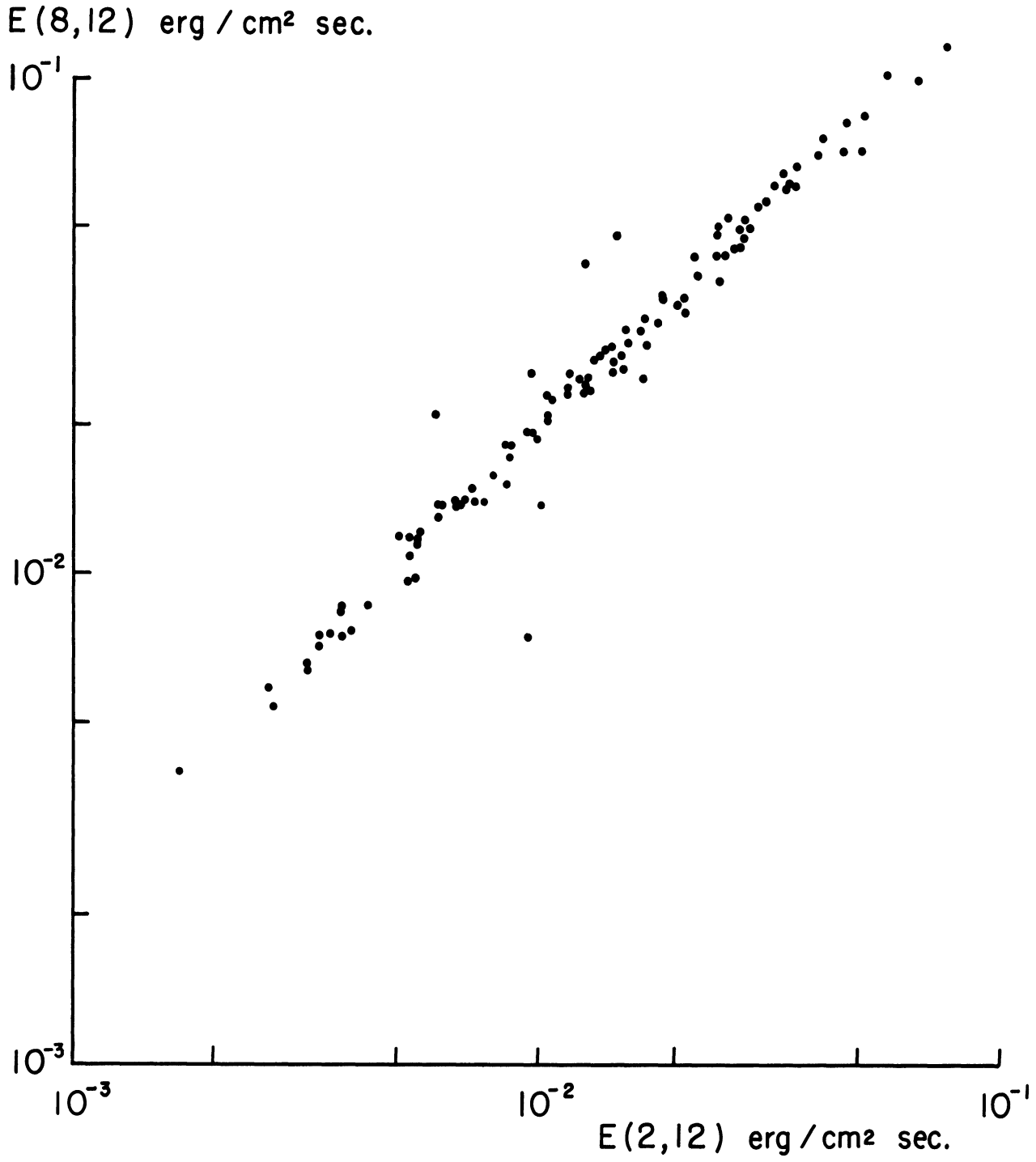

Figure 2-9. Comparison of the peak rates of E(8,12) and E(2,12) for X-ray bursts associated with major Hα flares. The values of E(2,12) were derived from a University of Iowa experiment aboard Explorer 35.

According to the many comparisons just described, it appears probable that the absolute values of the E(8,12) measurements which will be used in the remainder of this study are systematically too high, perhaps by as much as a factor of two or three. But the excellent time resolution, dynamic range, sensitivity, stability, and relative accuracy of the Michigan experiment, as well as its notable longevity, make the data obtained from this instrument extremely valuable for the study of solar soft X-radiation.

In summary, the various characteristics of the Michigan ion chamber experiment discussed in this chapter are compiled in Table 2.3.

TABLE 2.3

UNIVERSITY OF MICHIGAN SOLAR X-RAY EXPERIMENT ABOARD OSO-III
(All data refer to normal incidence)

Physical characteristics		
Window:	Metal foil	Al (99.45% pure)
	Surface density	0.00327 gm/cm^2
	Effective area	3.22 cm^2
Filler:	Gas	99% N_2 + 1% He
	Pressure	~ 1 atmosphere
	Surface density	0.00331 gm/cm^2
	Ionization efficiency	36.0 ev/ion-pair
General:	Chamber depth	2.58 cm
	Collimation cone	250 square degrees (window fully illuminated)
	Satellite rotation period	1.7 sec
	Instrumental calibration	± 6%
	Stability	± 1%
Data characteristics		
Effective bandpass		8-12 Å
Conversion factor		7.71 x 10^8 erg/(cm^2 sec amp)
Effective time resolution		6.4 sec
Time accuracy		better than 1 sec
Extensive coverage		10 March 1967 - 28 June 1968
Limited coverage		28 June 1968 - 17 August 1969
Flux absolute error		factor of 2-3 (?) (flux values probably high)
Flux relative error		± 30%

CHAPTER III

THE X-RAY SLOWLY VARYING COMPONENT

Solar radio emission is often divided into a slowly varying component with a time scale of 27 days and a burst component which shows significant variations within minutes. The same scheme of classification can be applied to the X-ray region of the spectrum (e.g., Kundu, 1963, 1965; Friedman, 1963a; Mandel'shtam, 1965a). This chapter will describe some investigations of the slowly varying component of solar X-radiation; Chapters IV and V will consider its burst component.

1. DETERMINATION OF THE DAILY E(8,12) BASE-LEVEL

A great deal of care must be exercised to identify the correct value of the nonburst X-ray flux for a study of the slowly varying component. During the period observed by the Michigan experiment aboard OSO-III, the sun was near its level of maximum activity and X-ray bursts occurred frequently. Long intervals exist in which the E(8,12) record is continuously disturbed, with bursts often overlapping one another. This is especially bothersome since X-ray bursts normally have greater durations than their optical or radio counterparts (as shown in Chapter IV). Moreover, the Michigan detector observes the entire solar disk, so that the true X-ray base-level can be attained only when no optical or radio event has occurred anywhere on the visible hemisphere for some period of time. But even this condition is not adequate because many X-ray bursts are not associated with a reported optical or radio event (e.g., Yefremov et al., 1962; Acton et al., 1963; Conner et al., 1964; Teske, 1969a). A final

difficulty is that the base-level flux is usually just a fraction of the flux during a burst. Therefore, any mistake in identifying the nonburst intervals can lead to substantial errors in the base-level values derived.

To avoid some of these problems, no attempt was made to select those specific intervals which were thought to be devoid of burst activity. Rather, the base-level for a given day was defined as the lowest flux value observed between 0400-2000 UT on that day (except that anomalously low measurements of short duration were discarded as spurious). While the above procedure is not ideal, we believe that it is more useful than presuming to identify the day's "nonburst" observations as is done for many other studies (e.g., Pounds, 1965a; Michard and Ribes, 1968; Wende, 1969). It definitely gives base-level values that are less misleading than those obtained from real-time observations, which include only 4 or 5 ten-minute intervals each day (Chitnis and Kale, 1966).

The daily E(8,12) base-level fluxes, as defined here, are thus taken to measure the slowly varying component of solar X-radiation. These values will be used in the following investigations and will be referred to as $E_b(8,12)$.

2. COMPARISON WITH Ca^+ PLAGE INDICES

Essentially all of the quiet-sun X-radiation (< 50 Å) originates from coronal enhancements which overlie active regions roughly delineated by chromospheric calcium plages. This had been suggested indirectly by some early studies (e.g., Waldmeier, 1947; Elwert, 1956); but it is shown directly by observations of individual regions using pin-hole cameras (Blake et al., 1963b; Broadfoot, 1967; Pounds et al., 1968), slit-telescopes (Blake et al., 1963a),

Fresnel zone-plate optics (Elwert, 1968), grazing-incidence telescopes (Lindsay, 1965; Underwood and Muney, 1967; Vaiana et al., 1968), and raster-scanning devices (Negus and Glencross, 1968; Paolini et al., 1968; Beigman et al., 1969), as well as measurements during a solar eclipse (Kreplin, 1961).

However, to study this relation by means of the OSO-III data, the sum of all Ca^+ plages on the disk must be considered, since Michigan's experiment has no spatial resolution of solar features. Therefore, the $E_b(8,12)$ fluxes were compared with the Ca^+ plage indices ΣA, ΣAxI, and $\Sigma A^{3/2}xI$ for the corresponding dates, obtained from measurements of the daily calcium spectroheliograms made at the McMath-Hulbert Observatory. Only the reports which were rated at least fair in quality between 10 March 1967 and 1 June 1967 were used here. The resulting correlation coefficients are shown in Table 3.1.

TABLE 3.1

CORRELATION OF $E_b(8,12)$ WITH Ca^+ PLAGE INDICES

Ca^+ Plage Index	Correlation Coefficient
ΣA	0.64
ΣAxI	0.70
$\Sigma A^{3/2}xI$	0.69

The value ΣA represents the total area of the visible plages, the individual plage areas having been corrected for foreshortening. The strong correlation of this index with $E_b(8,12)$ indicates again the close relation between the plage regions and the source of soft X-radiation. Moreover, the size of the region seems to be a measure of its associated X-ray emission, which confirms the results

of several image-forming experiments (e.g., Underwood and Muney, 1967; Negus and Glencross, 1968).

But the correlation of $E_b(8,12)$ is even stronger with ΣAxI, a rough indicator of the total Ca^+K excess flux due to the visible plages. The intensity values for this index are derived by estimating the rank of the brightest part of each plage on a scale of 1 to 5, which is then converted into the appropriate excess intensity I by means of Table 3.2. (This table is courtesy of the McMath-Hulbert Observatory.) Such a result implies that the conditions which determine the chromospheric plage brightness (that is, the level of the enhanced temperature, density, and magnetic field strength) extend into the overlying, X-ray emitting region.

TABLE 3.2

RELATIONSHIP BETWEEN ARBITRARY Ca^+ PLAGE INTENSITY SCALE AND PHOTOMETRIC MEASUREMENTS OF Ca^+ PLAGES

Scale	Intensity in Units of Ca^+ Background	Excess Intensity
1	1.3	.3
1.5	1.5	.5
2	1.7	.7
2.5	1.85	.85
3	2.0	1.0
3.5	2.15	1.15
4	2.3	1.3
5?	> 2.3	> 1.3

Teske (1969b) has continued this comparison through 30 April 1968 using the Michigan data and finds a correlation coefficient of 0.73 between $E_b(8,12)$ and ΣAxI for this period. Therefore, the time interval considered in the present study does not seem to be atypical. The fact that others (e.g., Michard and Ribes, 1968) find a much weaker correlation shows the advantage of the $E_b(8,12)$ definition used here. Direct observations of individual X-ray regions indicate also that the X-ray emission is related to the area and intensity of the associated Ca^+ plage (Blake et al., 1963b; Pounds and Russell, 1966; Reidy et al., 1968).

On the other hand, the X-ray emitting region is known to have an extensive three-dimensional structure (Vaiana et al., 1968; many others) so that it clearly must be treated as a volume source. It would be interesting to determine how this volume depends on the area of the underlying chromospheric plage. W. A. White (1964) finds that it is much better to assume that the thickness of the X-ray source is directly related to the mean plage diameter rather than to assume a constant thickness. Therefore, he sets the X-ray emitting volume proportional to $A^{3/2}$. Unfortunately, his analysis is based on an incorrect interpretation of the intensity index for the Ca^+ plage as estimated by the McMath-Hulbert Observatory.

Probably for that reason, the present study does not substantiate White's result. Table 3.1 shows that the correlation of $E_b(8,12)$ with $\Sigma A^{3/2}xI$ is no better than that with ΣAxI. It follows that the major part of the soft X-ray emission originates from a volume whose thickness does not strongly depend on the size of the underlying plage. This would be the case if, for example, the

X-ray emitting region consisted of many small volume elements, each associated with the filamentary structure of the chromospheric plage. As the plage area grew by the addition of more such elements, there would not necessarily be any concurrent increase in the thickness of the X-ray emitting source.

Although the correlation between $E_b(8,12)$ and ΣAxI is quite good in general, the relation appears much weaker when examined in detail. This can be seen in Figure 3-1, which plots the daily values used to find the correlation coefficient discussed above. By following the time development of this relation, two intervals were identified whose daily values fell in totally different regions of the figure. $E_b(8,12)$ was higher than would be predicted from ΣAxI for the period 15-17 April 1967, and at that time the largest plage on the disk was a region near the limb (McMath #8776) which was in its first rotation. (Unfortunately, there were no adequate Ca^+ observations by McMath-Hulbert for 13-14 April when this region was directly on the limb.) In contrast, the major feature of the disk between 22-28 April was a very large, but fragmented plage near the central meridian (McMath #8778) which was four rotations old. During the latter interval, $E_b(8,12)$ was noticeably low relative to ΣAxI. Although McMath-Hulbert's spectroheliograph was readjusted between the two intervals considered here, an examination of data during the two-month period bracketing the readjustment shows that this had no systematic effect on the relation of $E_b(8,12)$ to ΣAxI.

One interpretation of the above result is that a region's X-ray emission gradually decays over a period of several solar rotations. This would be consistent with the observations of Neupert (1967, 1968), who finds that both the

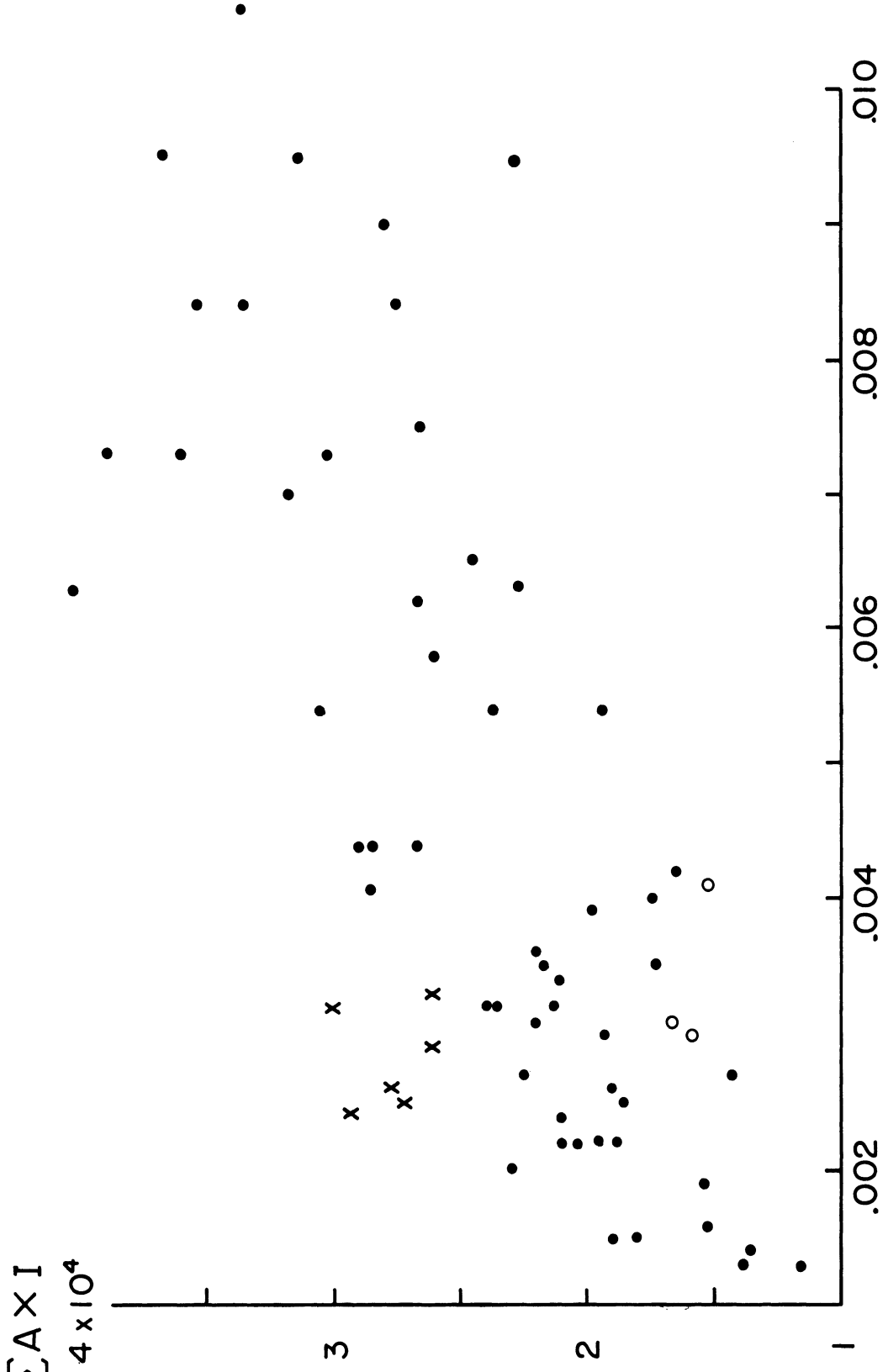

Figure 3-1. Relation between the daily values of $E_b(8,12)$ and the calcium plage index $\sum$ A x I for the period 10 March to 1 June 1967. The units for A are millionths of the solar hemisphere; I is in units of the Ca^+ background intensity. Points for the dates 15-17 April are marked as o; those for 22-28 April as x.

temperature and density of a coronal condensation decrease as the associated active region ages. Another possibility is that X-ray sources display a "limb-brightening" effect. Such an effect has been suggested by Teske's (1969a) study, which shows that $E_b(8,12)$ is high relative to other solar activity indices during both limb passages of a major active center. The observed "limb-brightening" is undoubtedly due to the height at which soft X-radiation is emitted. X-ray sources overlying plages at the limb are typically reported to have heights of roughly 100,000 km (e.g., Negus and Glencross, 1968; Paolini et al., 1968; Vaiana et al., 1968; Beigman et al., 1969). Thus a region's X-ray emission can be observed even if its chromospheric plage is just beyond the limb.

3. COMPARISON WITH X-RAYS OF OTHER WAVELENGTHS

It is not possible to derive any information about the shape of the X-ray spectral distribution from measurements by a single ion chamber, as discussed in Chapter II. However, a rough estimate of the average spectral slope can be obtained from a comparison of equivalent observations made by two or more dissimilar broad-band detectors.

Figure 3-2 shows such "composite" spectra of the slowly varying component between 1/2-60 Å for two different dates. The spectra are based on data from four NRL experiments (all carried by the satellite OGO-4) as well as from The University of Michigan's experiment. Table 3.3 gives the bandpass of each experiment and the gray-body temperature that was used in the reduction of each detector's response. For clarity of presentation, the spectra have been plotted on an arbitrary flux scale with a convenient separation between the data for

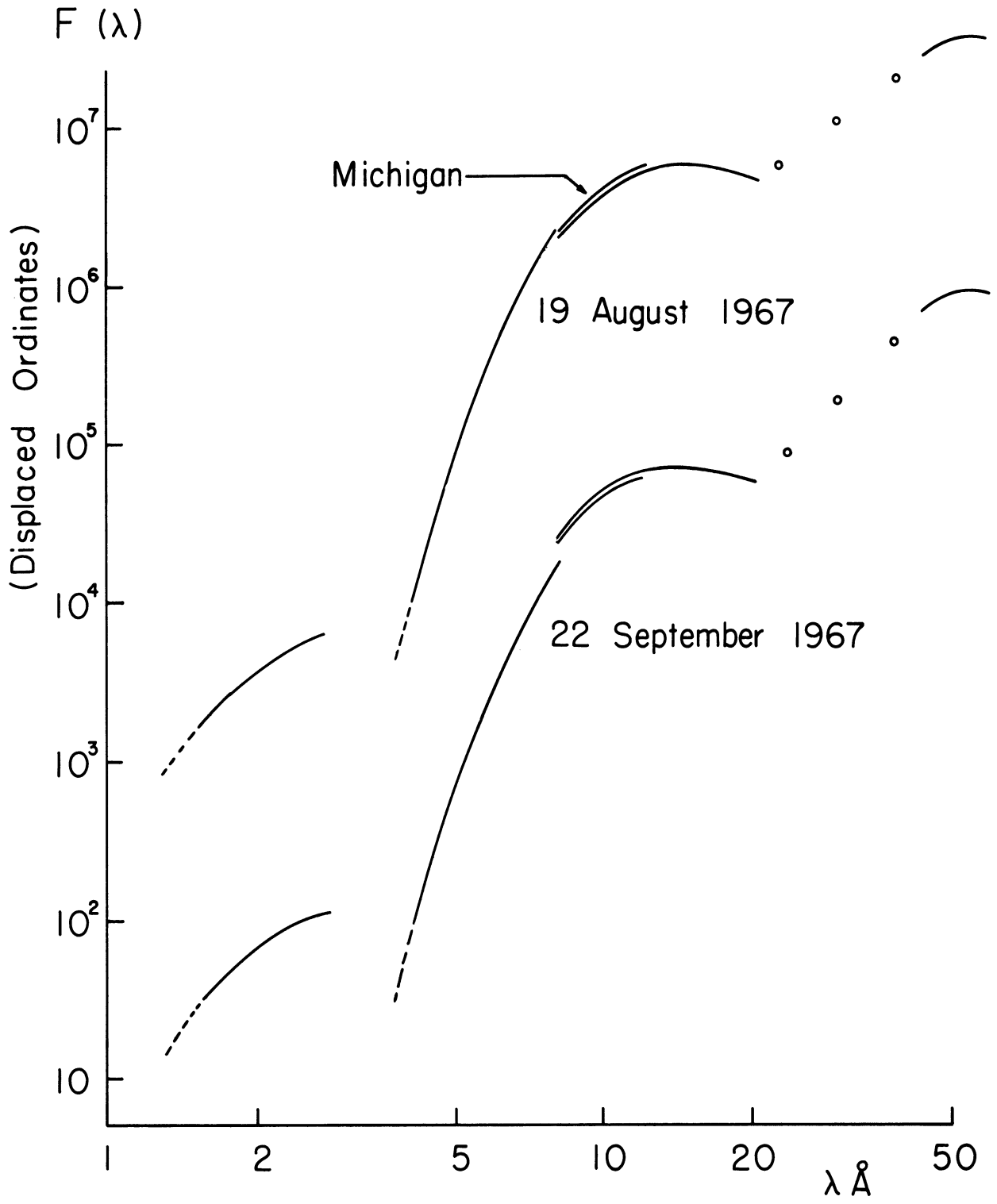

Figure 3-2. Composite average spectra of the slowly varying component between 1/2 - 60 Å for two dates. The spectra are plotted on an arbitrary ordinate with a convenient separation. The spectral slopes of individual segments reflect the gray-body distribution assumed for each measurement. 19 August and 22 September 1967 represent dates of high and low base-level flux, respectively.

these two dates. The spectral slopes of the individual segments shown have been derived from the gray-body distribution assumed for each experiment.

TABLE 3.3

CHARACTERISTICS OF COMPARED EXPERIMENTS

Bandpass (Å)	Assumed Gray-Body Temperature (10^6 K)	Investigator
1/2 - 3	10	NRL
1 - 8	2	NRL
8 - 12	2	Michigan
8 - 20	2	NRL
44 - 60	0.5	NRL

This figure shows, first of all, how well the Michigan results agree with those of NRL, the largest difference at 8 Å being about 30%. Secondly, the rough spectral slope around 10 Å seems to be quite close to the 2 x 10^6 K gray-body slope assumed in the reduction procedure for E(8,12). Both of these findings offer further support for the analysis of the Michigan experiment's reliability as discussed in Chapter II. Finally, it is obvious that the entire spectrum between 1/2 - 60 Å cannot be represented correctly by a single temperature, a result which also agrees with observations made by other techniques (e.g., Pounds and Sanford, 1963; Bowen et al., 1964; Mandel'shtam, 1965a). Therefore, the X-ray emitting source is not isothermal, but apparently consists of a small, very hot nucleus surrounded by more extensive regions of cooler and cooler material (although still hotter than the ambient corona). Such a model has been proposed by Blake et al. (1963a), and Evans and Pounds

(1968), and is consistent with the results of image-forming experiments which show that the size of a coronal X-ray source decreases as the wavelength of the observation becomes smaller (Blake et al., 1965a; Underwood and Muney, 1967).

Since all of the experiments which were used to derive Figure 3-2 observed the sum of the X-ray emission from the entire solar disk, another interpretation of this figure is conceivable. Namely, each X-ray source on the sun is isothermal itself, but different temperatures apply to the various regions on the disk at any given time. However, this explanation is not tenable for the following reason. The dates for the spectra shown in Figure 3-2 were chosen because they represented the highest (19 August 1967) and the lowest (22 September 1967) daily base-level fluxes encountered in the time period studied. The Ca^{+} plages seen on the disk differed greatly in number, intensity, and total area on those two dates. Thus, the X-ray emitting regions associated with these plages also should have very different characteristics, according to the results discussed in the previous section. Yet Figure 3-2 indicates that the overall spectral shape has changed very little between the dates in question, although each spectrum represents the contributions from a completely different set of emission sources. This would be highly unlikely if the "isothermal hypothesis" just described were correct.

Striking changes in the average spectral slope of the slowly varying component have never been observed, but a subtle hardening of the spectrum as the daily base-level increases can be detected by a statistical study of many days' observations. For this purpose, data from the NRL 1/2 - 3 Å, 1-8 Å, and 8-20 Å detectors aboard OGO-4 were again used. Lists of hourly averages of the

"nonburst" measurements made by these detectors between 1 August 1967 and 31 March 1968 were searched to find the daily base-level fluxes in a manner identical to that described in Section III-1. Hereafter, these values will be referred to as $E_b(1/2,3)$, $E_b(1,8)$, and $E_b(8,20)$. Unfortunately, the 44-60 Å experiment aboard OGO-4 failed very early in November 1967 and so could not be used in this study.

The resulting relation between $E_b(8,12)$ and $E_b(1/2,3)$ is given in Figure 3-3, along with that between $E_b(8,12)$ and $E_b(8,20)$. The comparison between $E_b(8,12)$ and $E_b(1,8)$ has been presented already as Figure 2-8 of Chapter II. Note that the poorest correlation is with $E_b(1/2,3)$, which represents the emission of a coronal region's hottest portions. One possible explanation is that only certain regions have such a high-temperature component. This hypothesis therefore implies that the "quality" of the X-ray emitting sources is the most important criterion for $E_b(1/2,3)$, rather than their "quantity" which is so important for $E_b(8,12)$. An interesting problem for future investigation is to attempt an identification of any special characteristics which might exist for the chromospheric plages observed on days with anomalous $E_b(1/2,3) : E_b(8,12)$ ratios. This would be a valuable test of the hypothesis just described.

Although the correlation between $E_b(1/2,3)$ and $E_b(8,12)$ is relatively weak, a straight line can be fitted to the points in Figure 3-3(a). An eye-estimate of this fit gives:

$$E_b(1/2,3) = 2.2 \times 10^{-3} E_b(8,12)^{1.24} \qquad (3.1)$$

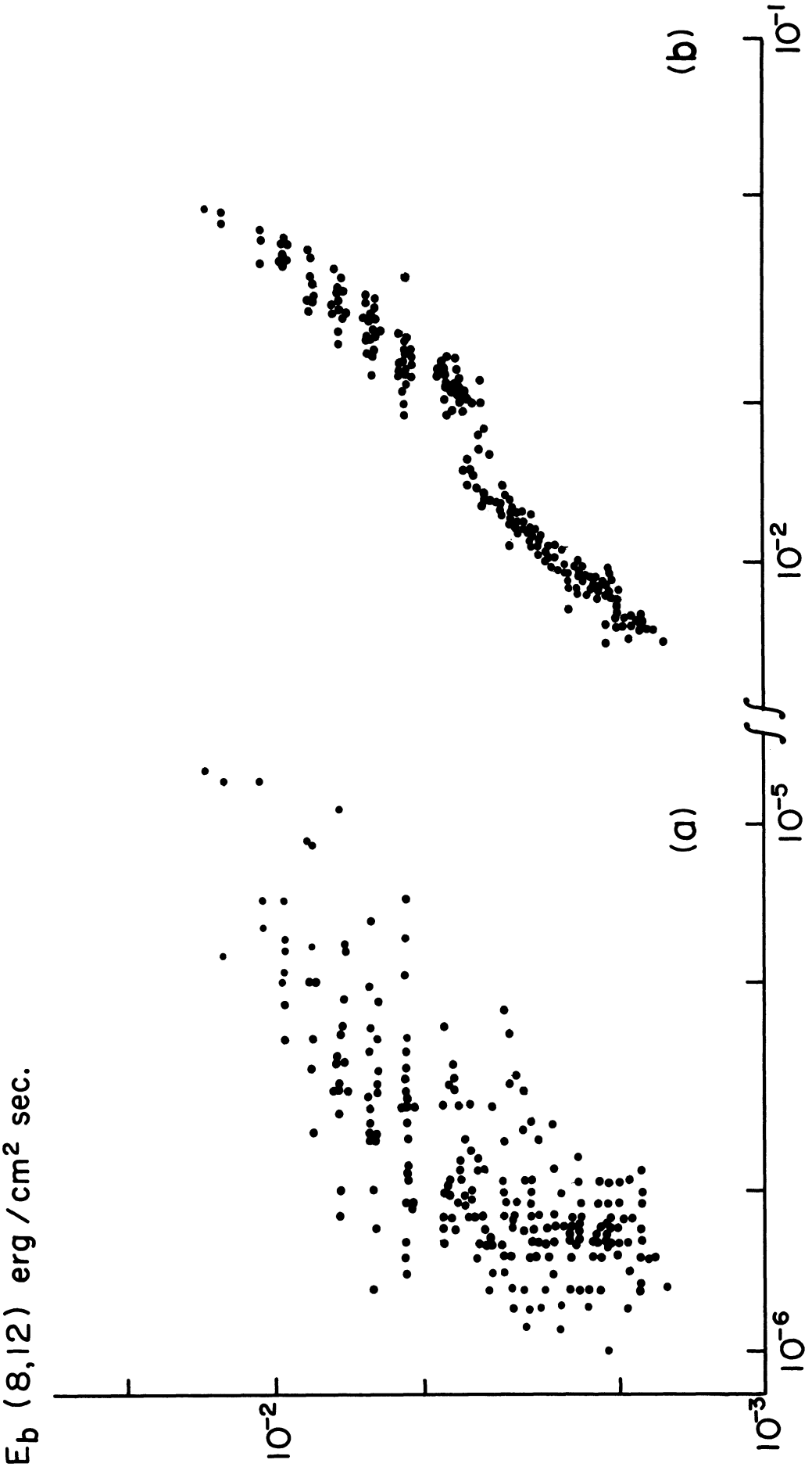

Figure 3-3. Comparison of $E_b(8,12)$ with (a) $E_b(1/2,3)$ and (b) $E_b(8,20)$ for the interval 1 August 1967 to 31 March 1968.

Since the exponent in this expression is greater than unity, $E_b(1/2,3)$ becomes larger relative to $E_b(8,12)$ on the average as the base-level flux increases, thus giving rise to the spectral hardening mentioned above.

This hardening of the X-ray spectrum is seen much more convincingly in Figure 2-8, because the relation of $E_b(8,12)$ with $E_b(1,8)$ is clearly much better than with $E_b(1/2,3)$. An eye-estimate of the best straight line fit to Figure 2-8 gives:

$$E_b(1,8) = 1.04\ E_b(8,12)^{1.32} \qquad (3.2)$$

implying again that the shorter wavelength emission increases relative to $E_b(8,12)$ on the average during periods of higher base-level flux.

As might be expected, the "tightest" relation is between $E_b(8,12)$ and $E_b(8,20)$ shown in Figure 3-3(b). However, there is a very pronounced break in the relation at about $E_b(8,12) = 0.0038$ erg/cm^{2}sec. This is probably unrelated to the Michigan experiment because it does not appear in any other comparison with $E_b(8,12)$. It is more likely to be caused by an improper alignment of the flux scales for the high and low sensitivity modes of the NRL instrument. (Note that the break occurs well below the point where the Michigan detector changes its sensitivity.) By shifting each part of the curve horizontally toward the other an equal amount, the relation becomes approximately:

$$E_b(8,20) = 0.95\ E_b(8,12)^{0.73} \qquad (3.3)$$

which once again, has an exponent appropriate for a spectrum that hardens, on the average, with increasing flux.

The change in spectral slope of the slowly varying component, although minor, occurs throughout the range 1/2-20 Å and has been reported by many others (e.g., Kreplin, 1961; Michard and Ribes, 1968; Wende, 1969). (One exception is Noci and Russo (1964) who correlated 0-8 Å flux with ionospheric parameters to find that the spectrum does not vary with changes in the quiet sun's X-ray flux level. But the evidence from direct observations is overwhelming that this interpretation is incorrect.) Therefore, we cannot consider changes in the slowly varying component as being due solely to differences in the number or total volume of otherwise similar X-ray sources. At least some of the regions that exist during periods of high base-level flux must be substantially hotter than the regions observed when the base-level flux is low. Most likely, the same basic mechanism which is responsible for the increased level of general solar activity also gives rise to further enhancements in the temperatures of the X-ray sources overlying active regions.

CHAPTER IV

THE X-RAY BURST COMPONENT: STATISTICAL STUDIES

Rapidly-varying bursts of solar X-radiation are often superimposed on the sun's X-ray base-level. These bursts usually accompany some optical phenomenon such as an Hα flare, disparition brusque, limb surge, or prominence eruption (Kreplin et al., 1962; Friedman, 1963b; Muney and Underwood, 1968), but they can also occur in the absence of any other reported events (e.g., Pounds, 1965b; Drake, 1969; Teske, 1967, 1969a, 1969b). The present study will consider only the enhanced X-ray emission associated with well confirmed Hα flares. Specifically, we will examine the general time-profiles of such bursts, both in an absolute sense and relative to the associated Hα flares. We will also compare the peak emission rates of the soft X-ray and Hα events, as well as the total energies emitted by these two radiations during flares of various importances. In addition, an attempt will be made to identify some parameters accessible to ground-based observers which correlate with the X-ray burst's amplitude. A statistical approach will be used in this chapter, and in Chapter V three well observed events will be investigated in some detail.

1. SELECTION OF Hα FLARE EVENTS

In order to facilitate the statistical study of flare-associated X-radiation, a catalog was compiled of all well confirmed flares of importance ≥ 1 which occurred between 10 March and 31 December 1967. Since all reports of Hα flares are not equally reliable (Dodson and Hedeman, 1968), an attempt was made to eliminate events which were not clearly verified. The first such cata-

log included only those flares which were reported by three or more stations and rated importance 1 or greater in the Quarterly Bulletin on Solar Activity. This list formed the basis of the studies reported by Teske and Thomas (1969), hereafter referred to as Paper I.

Unfortunately, the above selection procedure strongly biased the sample toward those events which occurred in summer months and during European observing hours, when the number of stations monitoring the sun can reach three times the world-wide yearly average (Dodson-Prince, personal communication). To avoid this difficulty, a second approach was taken for the catalog used in the present investigation. Each flare had to satisfy all of the following conditions to be included in this list:

(1) at least two stations report the event,

(2) more than 50% of the stations observing at its time of maximum report the event,

(3) at least 50% of the stations observing at its time of maximum rate its importance as 1 or greater,

(4) at least one station reporting the event must be photographic or cinematographic, and

(5) the Quarterly Bulletin rates its importance as 1 or greater.

This set of criteria requires that a photographic record of the flare exists, and that most of the stations which were monitoring the sun at the time actually saw the flare and agreed that it was indeed greater than just a subflare. To determine exactly which stations were observing at any given time, lists were used of the daily patrol-times for all flare-monitoring observatories which re-

port to the World Data Center at Boulder, Colorado. (These patrol-times were obtained through the kind offices of J. Virginia Lincoln.) The individual flare reports, which are tabulated in the "Revised" list of the ESSA Solar-Geophysical Data Bulletin (SGDB), gave data on the number of stations reporting the event and the various assessments of its importance.

In addition to the above screening procedure, events were eliminated whenever it appeared that the X-ray record might be seriously affected by particle interference (discussed in Section II-6) or by the occurrence of two or more flares close together in time. The latter requirement is necessitated by the Michigan detector's lack of spatial resolution, which does not allow the individual contributions of simultaneous bursts to be determined. Unfortunately, this eliminates any possible examples of the so-called sympathetic class of flares discovered by Richardson (1951) and shown to be due to the "triggering" of one flare by another (Becker, 1958). Therefore, the results of the present study do not necessarily apply to this very interesting class of events.

2. THE LIST OF Hα FLARES HAVING X-RAY COVERAGE

After the culling process described in the previous section, we are left with 283 flares for which we have at least partial X-ray coverage. Although many valid events were no doubt excluded by this procedure, the flare reports which remain can be safely considered as highly reliable. Table 4.1 presents the resulting list of Hα flares along with some information about the associated 8-12 Å X-radiation. (Since this list represents the second flare catalog constructed for events observed by the Michigan experiment, it will also be referred to as Catalog II in the following discussion.) The times of start and

TABLE 4.1

Hα FLARES WITH X-RAY COVERAGE (CATALOG II)

Date	Hα Flare Data					E(8,12) Burst Data					No.
	Start	Max.	End	Imp.	Location	Start	Max.	End	Base	Ampl.	
					March 1967						
16	2342	2349*	2402	1n	N18E79 8733	2343	2349	-	39	56	1
17	2152	2202	2222	1f	N24E53 8733	2152.5	2200	-	54	41	2
18	0835E	0853	0948D	1f	S15E08 8727	-	0850.5	-	42	48'	3
20	1344	1350	1418	1n	N18E35 8733	-	1403.5	-	130	92'	4
		1401									
20	2310	2345	2420	1n	N23E21 8733	2302.5	-	-	73	84	5
21	1814	1820	1835	1n	N20E77 8740	1818	1824	-	73	54	6
22	0022	0033	0240	2b	N24E68 8740	0017.5	0038'	-	84	1211"	7
		0155					0157				
23	1917	1932	2017	1b	N24E31 8740	-	1935	2018	53	257	8
25	0709	0714*	0730	1n	N23E26 8740	0705.5	0714	-	53	104	9
25	1856	1914	2024	1n	N26E20 8740	-	1925	2055	106	94	10
26	0458	0509	0540	2n	N23W01 8740	0504.5	0513	0534	73	231	11
26	1402	-	1428	1n	S19E67 8745	-	-	1426	53	-	12
26	1603	1605	1619	1b	N24E02 8740	1604	1608	1630'	84	236	13
26	1630	1652	1750	3n	N26E05 8740	-	-	1812	84	-	14
27	1558	1614	1650	1n	N24W06 8740	1557	1617	-	62	107	15
27	1718	1730	1800	1n	N25W23 8740	-	1726.5	-	53	82	16
27	2107	2113	2205	1b	N23W24 8740	2110.5	2117	-	84	363	17
		2129					2129				
28	0615	0618	0626	1n	N24W29 8740	0614	0619.5	0642	116	225	18
29	1726	1740	1820	1b	N21W30 8740	1722	1743	-	137	388'	19
30	0756	0800	0835	1n	N22W40 8740	-	0807	-	175	272'	20
30	0851	0902	0930	2n	N24W49 8740	-	0906'	-	258	592'	21
30	2336	2347*	2420	1n	N24W59 8740	2340.5	2349.5	-	116	215	22
31	1258E	1305	1420	1n	N18W32 8741	1257	1311	-	128	29	23

TABLE 4.1 (Continued)

Date	Hα Flare Data					E(8,12) Burst Data					No.
	Start	Max.	End	Imp.	Location	Start	Max.	End	Base	Ampl.	
					March 1967 (Concluded)						
31	2212	2218 2232	2300	1n	N18W63 8740	2212.5	2219	2239	128	102	24
					April 1967						
1	0119	0122	0140	1n	N24W75 8740	0118	0128.5	-	148	369	25
1	0618	0621	0632	1b	N19W70 8740	0615.5	0622	0637	270	500	26
1	0810	-	0848	1n	S20W07 8745	0814.5	0822	-	169	164	27
2	0407	0418 0424	0440	1n	N24W86 8740	-	0421 0425.5	-	84	116	28
2	0818	0823	0840	1n	S24W79 8739	0800.5	0801	0802	95	5	29
2	1116	1120	1150	1n	S23W81 8739	1116.5	1125	-	100	163'	30
9	0912	-	0938D	1f	S20W40 8753	0910.5	-	-	39	-	31
11	1112	1119 1124	1142	1n	S21W65 8753	-	1122' 1132	1220	40	330'	32
11	1336	1344	1440	1b	N22W24 8760	1315	1343	-	34	93	33
12	0533	0542*	0558	1b	S22W74 8753	-	0542.5	-	35	262	34
14	2236	2241	2256	1f	N21W66 8760	2231	2240	2252	38	16	35
23	0020	0036*	0050	1n	S22W67 8777	-	0037	0113	30	86'	36
27	1602	1606	1620	1n	S22E80 8791	-	-	1653	33	-	37
30	0938E	0945	1010	1n	S20E42 8791	0939	0946.5	-	40	35	38
30	1304	1309	1333	1n	S22E40 8791	1302	1310	-	37	47	39
					May 1967						
1	0519	0523 0531	0545	1n	S22E31 8791	0507	0522	-	28	67	40
1	0745	0755*	0815	1n	S22E30 8791	-	0754	0824	26	38	41
6	0435	0439	0545D	3n	S20W34 8791	0422	0457	0613	22	1328"	42
10	1145	1153	1240	2n	S22W87 8791	-	1212.5	-	15	316	43
12	1755	1802	1830	1n	N24W68 8798	1758	1801	1809	14	8	44

TABLE 4.1 (Continued)

Date	Hα Flare Data					E(8,12) Burst Data					No.
	Start	Max.	End	Imp.	Location	Start	Max.	End	Base	Ampl.	
					May 1967 (Concluded)						
14	1533	1547	1640	1n	S27E08 8807	1532	-	-	20	-	45
18	1934	1937*	1951	1n	N25E80 8818	1933.5	1935.5	2007	175	145	46
19	1239	1257	1310	1b	N24E65 8818	1241	-	1325	73	-	47
19	1524	1538	1615	1b	N24E70 8818	-	-	1649	100	-	48
20	1005	1009	1025	1b	N25E53 8818	1006	1009	-	63	43	49
20	1508	-	1615	1b	N23E51 8818	-	-	1641	95	-	50
21	1300	1302	1316	1n	N26E61 8818	-	1306	-	73	353	51
21	1535	1539	1600	1b	N23E58 8818	-	1540	1611	75	393'	52
21	1919	1926	2025	2n	N24E39 8818	1917.5	-	2042	90	2635"	53
21	2354	2411	2427	2b	N24E55 8818	2351	2410 2414 2417	-	95	403	54
23	1802	1814 1844 1947	2200	3b	N28E26 8818	1758	-	-	175	8060"	55
24	0300	0321	0420	1n	N22E10 8818	0250	0330	0503	137	371	56
25	0222	0227*	0313	1n	S20E15 8819	-	0230'	0308	73	102'	57
25	0632	0646	0720	1b	N28E11 8818	0631.5	0637	0803	84	-	58
25	1039	1053	1225	1b	N22W06 8818	-	1101.5	1229	100	738'	59
25	2043E	2054	2125	1n	N27E05 8818	2028.5	2055	-	73	83	60
26	1516	1531 1555	1700D	1n	N30W05 8818	-	1608	-	150	161'	61
27	0129	0203	0257D	1n	N26W18 8818	0127	-	0330'	137	-	62
28	0529E	0543	0700	2b	N28W32 8818	-	0555'	-	90	3909"	63
28	0714	0732 0750	0820	1n	N24W44 8818	-	0734 0757.5	-	150	170'	64
29	1856	-	1930	1n	N30W68 8818	1853	-	1944	84	-	65

TABLE 4.1 (Continued)

Date	Hα Flare Data					E(8,12) Burst Data					No.
	Start	Max.	End	Imp.	Location	Start	Max.	End	Base	Ampl.	
					June 1967						
1	1451	1457	1512	1n	N24E27 8831	-	1458'	1531	138	94	66
2	0056	0105	0142	1n	N21W39 8824	0057.5	-	-	118	-	67
2	0825	0832	0856	1n	N10W77 8821	0823.5	0836	-	127	98	68
2	0847	0852	0920	1n	N20W45 8824	0842.5	0852.5	-	175	365'	69
2	2302	2306	2345	1b	N20W53 8824	2303.5	2317'	-	84	66'	70
3	0226	0304	0352	1n	N23E12 8831	0230.5	-	-	84	-	71
4	0753	0758	0840	1n	S17W39 8829	-	0759'	-	84	127'	72
5	1839	1844 1938	2032	2n	S18W58 8829	-	1950	-	39	-	73
11	1107E	1115	1155	1n	N19E58 8843	1105	1117	-	11	12	74
16	0021	0026	0040	1f	S16W90 8836	-	0026	0059	40	22	75
17	2120	2125	2220	1n	N28E63 8854	2106	2131 2144	-	20	159	76
18	1306	1315	1415	1n	N26E55 8854	1258	1313 1319	-	44	256	77
23	0037	0039 0052	0110	1n	N15E33 8863	0033.5	-	-	27	-	78
25	0105	0135	0200D	1n	N22E16 8863	-	0138	-	27	120	79
29	2331	2339	2359	1n	N15W57 8863	2332	2341	-	26	47	80
					July 1967						
2	0920	0928*	0945	1b	N20W90 8863	0917	0927	-	29	55	81
4	0643E	0648	0700	1n	S21W01 8875	-	0649	-	22	51	82
5	1832	1855	1935	1b	S21W18 8875	1832	-	2005	27	-	83
7	1946	1953	2016	1n	N27E24 8880	-	1954	-	25	48'	84
9	0110	0142	0230	1n	S23W64 8875	-	0141	-	25	70'	85
20	0547	0551	0630	1n	S22E50 8901	0547.5	0555.5	-	32	136	86

TABLE 4.1 (Continued)

Date	Hα Flare Data					E(8,12) Burst Data					No.
	Start	Max.	End	Imp.	Location	Start	Max.	End	Base	Ampl.	
					July 1967 (Continued)						
20	0717	0724 0739*	0810	1n	S22E49 8901	0719.5	0727.5 0741.5	-	32	209	87
21	2250	2303	2340	1f	N24E82 8905	-	-	-	63	0	88
23	0538	0543	0600D	1n	N12E84 8907	0515.5	0546.5	-	84	191	89
23	1244	1302	1310	1b	N12E75 8907	-	1301'	1309	63	187'	90
24	0024	0035	0050	1n	N11E66 8907	0018	0037	0057	63	356	91
24	0928E	0933*	1015	1n	N27E54 8905	-	0947	-	75	199'	92
24	0959	1000	1008	1b	N10E63 8907	0957	1001	1009	235	213	93
24	1148	1154	1210	1n	S23W04 8901	1142	1156'	-	100	143'	94
24	1152	1202*	1220	1n	N27E53 8905	-	1203.5	-	200	266'	95
25	0010	0014 0039	0100	1f	N29E43 8905	0012'	0013.5 0039.5 0046.5	-	84	-	96
25	1055	1058 1120	1130	1b	N27E38 8905	-	1114' 1138.5	1158	120	230'	97
25	1425	1429	1500	1b	N28E39 8905	1418	1429.5	1520'	137	843	98
25	1720	1728	1740	1n	N27E37 8905	-	1733	1810	179	106	99
25	2132E	-	2157D	1n	N28E36 8905	2112	2119'	-	250	130'	100
26	0654	0700	0720	1n	N26E30 8905	0644.5	0701	-	128	247	101
26	0918	0921 0940	0955	1n	N13E36 8907	-	-	0946	116	-	102
28	1130E	1136*	1150	1n	N17E33 8911	1133	1138	1146	84	85	103
28	1849	1854	1910	1n	N12E02 8907	1851.5	1854	1913	135	44	104
29	0242	0246	0320	1b	N16E19 8911	-	0244.5	-	95	112	105
29	0402	0432	0511	2n	S26W63 8901	-	0436	-	95	130	106
30	0508	0513	0532	1b	N24W27 8905	0508.5	-	-	106	-	107
30	0615E	0620	0700D	2b	N26W29 8905	0618.5	0627.5	0645	116	390	108
30	1410	1417	1445	1b	N15W10 8907	1408	1419	1450'	84	190	109
30	1555	1601	1615	1b	N13W07 8907	1556	1603	1612	95	119	110

TABLE 4.1 (Continued)

Date	Hα Flare Data					E(8,12) Burst Data					No.
	Start	Max.	End	Imp.	Location	Start	Max.	End	Base	Ampl.	
					July 1967 (Concluded)						
30	1612	1635	1654	1n	N26W36 8905	1613	-	-	95	-	111
31	0808	-	0850	1n	N25W42 8905	0808.5	-	-	63	-	112
31	0855	0857	0920	1n	N13E11 8913	0855	0900	0939	73	169	113
31	1115	1120	1200	1b	S24E35 8914	1115.5	1124	-	63	126	114
31	1225	1228	1250	1b	N23W44 8905	1225	1228	1242	73	129	115
31	1950	2004	2040	1n	N27W45 8905	-	2005	2045	73	228	116
31	2047	2114	2140	1b	N23W50 8905	2048	-	-	73	-	117
					August 1967						
1	1721	1738	1810	2b	N27W62 8905	1725	1739.5	-	63	930	118
2	0043	0048	0102	1n	N26W58 8905	-	0049	-	63	913	119
2	1516	1522	1544	1n	N20W06 8913	1513.5	1521	1545	71	65	120
3	0918	0920 0930	0950	1b	N27W85 8905	0917.5	0922.5 0933	-	73	516	121
6	1433	1449	1520	1n	S23E75 8926	-	1449.5	1540'	84	268	122
9	0812	-	0930	1n	N25W38 8916	0807.	0841	-	33	30	123
9	1758	1813 1830	1930	2b	S24E32 8926	1755	1811.5	-	31	-	124
12	1547	1610	1720	2n	S24W06 8926	-	1612	1745	35	202'	125
15	2138	2145	2205	1n	S23W28 8929	-	2145.5	2230	32	25	126
17	1206	1214	1245	1n	S22W77 8926	-	1214	-	63	159	127
18	0043E	0046	0130	1n	N08W17 8941	-	0046	0150'	73	620	128
18	1955E	1958 2026	2050	1n	N24E87 8942	-	2027.5	-	106	419'	129
18	2131	2138	2156D	1n	N26E90 8942	-	-	2355'	300	2163"	130
19	0530E	-	0620D	1b	N16E85 8942	0530'	0616	-	125	501	131
20	0025	0026 0037	0048	1n	N22E79 8942	-	0040	0048	84	-	132

TABLE 4.1 (Continued)

Date	Hα Flare Data					E(8,12) Burst Data					No.
	Start	Max.	End	Imp.	Location	Start	Max.	End	Base	Ampl.	
					August 1967 (Concluded)						
21	0057	0110	0140	1n	N15E54 8942	0107	0116	-	73	43	133
21	1830	1844	2000	2n	N23E48 8942	1817.5	1857	-	95	255	134
22	0156	0206	0255	1n	N22E52 8942	-	0210.5	0259	63	116	135
23	0515E	-	0540	1b	N23E36 8942	0514	0522	0546	63	289	136
23	1016	1020	1040	1n	N25E32 8942	-	1024	1042	73	81	137
24	0957	-	1012	1n	N23E21 8942	0955.5	-	1022	63	-	138
25	0625	0630	0700	1n	S20E11 8949	-	0631.5	0710	53	152	139
26	0014	0023	0108	1b	S19E00 8949	0012.5	0025	-	53	460	140
26	0940	0947	1022	1n	N22W05 8942	0938	-	1012	73	-	141
26	2101	2111	2140	1n	N13W06 8942	2059.5	2116	2148	95	122	142
28	1402	1404 1414	1430	1n	S22W32 8949	-	1415	-	73	177'	143
29	1330	1335	1444	2b	N22W46 8942	1328.5	-	-	146	-	144
29	1942	1948	2020	1b	N22W50 8942	1942	1946 1950	-	73	467	145
29	2036	2053	2135	1b	N22W50 8942	2037	2055	-	84	506	146
30	0020E	0030	0122	1n	N22W52 8942	0007	0034'	0128	79	241'	147
30	0458	0503	0528	1b	N24W53 8942	0453	0505.5	-	84	328	148
31	0826E	0827	0840D	1n	N17W71 8942	0825	0827.5	-	63	267	149
					September 1967						
1	0810	0810*	0830	1n	N23W85 8942	0806.5	0820	-	73	64	150
1	0911	0928	0934D	1n	N22E63 8961	-	0928'	-	73	43'	151
2	2030	2040	2105	1n	N27E23 8957	2036	2042.5	-	53	383	152
10	1156E	1215 1318	1338	1n	N25W33 8963	1129	1215	-	29	154	153
11	1323	1328	1340	1f	N22W87 9861	1321	1334	-	27	12	154
17	1050	-	1200D	1n	N18W38 8973	1047	-	-	27	-	155

TABLE 4.1 (Continued)

Date	Hα Flare Data					E(8,12) Burst Data					No.
	Start	Max.	End	Imp.	Location	Start	Max.	End	Base	Ampl.	
					September 1967 (Concluded)						
18	2316	2344	2545	2b	N16W60 8973	-	2350'	-	30	400'	156
28	0338E	0342	0407	1n	N19E55 9002	0328	0341.5	-	44	30	157
28	1127	-	1245	2n	N14E41 8999	-	1158	1330'	35	103'	158
30	1300E	1305	1345	1n	N17E17 8999	1245	1319	-	29	55	159
					October 1967						
1	0935E	0955*	1035	1n	N12E03 8999	0932	0957	-	53	63	160
2	0756	0758	0815	1n	N16W34 8998	0754	0758.5	-	24	114'	161
2	2151	2154	2212	1n	S20E46 9006	-	2158	-	25	113'	162
4	0600	-	0633	1n	N17W31 8999	0554	0609	0643	33	30	163
5	1040	1044	1110	1n	S18W22 9004	1036	1045.5	-	28	56	164
6	1102	1103 1116	1130	1n	S18W36 9004	-	1116.5	-	26	112	165
6	1218	1225	1245D	1n	S17W37 9004	-	1236	-	39	211	166
8	2029	-	2106D	1n	S17W69 9004	2000	-	-	23	-	167
14	2120	-	2225	1n	N17W49 9018	2113	-	-	29	-	168
20	0004	0009	0035	1b	N16E27 9032	0003.5	0010.5	0107	28	287	169
20	0225	0228	0240	1n	N16E25 9032	-	0234	0259	30	43'	170
20	1050	1114	1138	1n	N17E21 9032	-	1115	-	25	38'	171
21	1945	2005	2035	1n	N14E58 9037	-	2006	2048	20	33	172
22	2211	2218	2310	1b	N10E15 9034	2207	2219'	-	30	320'	173
24	0740	0750	0820	1n	N20E29 9037	0724	0750	-	41	43	174
24	2014E	-	2200	1n	S21W01 9035	2014	-	-	30	-	175
25	1327E	1335 1350	1445	1n	N09W24 9034	-	1355	-	44	83'	176
25	2312E	2328	2400	1b	N10W28 9034	2307.5	2331	2432	84	406	177
26	1012	1015	1030	1n	N10W42 9034	-	1016.5	1041	116	104'	178

TABLE 4.1 (Continued)

Date	Hα Flare Data					E(8,12) Burst Data					No.
	Start	Max.	End	Imp.	Location	Start	Max.	End	Base	Ampl.	
					October 1967 (Concluded)						
29	2347	2351 2414	2500D	2b	N10W90 9034	-	-	2558	125	1294"	179
31	1124	1130	1200	2n	S19E21 9047	1121	1132	1200'	53	190'	180
					November 1967						
2	0852	0856	0914	2b	S18W02 9047	-	-	0918	32	-	181
2	1141	1210 1232	1250	1n	N20W59 9041	1121	-	1317'	30	-	182
3	1159	1210	1240	1n	N18W76 9041	-	1214	-	30	417'	183
4	1151	1154	1220	1b	S18W33 9047	-	-	1240	53	-	184
5	0900	0906	0945	1n	S25W41 9053	0854	0908.5	-	36	34	185
5	2234	2238	2253	1n	S18W48 9047	2209	2237.5	2340	29	34	186
10	0853E	0855*	0913	1b	S26W78 9047	0851	0901.5	-	36	305	187
10	1317	1330	1410	1n	S26W82 9047	-	1344	-	73	159	188
10	1517	1530	1540	1f	S26W84 9047	1526	1531.5	-	63	126	189
10	2130	2133	2140	1n	S25W83 9047	2130.5	2135	2149	146	54	190
13	1808	1816	1900	1f	N11E74 9073	1757	1818	1936	30	149	191
16	1002	1011	1100D	2n	N10E38 9073	0951.5	1012.5	-	42	228	192
17	0817	0821 0840	0935	1b	N10E26 9073	0818	0838	1009	38	448	193
27	1602E	1610	1625	1f	N25W53 9093	-	1613	1634	44	29	194
29	1852	1902	1912	1f	S29W54 9091	-	-	1921	53	-	195
					December 1967						
1	0335E	0345	0416	1n	S27W70 9091	0304	0339.5	0448	189	951	196
1	1250	1252 1304	1315	1b	S28W75 9091	1247.5	-	-	127	-	197

TABLE 4.1 (Continued)

Date	Hα Flare Data					E(8,12) Burst Data					No.
	Start	Max.	End	Imp.	Location	Start	Max.	End	Base	Ampl.	
					December 1967 (Continued)						
1	1932	1947	2014D	1n	S27W82 9091	-	1946	-	95	21	198
4	1302E	1310	1326	1b	S19W90 9088	1301	1312	-	53	85	199
11	2154	2200 2215	2235	1b	N14W48 9101	2149	2200	-	30	-	200
13	0051	0056	0108	1n	N12W64 9101	0047	0057	-	39	213	201
13	0332	0338	0341D	2f	N12W65 9101	0331.5	0337	0408	37	248	202
13	0851	0856*	0905	1n	N13W70 9101	0852	0858	-	39	291	203
16	0941	0944 0956	1030	1n	N20E13 9115	-	0944	-	100	315'	204
16	1251	1255	1300	1n	N19E11 9115	-	1255	1311	106	51	205
17	0440E	0441	0457	1n	N18E03 9115	-	0444.5	0515'	125	268'	206
17	0643E	0646 0702	0750	1b	N19E02 9115	-	0647 0705'	-	137	563'	207
18	0242	0259	0320	1n	N19W11 9115	-	-	0350'	150	-	208
18	1015E	-	1030D	1n	N19W19 9115	1001	-	-	147	-	209
21	0910	0914	0940	1b	N26E04 9118	0911.5	0917	0940'	116	52	210
22	1315	1320	1330	1n	N17W70 9115	-	-	1400'	95	-	211
23	2101	2106	2200	1n	N25W19 9118	-	-	2203	84	-	212
26	0611	0627	0714	1n	S16E14 9128	0547.5	-	-	73	-	213
26	1304E	1309	1325	1n	S14E80 9132	-	1310.5	-	147	138	214
26	2023	2027	2045	1n	S15E73 9132	2020'	2030'	-	100	170'	215
27	0838	0843 0905	0920	1n	S17E59 9132	0838	0847 0853 0909	-	73	211	216
27	1942	1948 2008	2055	1b	S16W09 9128	1940.5	1949	-	84	212	217
28	0218	0223	0304	1b	S17W12 9128	0217.5	0227	-	84	180	218
28	1335	-	1530	1n	S21W19 9128	1336	-	1530	75	-	219

TABLE 4.1 (Continued)

Date	Hα Flare Data					E(8,12) Burst Data					No.
	Start	Max.	End	Imp.	Location	Start	Max.	End	Base	Ampl.	
					December 1967 (Concluded)						
29	0047	0050	0100	1n	S27W78 9120	0046	0050.5	-	73	362	220
29	1120	1122	1135	1b	S15W28 9128	-	-	1137	73	-	221
29	1144	1149 1200	1225	1n	S14E31 9132	1146.5	1149 1206.5	-	73	47	222
					January 1968						
2	0519	0531	0545	1b	S22E89 9145	0520	-	-	168	1912"	223
3	1524	1530	1543	1n	S22W41 9133	-	1535	1619'	100	164'	224
4	1719	1721* 1724*	1735	1n	N21E49 9144	1716	1723 1729	-	137	193	225
5	0210	0217	0240	1n	N20E49 9144	-	-	0326	116	-	226
5	0458	0459	0504	2b	N12E72 9146	0457	0502.5	-	106	434	227
6	0619	0622	0641	1b	N11E64 9146	0613.5	0623	-	137	338'	228
7	2153	2157	2227	1b	S22E13 9145	2152.5	2201	2226'	146	454	229
8	2209	2218 2232	2335	1n	N23E67 9153	2212.5	-	2340	106	-	230
9	0507	0511	0530	2n	N09E26 9146	-	-	0548	95	-	231
11	1659	1701 1708	1728	1b	S25W38 9145	-	1705	-	100	643'	232
12	1807	1811	1832	2b	S25W53 9145	1807.5	1813.5	-	73	476	233
14	0040	0046	0120	1n	N12W47 9146	0040	0052	-	95	137	234
14	2400	2407	2435	2b	N17W44 9146	2400.5	2410	2434	73	749	235
17	0430	0436	0442	1n	N16W80 9146	0436.5	0437.5	0440	95	11	236
17	1228	1232 1245	1300	1n	S16E85 9171	-	-	-	127	183'	237
18	0616	0619	0632	1b	S14E77 9171	0617	0619	0630	62	127	238
18	1514	1525	1600	1n	S15E70 9171	-	1530	-	73	372'	239
20	0113	0117 0124	0134	2n	N27W90 9153	0114	0120	0139	44	31	240

TABLE 4.1 (Continued)

Date	Hα Flare Data					E(8,12) Burst Data					No.
	Start	Max.	End	Imp.	Location	Start	Max.	End	Base	Ampl.	
					January 1968 (Concluded)						
20	0317	0319	0329	1n	S16E50 9171	0316	0320.5	-	43	73	241
22	0440	0445	0515	1b	S20W23 9167	0437	0446.5	-	36	70	242
28	0840	0844	0950D	2n	N15E35 9184	0839.5	-	-	158	267'	243
29	0801	0807	0850	1b	N14E32 9184	-	0813	-	116	685'	244
29	1537	1540	1558	1b	N14E28 9184	-	-	1606	95	-	245
30	0503	0506	0525	1n	N21E42 9188	0501	0506.5	-	95	1205'	246
30	1603	1608	1652	1n	N23E37 9188	-	1620'	-	116	127'	247
30	2006	2022	2045	1n	N13W04 9184	-	-	2110	116	127'	248
31	1920	1923	1937	1n	N11E77 9196	1920	1928'	1939	127	-	249
					February 1968						
1	0925	0930	1030	1n	N12W24 9184	0928'	0949	-	243	243	250
1	1058	-	1200	1n	N15W24 9184	1055.5	1132	-	236	364	251
1	1613	1618 1629	1649	1n	N17W26 9184	1614	1623	-	139	-	252
1	1915	1920	2005	1n	N16W16 9184	1916	1920	-	159	541'	253
1	2042	2044 2052	2110	1f	N13W32 9184	2043	2056.5	-	212	99	254
2	0915E	0921*	0935	1n	N10W38 9184	-	0923.5	0944	150	348	255
2	1030E	1103	1130	2b	N13W37 9184	-	1107	-	175	471'	256
2	1256	1303	1322	1b	N17W29 9184	1257	1308	-	243	193	257
8	1823	1827	1832	1n	S17E85 9206	1824.5	-	1857	62	-	258
10	1615E	1617 1628	1636D	2n	S17E57 9206	1606	1630	-	62	319	259
10	1915	1917	2000	1n	N20E45 9204	-	1931.5	2016	95	588	260
12	0758	0803	0843	1n	N17E22 9204	0755.5	0804	-	44	103	261
15	0034	0041	0120	1n	N20W10 9204	0027.5	-	-	40	-	262

TABLE 4.1 (Continued)

Date	Hα Flare Data					E(8,12) Burst Data					No.
	Start	Max.	End	Imp.	Location	Start	Max.	End	Base	Ampl.	
					February 1968 (Concluded)						
15	1450	1508 1524	1540D	1b	S14W11 9206	1449	-	-	36	-	263
15	1809	1828	1855	1n	N15W24 9204	1803.5	-	-	44	-	264
16	2008	2015	2100	1b	S27E03 9211	-	2019	2100	40	-	265
17	0252	0254	0313	1b	N17W47 9204	0250	0257	0319	39	266	266
17	0928	0934	0943	1n	N05E67 9216	0920	0936	0950	38	100	267
17	1254	1255	1312	1b	N07E65 9216	1255	1258.5	-	35	236	268
17	2345	2351	2420	1n	N17W54 9204	2343	2358	-	31	97	269
18	1055	1110	1135	1n	N25W14 9209	1102.5	1111	1131	44	29	270
18	1422	1424 1443	1500	1f	N19W61 9204	1423.5	1437	-	62	33	271
19	1520	1526	1550	1n	N17W77 9204	1518	-	-	44	-	272
21	0707	0714	0800	1n	S28E32 9218	0709	0738	-	73	138	273
26	0623E	0625	0642D	1n	S25E23 9224	-	0629	0702	73	177	274
26	0817	0822	0840	1n	S26E23 9224	0815.5	0823.5	0845	73	191	275
26	1654E	1657 1706	1724	1n	N12W90 9226	1619.5	-	-	84	-	276
					March 1968						
13	0644	0646	0655	1n	N29E80 9267	0638	0647	-	28	119	277
15	1111E	1123*	1207	1n	N29E51 9267	-	1126	-	22	73'	278
22	0543E	0543	0556	1n	N10W06 9281	0525	0545	-	32	63	279
24	1635	1645	1735	1b	S12W02 9273	1633.5	1647	1833	53	412	280
25	1442	1449 1507	1600	1b	S12W14 9273	1444	1452 1507.5	-	40	435	281

TABLE 4.1 (Concluded)

Date	Hα Flare Data					E(8,12) Burst Data					No.
	Start	Max.	End	Imp.	Location	Start	Max.	End	Base	Ampl.	
					March 1968 (Concluded)						
27	1133E	1140*	1155	1n	N18E44 9286	1135	1142	1152	53	31	282
28	0321	0329	0400	1n	S15W51 9273	0322	0337	-	62	75	283

maximum for each X-ray burst are measured to the nearest 1/2-minute; other times are to the nearest minute. All are given in Universal Time (UT). The standard notation E (or D) implies that the event started before (ended after) the time listed. The flare's importance is indicated by means of the present I.A.U. (International Astronomical Union) scheme which rates its area on a scale 1 to 4, as shown in Table 4.2, and the intensity of its brightest point as f (faint), n (normal), or b (bright). The location of the flare is given by its mean heliographic coordinates and the McMath serial number of its plage region. All Hα flare data were taken from the Quarterly Bulletin, except when that source did not give a time of maximum. In such cases, the value given by the SGDB was used if the individual reports of maximum were in agreement to the author's satisfaction. These are marked by * in Table 4.1.

TABLE 4.2

CLASSIFICATION OF FLARE AREA

Class	Corrected Area (millionths of hemisphere)
S	< 100 (subflare)
1	100 - 250
2	250 - 600
3	600 - 1200
4	> 1200

In addition to the timing values for the associated X-ray events, the table includes information on the E(8,12) base fluxes and burst amplitudes, both in units of 10^{-4} erg/cm^{2}sec. The base flux (not to be confused with the daily base-level $E_b(8,12)$ defined in Chapter III) is an estimate of the nonburst com-

ponent of E(8,12) at the time of burst maximum, and is usually taken to be the flux value just prior to the onset of the event. This quantity will be referred to hereafter as $E_B(8,12)$. The burst amplitude $\Delta E(8,12)$ is defined as $E_P(8,12)$ minus $E_B(8,12)$, where $E_P(8,12)$ is the total flux at the peak of the X-ray burst. Whenever an event has more than one maximum, the tabulated value of $\Delta E(8,12)$ refers to the largest amplitude. In all cases, the symbol ' means that a measurement is somewhat uncertain. The last column of Table 4.1 lists an identification number for each event of Catalog II.

Three exceptions were made to the screening procedure described above. Flares #136 and #148 of the table were included even though no photographic record of either event exists in the ESSA flare-patrol network. However, both flares were reported by all the observatories which were monitoring the sun at the time (a disappointingly rare occurrence) and the internal agreement among the various reports for each flare was good, indicating that the time development of these two events was clearly marked. The third case, flare #202, was included because it is the only example during the period studied of a flare with an importance rating of 2f which might be considered valid. This event was reported by just one station, Mitaka (Tokyo), which was the only station monitoring the sun at the time. Furthermore, it was recorded by cinematography, the most reliable flare-patrol technique. Therefore, the event was retained in this catalog, but with the explicit warning that it should be given little weight since it has not been properly verified.

For one flare, #55 in Catalog II, the importance rating was not taken from the Quarterly Bulletin. This great event on 23 May 1967, one of only about two

dozen flares ever observed in white-light (DeMastus and Stover, 1967; McIntosh, 1967), gave rise to the largest hard X-ray burst (Kane and Winckler, 1969) and soft X-ray burst (Van Allen, 1968) yet recorded, and was accompanied by one of the greatest solar radio bursts measured to date (Castelli et al., 1968a, 1968b). Although the Quarterly Bulletin lists the event as three separate 2b flares, Dodson and Hedeman (1969a) conclude that the most plausible interpretation of the Hα film record is that a single flare of importance 3b occurred which had three distinct phases. This evaluation is used to describe the event in Catalog II.

The 23 May 1967 flare also caused the greatest X-ray burst observed by the Michigan ion chamber, saturating the detector for over two hours. Even so, an estimate of $\Delta E(8,12)$ for this burst can be made by means of data from the University of Iowa's 2-12 Å detector aboard Explorer 35. There is an excellent relation between the 2-12 Å and 8-12 Å peak fluxes for bursts measured simultaneously by the Iowa and Michigan instruments, as shown in Figure 2-9 of Chapter II. Since the relation applies over a range of nearly two orders of magnitude, it seems unlikely that an extrapolation of another factor of 10 would be too much in error. On this assumption, the relation derived from Figure 2-9 was used with the Iowa measurement of the peak 2-12 Å flux to determine $E_p(8,12)$ for the 23 May 1967 burst. Then, subtraction of the observed 8-12 Å base flux gives the value of $\Delta E(8,12)$ which is listed in Catalog II for this event.

The identical procedure was used to find the approximate $\Delta E(8,12)$ for six other events which saturated the Michigan detector: #7, 53, 63, 130, 179, and 223 in the catalog. The burst on 6 May 1967 (#42) also saturated the instru-

ment, but for such a short period of time that its peak flux could be estimated easily by inspection. (This X-ray burst is shown in Figure 2-2 of Chapter II.) The resulting values of $\Delta E(8,12)$ for all of the events just discussed are marked by the symbol " in the catalog to indicate that they were not measured directly.

3. CHARACTERISTICS OF THE Hα FLARES IN CATALOG II

Several tests were made to investigate the possibility of bias in the selection of flares for this catalog. First, the frequency of occurrence N as a function of flare importance was considered, and the results are shown in Table 4.3 along with the "nominal" frequency distribution taken from Smith and Smith (1963). The latter distribution for given area classes is not significantly different from that found for the events of Catalog II. Unfortunately, no study has yet been made, to the author's knowledge, of this "nominal" distribution using the new I.A.U. classification scheme.

TABLE 4.3

FREQUENCY DISTRIBUTION WITH FLARE IMPORTANCE

Flare Importance	This Study N	This Study %	Smith and Smith %
1f	14	4.9	
1n	172	60.8	
1b	63	22.3	
1 (all)	249	88.0	78.6
2f	1	0.4	
2n	15	5.3	
2b	15	5.3	
2 (all)	31	11.0	19.2
3n	2	0.7	
3b	1	0.4	
3 (all)	3	1.1	2.2

Next, the number of cataloged flares occurring in the northern or southern hemispheres and eastern or western hemispheres was investigated. The results are given in Table 4.4, which also includes the probability P (derived from Chi-squared tests) that the observed north-south or east-west differences in flare occurrence are significant. For sunspots, an east-west asymmetry has been known since Maunder's (1907) early study, but apparently none exists for flares in general (Smith and Smith, 1963). Thus, the occurrence of events in Catalog II is not clearly atypical, since there is a large likelihood that its east-west difference (opposite in sense from the sunspot's east-west asymmetry) is due purely to chance. On the other hand, the north-south asymmetry of the cataloged events is very striking and is almost certainly a real effect; but this is not unexpected. Behr and Siedentopf (1952) have shown that in both sunspot and flare occurrence there is a definite north-south asymmetry which changes sense pseudo-periodically with the solar cycle. During the interval covered by the present study, the sun's activity was clearly concentrated in its northern hemisphere, and Catalog II merely reflects this effect. In fact, Dodson and Hedeman (1969b) report that the north-south asymmetry in solar activity was stronger at the start of solar cycle 20 (1964-1966) than at the onset of any other solar cycle in the past 100 years.

TABLE 4.4

FREQUENCY DISTRIBUTION WITH HEMISPHERE OF OCCURRENCE

Hemisphere	N	%	P
North	196	69.3	>99%
South	87	30.7	
East	134	47.3	~60%
West	149	52.7	

One investigation of the catalog did reveal a bias, however. As mentioned earlier, the major motivation for constructing another catalog was that a disproportionate number of events in Catalog I occurred during European observing hours. Unfortunately, Figure 4-1 shows that the second effort did not completely eliminate this effect since the number of events in Catalog II which occurred between 0800 and 1359 UT is again significantly too large (more than 3σ above the mean). The effect cannot be attributed to the selection procedure described in Section IV-1, since it also exists for flare reports in general (Dodson and Hedeman, 1960). A more likely explanation is that European observatories may tend to assign a somewhat greater importance classification to a given flare than would their American counterparts, so that they may rate some events as importance 1 which would have been called subflares by observers in other parts of the world (Dodson and Hedeman, 1960; C. S. Warwick, 1965). This possibility will be discussed further in Section IV-6b.

4. CHARACTERISTICS OF THE SOFT X-RAY BURSTS IN CATALOG II

Catalog II was constructed as a list of well-verified Hα flares for which valid X-ray coverage by the Michigan ion chamber was available; there were no requirements as to the nature of that X-radiation. However, all but one of the listed flares were accompanied by a measurable E(8,12) enhancement in excellent time-relation to the optical event. This section considers some of the general characteristics of these X-ray bursts themselves, and following sections will investigate the relation of these bursts to other phenomena. But it must be emphasized again that these studies relate to a very special type of soft X-ray

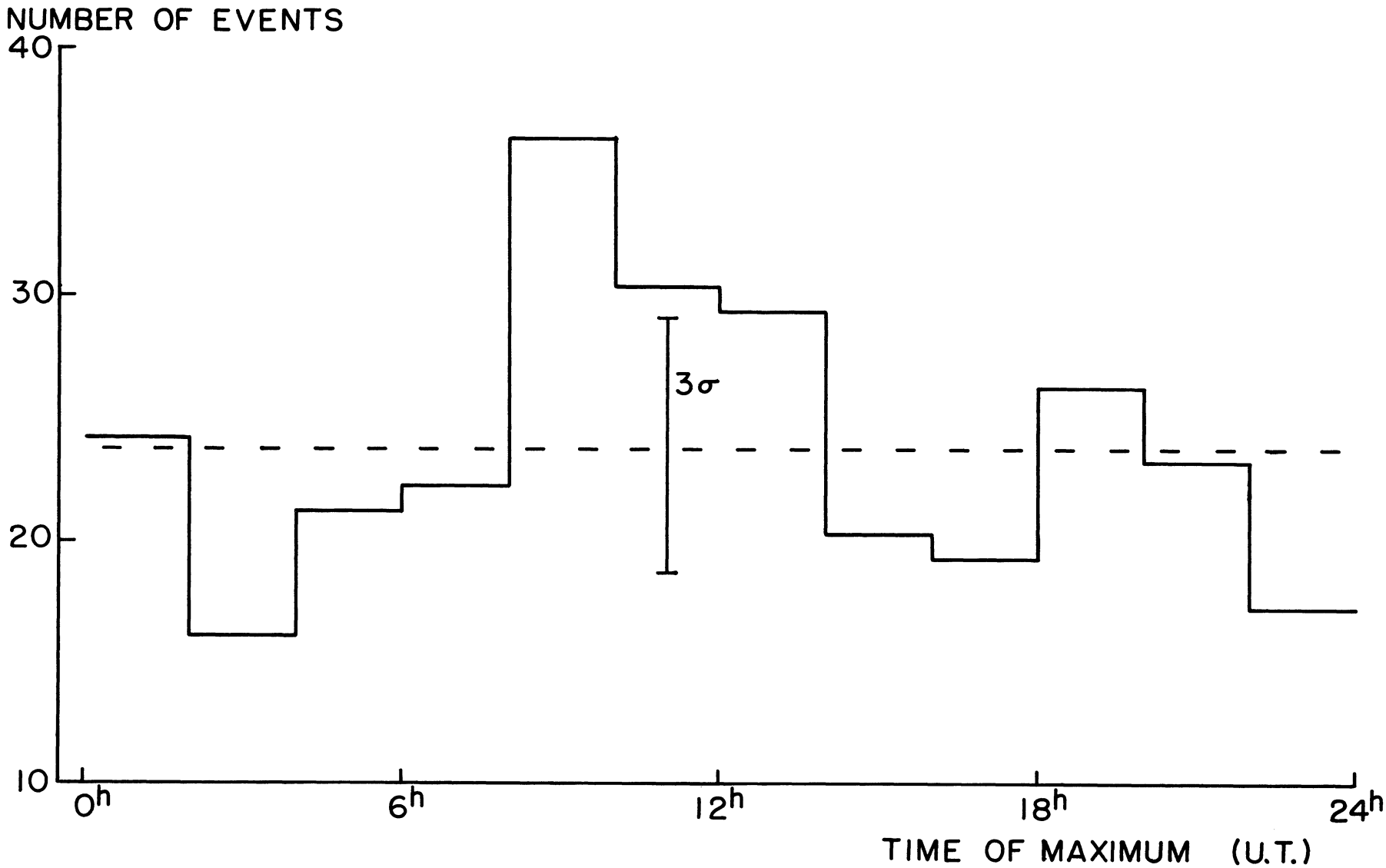

Figure 4-1. Frequency distribution of Catalog II flares with Universal Time. The mean frequency is indicated by the dashed line. The "Universal day" is divided into 12 two-hour blocks, and flare membership is defined by the time of the Hα intensity maximum. If more than one maximum is listed in the Quarterly Bulletin, the time of the first is used here. Note the significant excess of flares between 0800-1359 UT, the period when European observatories are monitoring the sun.

enhancement, one associated with an Hα flare of importance $\geq$ 1. The results found here may not necessarily apply to all X-ray bursts in general.

a. Occurrence of the Bursts

Many investigators have claimed that a substantial fraction of Hα flares of importance $\geq$ 1 are not accompanied by an enhancement of solar X-ray emission (Kreplin et al., 1962; Acton, 1964; Lindsay et al., 1965; Culhane et al., 1968; Culhane and Phillips, 1969; Hudson et al., 1969a). As just mentioned, the present study does not substantiate that claim. Of the 283 flares listed in Catalog II, only one (#88) had no measurable X-ray burst associated with it, and that event was marginal in many respects. It was rated importance 1f, the weakest type considered for the catalog, and occurred very near the solar limb, where importance ratings are most difficult to assign. It was reported by just two stations, Lockheed and Ikomasan (Japan), the only observatories monitoring the sun at the time of flare maximum, which was 2303 UT on 21 July 1967. Ikomasan is a visual station and reported merely that the event began before 2302 and ended after 2306 UT, although it was observing continuously before and after these times. This might indicate that the flare was very faint indeed. Therefore, the reports of this flare were not as well verified as one would like.

Furthermore, at the time of the event, the Michigan ion chamber was in its operating mode of low sensitivity, so that it could only detect changes in the solar X-ray flux of at least 95 x 10^{-4} erg/cm^{2}sec. Two other bursts in Catalog II had measurable amplitudes less than that value. But, even if event #88 is taken to be an example of a flare with no associated soft X-ray enhancement,

this study implies that at least 99% of flares of importance 1 or larger are accompanied by soft X-ray bursts. The failure of earlier investigators to find this result is undoubtedly due to their utilization of flare lists which include spurious reports, as suggested by Teske (1969a).

b. General Time-Profile Properties

Solar microwave bursts usually fall into one of two categories, normally called gradual rise and fall (GRF) and impulsive bursts (Covington and Harvey, 1958). This classification also applies to hard X-ray events (Kane, 1969), but the situation is not so clear for X-ray bursts at longer wavelengths. Some authors claim that such a distinction can be clearly made for soft X-ray events (Chambe and Sain, 1969), some find only slight evidence for it (Culhane et al., 1963; Culhane and Phillips, 1969), while others feel no such distinction exists (Drake, 1969). The resolution of this problem is of great importance because of the insight it would give into the physical characteristics of the solar X-ray emitting region. In the case of the microwave events, for example, it is generally agreed that the GRF bursts are thermal in nature, while impulsive bursts are due to nonthermal processes (e.g., Takakura and Kai, 1961, 1966; Holt and Cline, 1968).

Two semi-related parameters can be used to distinguish gradual events from impulsive ones: the time between the start and maximum of a burst Δt, and the mean rate of flux enhancement $\Delta E/\Delta t$. A total of 128 soft X-ray bursts in Catalog II were sufficiently well observed so that these parameters could be determined for them. The frequency distributions of events with various values of these parameters are depicted in Figure 4-2. Neither distribution shows any

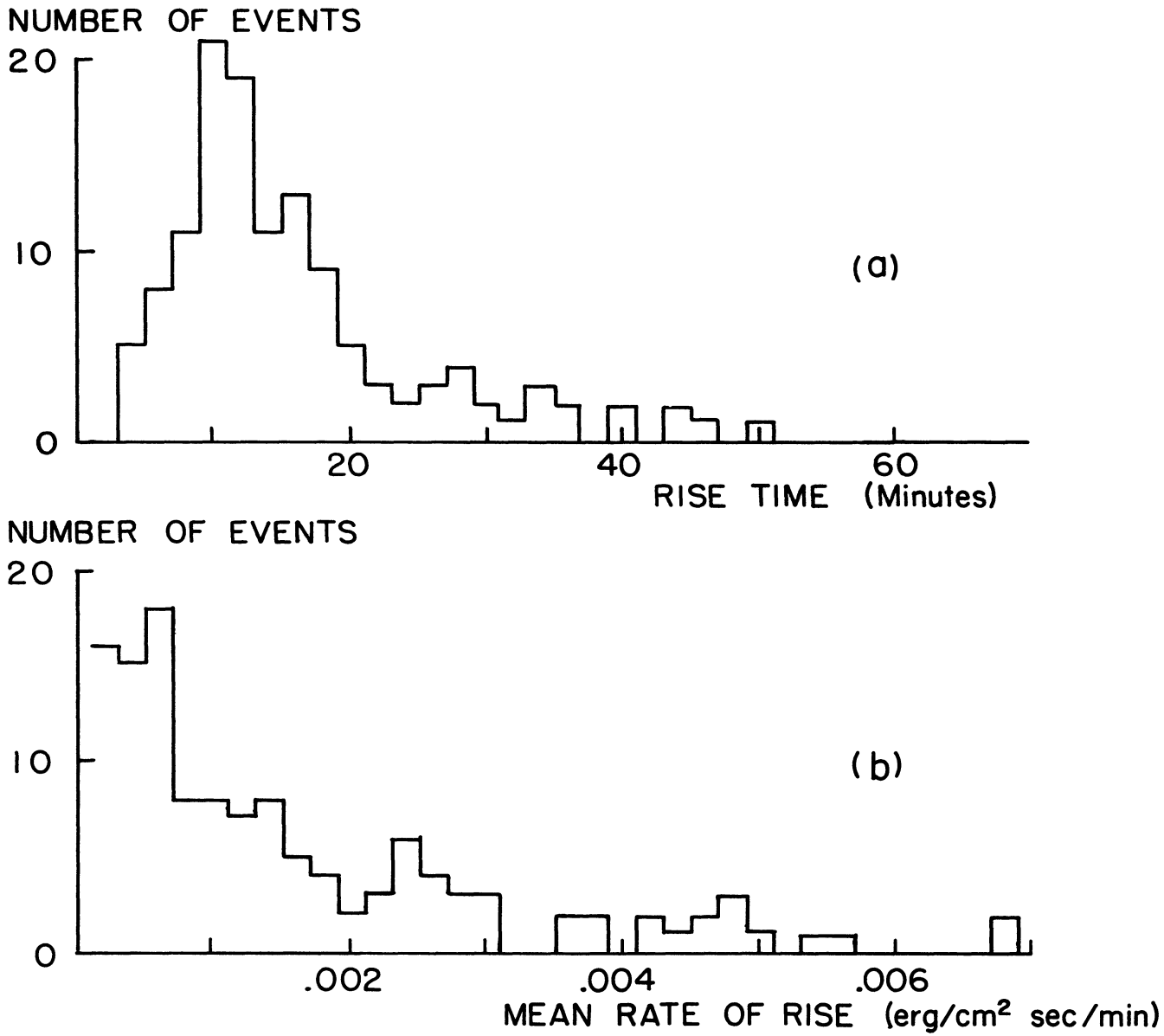

Figure 4-2. Frequency distributions of Catalog II bursts with (a) rise-time and (b) mean rate of E(8,12) rise. Neither distribution is bi-modal in character.

evidence for two distinct burst types, which suggests that all E(8,12) events can be considered of thermal origin. (The time-development is much too gradual on the average to assume that they are all nonthermal.) Yet another attempt to identify impulsive bursts in Catalog II is shown as Figure 4-3. This plot of the soft X-ray amplitude ΔE versus the rise-time Δt is essentially the same method originally used to distinguish the two types of microwave bursts (Covington, 1959). Again, no clear grouping occurs for the X-ray events considered here.

It must be pointed out once more that the list of X-ray bursts used in the present study is a very select one, consisting only of those which accompany well verified Hα flares. Thus, it is conceivable that the result found here does not apply to other soft X-ray bursts. But this does not seem to be the case, since it best agrees with Drake's (1969) investigation, the most extensive yet attempted, which includes over 2000 events observed during the period 2 July 1966 to 18 September 1968. DeJager (1965b), who first suggested that X-ray bursts be divided into "quasi-thermal" and "nonthermal" classes, also felt the majority of bursts observed at wavelengths longer than 1 Å should fall in the former category. Other theoretical investigations led to similar conclusions (Kawabata, 1963, 1966a; Kundu, 1964; Culhane and Phillips, 1969).

A possible explanation for the disagreement on this point among the observers mentioned earlier is that a relatively small, impulsive component is sometimes superimposed on the larger, more gradual soft X-ray burst (Donnelly, 1969b). Examples of such composite events have been recorded by the Michigan experiment (Figure 4-4), but they are infrequent. If this impulsive component

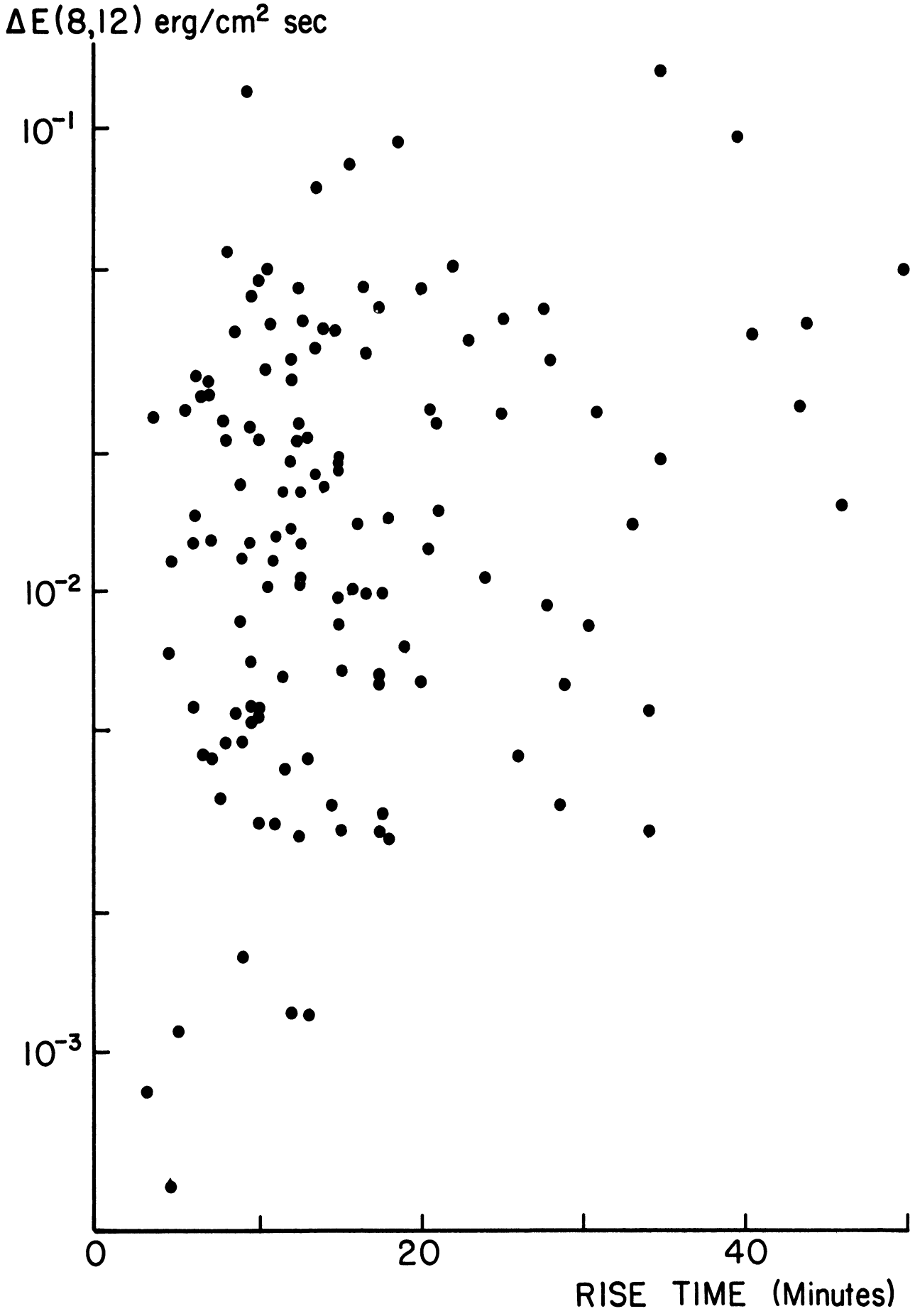

Figure 4-3. Scatter diagram of X-ray burst amplitude ΔE(8,12) versus rise-time for events of Catalog II. No evidence appears for distinct classes of soft X-ray bursts.

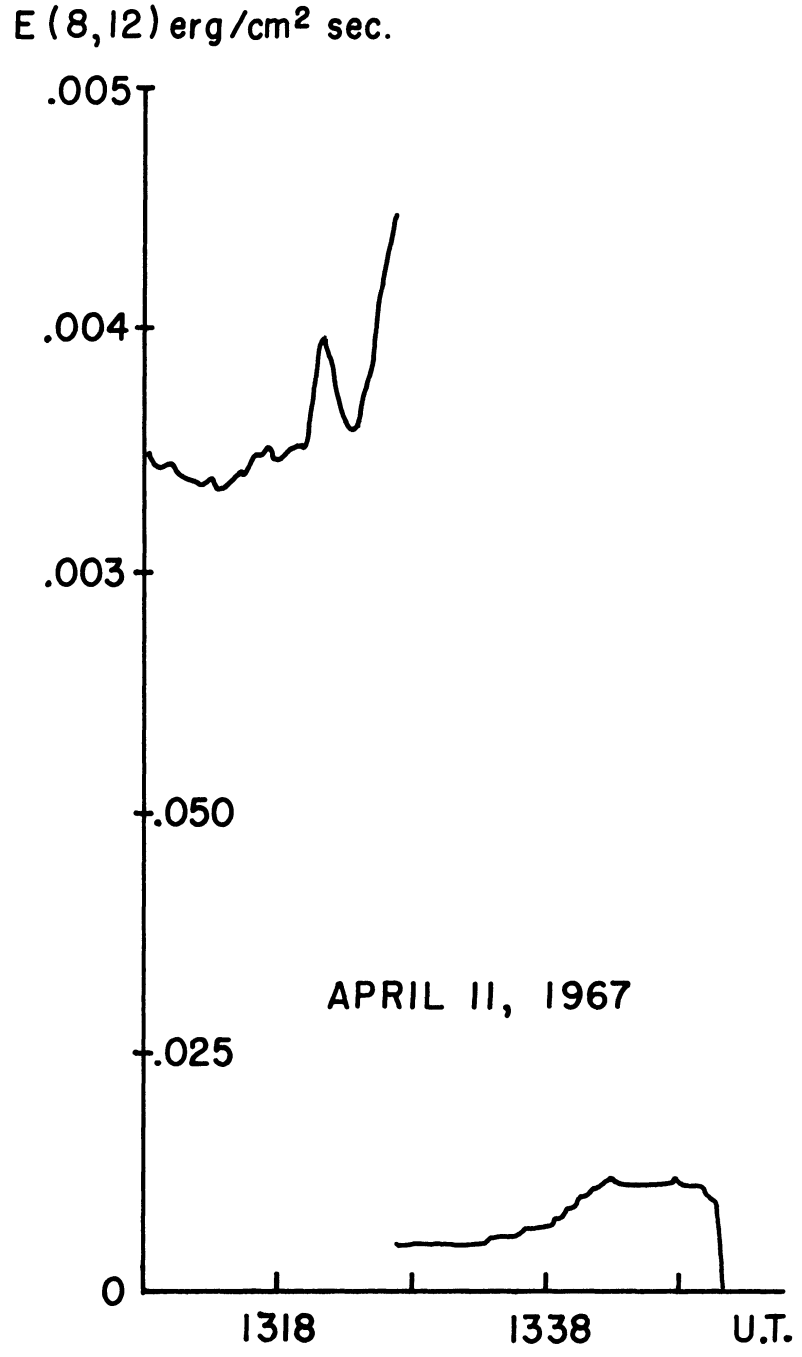

Figure 4-4. Time-profile of the soft X-ray burst on 11 April 1967. The Michigan detector switched its operating mode from high (flux scale on left side of ordinate axis) to low sensitivity (scale on right) at 1326 UT. Note the minor impulsive burst at about 1321 UT superimposed on the initial rising phase of the major event (#33 in Catalog II).

becomes stronger relative to the gradual component at shorter wavelengths (as observed by Kane, 1969), one can account for the above, apparently contradictory reports. In any case, it is clear that the soft X-ray bursts of Catalog II are almost exclusively thermal in character.

c. Mean Burst Durations

It is well known that the total durations of Hα flares depend upon their importance on the average (e.g., Waldmeier and Bachmann, 1959; H. J. Smith, 1962). Unfortunately, Catalog II is not extensive enough to permit a similar study for the X-ray bursts associated with these flares. Of the 60 bursts in the catalog which had observed beginning and ending times, 52 accompanied importance 1 flares. For these, the median burst duration is 33 minutes, somewhat longer than the median duration of 24 minutes found for importance 1 Hα flares in general (H. J. Smith, 1962). The typical "importance 1" X-ray burst is probably of even greater extent, however, because the above procedure systematically discriminates against longer duration events. The end-time for such a burst is much less likely to be identified since it has more chance of being contaminated by other events or lasting into the unobserved period during satellite-night.

Therefore, it is safe to say that the soft X-ray bursts have a greater duration than their optical counterparts on the average, a result which agrees with the observations of others (Acton et al., 1963; Lindsay, 1964; Paolini et al., 1968). With regard to the burst duration as a function of the associated flare's size, we can only state that our subjective opinion supports Teske's (1969a) claim that the X-rays tend to outlast the visible event for a length of

time which depends upon flare importance. As an example, the E(8,12) flux remained above its pre-burst level for more than two hours after the reported end of the great 23 May 1967 flare described earlier. This question should be reconsidered quantitatively in the future when more extensive data are available.

d. Accuracy of Source Position and Burst Amplitude

Although the Michigan experiment has no resolution of the solar disk, the location of each X-ray burst in Catalog II can be assigned with confidence to the position of its associated Hα flare. This follows, for example, from the exquisite X-ray photographs of the sun during a 1n flare (Vaiana et al., 1968) which show not only that the X-ray and Hα flaring regions are coincident, but also that their general structures are remarkably similar. There is some indirect evidence that an X-ray burst which does not accompany a flare can occur in a region devoid of any type of solar activity (Zhitnik et al., 1966), but no examples exist, to the author's knowledge, of a flare-associated X-ray burst which was not located at the position of the optical event.

It is also necessary to defend the reliability of the burst amplitude values listed in Catalog II. These values were derived on the assumption that the X-ray spectrum mimics that of a 2×10^6 K gray body and remains constant at all times. In reality, the X-ray spectrum during a burst bears little resemblance to that of a gray body (e.g., Neupert et al., 1969: shown in this paper as Figure 2-4) and the spectral distribution varies rapidly as the burst develops (Chubb et al., 1960; Pounds and Willmore, 1963; Friedman, 1964; Lindsay, 1964; Takao, 1967).

The analysis of this problem discussed in Chapter II implies that the Michigan results are only slightly affected by the poor choice of assumed spectrum. In the worst case, the relative error of E(8,12) appears to be about 30%. One of the strongest arguments for this point of view is the excellent relation between the peak fluxes of X-ray bursts as measured by the Michigan and Iowa experiments, two detectors with quite different spectral responses (Figure 2-9). Therefore, the burst amplitudes of Catalog II can be considered as reasonably valid as far as relative error is concerned. However, bear in mind that the absolute values of E(8,12) may be too large, perhaps by as much as a factor of 2 or 3. But this will not vitiate the qualitative aspects of the studies which follow.

5. TIME-RELATIONS BETWEEN Hα FLARES AND SOFT X-RAY BURSTS

The timing of X-ray bursts relative to other solar events is naturally of interest for the information it would offer about the mechanisms giving rise to those events. But such a study gains additional significance because of the possibility that a soft X-ray enhancement is the very first manifestation of a solar flare (Donnelly, 1968b). This possibility is of obvious importance to a flare early-warning system, for example, in future manned space applications. The time-relations between Hα flares and X-ray bursts have already been examined in some detail in Paper I (Teske and Thomas, 1969) using our first flare catalog. But, because of its importance, this investigation has been redone here with the more extensive list of events in Catalog II.

a. Starting Times

As in the study for Paper I, the starting time used for the Hα event is the earliest flare start-time reported by a cinematographic station, if one was observing, or the earliest reported by a photographic station otherwise. (In general, this will not be the time listed in Table 4.1.) This procedure is followed since some Hα brightening must have appeared on the film at that time even though it may have been so subtle that other observers overlooked it. Unfortunately, possible clock errors at the various flare-patrol stations cannot be taken into account. However, if such errors exist in significant degree, they would bias the results of the present study toward earlier relative starting times for the Hα flares.

The start-time of the X-ray burst is defined as that time when the E(8,12) curve first begins to rise, even though the increase may not necessarily be monotonic after that point. Since the flares in Catalog II were carefully screened to include only isolated events, any initial fluctuations which may occur in the X-ray burst are considered to be a part of a single comprehensive event as long as the flux always remains above the pre-burst level. (This point will be reconsidered later.)

The bursts were divided into groups depending upon whether they started when our detector was in its operation mode of high or low sensitivity. Also, bursts associated with flares occurring within 60° heliocentric of the solar disk center were considered separately from those associated with flares nearer the limb. The latter groups will be referred to as "center" and "limb" events, respectively. Table 4.5 shows the results of this study, which included a total

of 173 events. The average differences between start-times are given in minutes, and negative values mean that the soft X-ray burst starts first. The numbers in parentheses indicate how many events were considered in each average. Also listed is a "confidence" parameter P (calculated by Student's t-test), which shows the significance of the observed difference between two sample means. More precisely, 1.0 minus P gives the probability that a difference between two averages as large or larger than the one observed could have resulted by the random selection of values from two identical sample populations.

TABLE 4.5

MEAN DIFFERENCES BETWEEN Hα AND SOFT X-RAY STARTING TIMES

(All time differences are in minutes)

	Center	Limb	P
Low sensitivity	+0.2 (88)	+0.1 (39)	8%
High sensitivity	-3.4 (33)	-4.8 (13)	57%
P:	> 99%	97%	

One can see that there is probably no center-to-limb effect, at least not in the way these data have been divided. On the other hand, the results do show a marked dependence on the sensitivity of the detector. With the instrument in its low sensitivity mode, no advance warning whatsoever of the Hα flare is gained from the soft X-ray observations. Only the high sensitivity results show that the X-ray burst does indeed begin on the average significantly before the reported start of the flare. This finding suggests that the initial rise of the "average" soft X-ray burst is very gradual and of small amplitude for

the first few minutes. (This preliminary phase is called the X-ray burst precursor and will be discussed in more detail below.) Then the coincidence of start-times when the low sensitivity X-ray data are used implies that there is a stronger rise in flux at the instant the Hα flare begins. Both of these features are often clearly seen in the time-profiles of individual events. As an example, the burst on 17 June 1967 which accompanied a 1n flare (#76) is shown in Figure 4-5.

Although the soft X-ray burst seems to begin early on the average relative to the Hα flare, there is a wide variation in the individual values. The range found in this study extends from X-rays starting early by 28 minutes to X-rays starting late by 12 minutes; and even when the detector is in its high sensitivity mode of operation, about 30% of the X-ray bursts begin after the reported start-time of their associated flares. This great dispersion of values is undoubtedly responsible for the conflicting results of timing studies which are based on only a few individual cases (cf. Landini et al., 1965; Falciani et al., 1968).

b. The X-Ray Precursor

Counterparts to the precursor component described above have also been reported for 1-1.5 Å (Hudson et al., 1969a) and 3-4 Å bursts (Culhane and Phillips, 1969). The possible existence of such a "pre-burst" phase is of interest not only for the flare-warning system mentioned earlier, but also for the information it would give concerning the physical mechanism which initiates the entire flare phenomenon. Unfortunately, the analysis leading to its "dis-

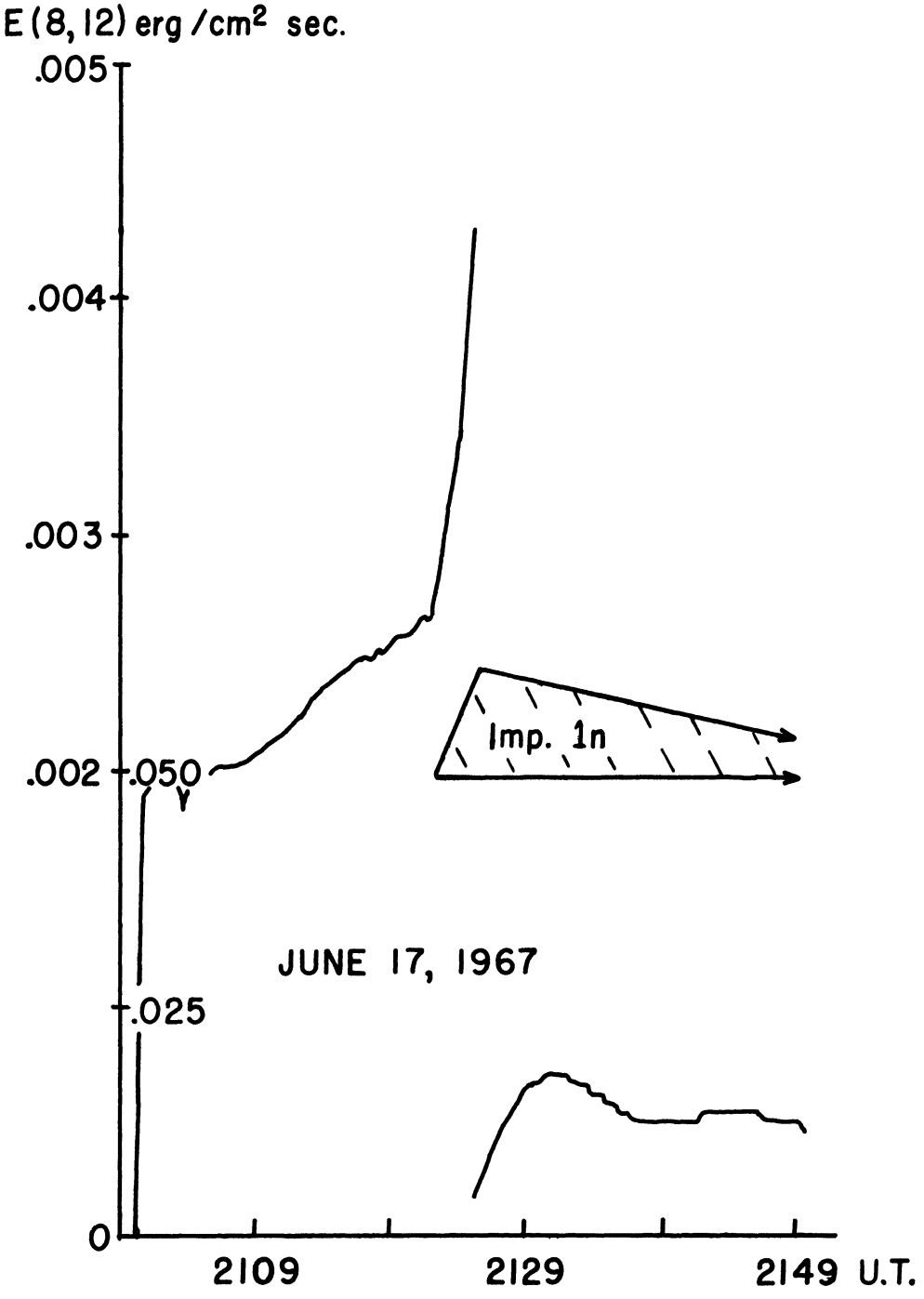

Figure 4-5. Time-profile of the soft X-ray burst on 17 June 1967 (Catalog #76). Note scale change at 2125 UT. The initial, very gradual rise in flux begins at 2106. A sharp increase in the rate of rise occurs at 2120, exactly coincident with the reported start of the Hα flare. A schematic representation of the flare's intensity development is also shown.

covery" contains two known sources of systematic error, at least in the case of 8-12 Å radiation.

The first involves the identification of the Hα flare's start, which was taken to be the earliest time reported by a cinematographic or photographic station in the present study. Cinematography offers the better time-resolution, but even so, filtroheliograms are normally made only once each 30 seconds. Furthermore, the observed flare start is given as the time of the first frame on which a visually detectable brightening appears. This combination of practices results in reported start-times which are consistently later than the "true" beginning of the event. In fact, photographic photometry indicates that the rapid-rise phase of an Hα flare may begin up to 1 to 1-1/2 minutes on the average before it is defined from a visual inspection of the film (Angle, 1968).

The second source of systematic error is the existence of E(8,12) enhancements which are not related to any reported optical events (Teske, 1967). These fluctuations may be due to subflares which are usually not reported by European observatories as a matter of course (Teske, 1969a); to flares which occur just beyond the limb (Teske, 1969b); or to still other sources. But whatever the cause of these flux variations, the Michigan detector's lack of spatial resolution makes it impossible to distinguish them from physically-connected components of flare associated bursts if the two should occur simultaneously. Although great care was taken to assure that the flares of Catalog II did not occur close in time to any other reported event, their X-ray bursts may still be contaminated by these background fluctuations. Thus, if a burst begins while such a flux enhancement is in progress, the start of the burst will be assigned mistakenly to the earlier start of the background fluctuation.

In order to estimate the influence of this systematic error on the mean start-time relation found in the previous section, the frequency and durations of such background fluctuations were investigated for the period of 10 March 1967 to 18 April 1967. Since the E(8,12) burst precursor normally appears just in data obtained by the detector's high sensitivity mode of operation (Section IV-5a), only these data were examined in detail, so that the total measured time came to 7371 minutes (called C hereafter). By determining the fraction of the test interval C affected by background fluctuations, one can calculate the amount of the average early rise given in Table 4.5 which is due to this effect.

If N(d) is defined as the number of such fluctuations with duration d occurring in the test interval, the fraction of this interval in which burst starting times would be misidentified by t or more minutes is given by:

$$x(t) = \sum_{d=t}^{\infty} (d - t) \cdot N(d)/C \qquad (4.1)$$

(Only integral values of d and t are considered for this study.) The fraction of the interval in which starting times would be assigned too early by exactly t minutes is then:

$$X(t) = x(t) - x(t + 1) \qquad (4.2)$$

Finally, the effect of background fluctuations accounts for y minutes in the average early rise-time of bursts occurring at random during the test interval, where y is given by:

$$y = \sum_{t=0}^{\infty} t \cdot X(t) \qquad (4.3)$$

The frequency distribution of N(d) for the time interval studied here is shown in Figure 4-6, and results in a value of y = 1.2 minutes. Since the interval 10 March 1967 to 18 April 1967 does not appear atypical, it seems reasonable to assume that this value can be applied to the relative start-time relations found for all Catalog II events. Thus, taking 1.2 minutes for the error caused by soft X-ray fluctuations and 1.5 minutes for the error due to the method of defining Hα flare start-times, we find that an E(8,12) burst begins just 1.1 minutes before its associated flare, on the average, if center and limb events are considered together.

The above analysis of the background fluctuations' effect assumes that they are not physically related to the flare event itself. Culhane (personal communication) points out another possibility: namely, that they are manifestations of a flare triggering mechanism which is not always successful. By this interpretation, all observed precursors are valid components of the total burst, and the average early rise of E(8,12) relative to the Hα flare thus becomes 2.3 minutes. The hypothesis also implies that two presumably independent conditions must obtain simultaneously in order for the total flare phenomenon to be initiated; first, the existence of the triggering agent (which always gives rise to a soft X-ray enhancement), and secondly, perhaps some metastable, high energy configuration of the potential flare source. Thus, if this suggestion is correct, a careful examination of plage regions during flare-producing and nonflare-producing precursors might indicate the active center configuration necessary for a flare event to occur. Such a study obviously merits future consideration.

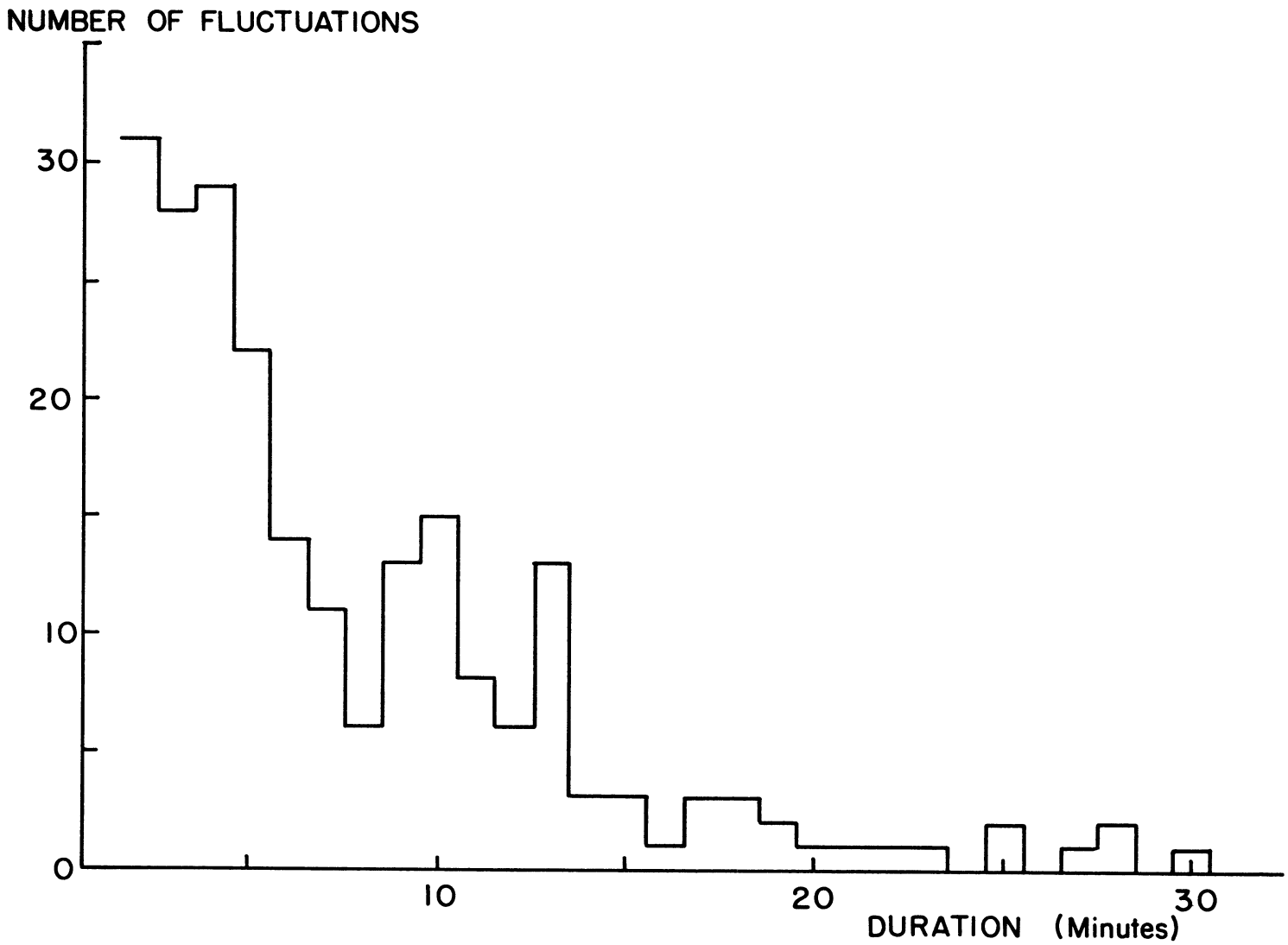

Figure 4-6. Frequency distribution of E(8,12) background fluctuations as a function of duration. Such fluctuations are soft X-ray enhancements which do not accompany any reported optical activity on the sun. This distribution refers to the 7371 minutes of high-sensitivity data recorded by the Michigan detector between 10 March 1967 and 18 April 1967.

In any case, the present study shows that the pre-flare warning provided by 8-12 Å X-rays is much shorter than previously believed, and that it exists only in a statistical sense even if high sensitivity data are used. Furthermore, the relatively frequent background fluctuations closely mimic the initial "early-rise" phase of flare-associated bursts. A soft X-ray monitor therefore appears somewhat less attractive as a flare-alarm device than first indications implied. But it is probably still the best technique available for at least three reasons (Friedman, 1964; Pounds, 1965a; Donnelly, 1968b):

(a) the soft X-ray enhancement is indeed one of the first known manifestations of the flare phenomenon on the average,

(b) soft X-ray bursts exhibit large percentage increases over the base-level flux of the total solar disk, thus permitting a simple patrol of the entire visible hemisphere, and

(c) a solar X-ray monitor is capable of very high time resolution.

An additional advantage is the fact that such relatively inexpensive X-ray monitors can be carried aboard polar-orbiting satellites, which would then allow completely continuous, "all-weather" coverage of solar activity by a single instrument, a truly noteworthy goal.

c. Maximum and Ending Times

The time-relations for the maximum and ending phases of the events in Catalog II have also been determined in a manner similar to that described in Section IV-5a. The results are shown in Table 4.6, where the terms "center" and "limb" and the confidence parameter P are defined as before. Here, the positive values mean that the relevant X-ray burst times all occurred <u>after</u>

their counterparts in the average Hα flare's intensity profile. No separation into sensitivity ranges was considered for the timings at maximum since these bursts almost invariably caused the detector to switch into its low sensitivity mode at their peak. Some events remained at their peak flux for several minutes, and in these cases the time of maximum used was one minute after the flux first reached this value. Thus, the difference of about 3 minutes between the times of Hα and X-ray maximum might actually be a slight underestimate of the true delay. It appears to be quite rare for the X-ray burst maximum to precede the peak intensity of the Hα flare; this occurred in only 5% of the events studied here.

TABLE 4.6

MEAN DIFFERENCES BETWEEN Hα AND SOFT X-RAY MAXIMUM AND ENDING TIMES

(All time differences are in minutes)

	Center	Limb	P
Times of Maximum	+ 3.6 (160)	+2.3 (71)	96%
Times of End	+13.9 (75)	+9.6 (31)	80%

The fact that the X-ray burst clearly reaches its maximum well after the Hα intensity peak may necessitate the reevaluation of some ionospheric parameters derived from SID studies. Mitra (1965) points out that such studies normally assume that the ionizing radiation (principally X-rays below 20 Å) follows the same time curve as the Hα flare's intensity, and in particular that their times of maximum are identical. The present results show that this assumption is incorrect.

The ending time for an X-ray burst is often difficult to identify correctly, and the difficulty may be even greater in the case of the Hα flare (Dodson and Hedeman, 1964). Thus, the time-relation given in Table 4.6 for the event's end must be treated as just an approximation. Even so, the result found here, that the X-ray burst outlasts the flare by roughly 10 minutes on the average, agrees nicely with the event duration study of the previous section where a different set of events was used for the investigation. The scatter among the individual values is very large, however, ranging from the X-rays ending early by 38 minutes to the X-rays ending late by 58 minutes.

Because of the uncertainties just described, the center-to-limb difference for the relative ending times in Table 4.6 cannot be considered as definitely established. On the other hand, the difference between relative times of maximum for flares at the center and near the limb, although small, does appear to be significant. If this effect is real, it may imply a variation of the optical flare's characteristics with height, since only the higher levels of the flare are visible when it is near the limb. No center-to-limb change is expected for the soft X-ray burst itself because the solar atmosphere is optically thin to X-radiation (Allen, 1969). Of course, the latter argument assumes that the X-ray emitting region radiates isotropically, but this is certainly a reasonable assumption for a thermal source (see Section IV-4b).

A word of caution must be given: the significance of the center-to-limb effect for maximum times and for starting times found in the present study are exactly opposite to the conclusions drawn in Paper I, although data from the same experiment were used for both. Since the events considered here are some-

what less biased (see Section IV-1) and are about three times as numerous as those in the previous study, the present results are probably more reliable. But this discrepancy does serve to point out that the significance of center-to-limb variations in these relative timings cannot be determined conclusively until more extensive data are available.

6. COMPARISON OF SOFT X-RAY BURST AMPLITUDES WITH OTHER PHENOMENA

The X-ray bursts listed in Catalog II display a wide range of E(8,12) amplitudes, spanning more than three orders of magnitude from the smallest measured, 0.0005 erg/cm^2 sec (#29), to the largest inferred, 0.806 erg/cm^2 sec (#55). (See Section IV-2 for the method used to estimate the amplitudes of bursts which saturated the Michigan detector.) The investigations discussed in this section were carried out in order to find some parameters accessible to ground-based observers which correlate with the amplitude of soft X-ray bursts. Such a study could be used to help identify those physical conditions which are important in influencing the production of soft X-radiation during a solar flare. Alternatively, it might form the basis for a purely empirical prediction of a soft X-ray burst's amplitude from ground-based observations (in addition to SID measurements, of course).

a. Hα Flare Importance

One obvious parameter to consider in this connection is the importance of the associated Hα flare. The results of previous studies regarding this point are quite contradictory. Some investigators report that there is a definite relationship between X-ray burst amplitude and Hα flare importance (Dodson et al.,

1956; Warwick and Wood, 1959 (both by means of SID data); Paolini et al., 1968; Teske, 1969a), some believe that the relation, if any, is either weak or variable (Culhane et al., 1968; Culhane and Phillips, 1969; Hudson et al., 1969a), while others claim that no such relationship exists (Conner et al., 1964; Friedman, 1964; Kreplin and Gregory, 1965).

The present study implies that soft X-ray burst amplitudes are indeed related to the importance of the associated flare, but only in a statistical manner. This was found by calculating the mean amplitude $\overline{\Delta E}$ for all E(8,12) bursts in Catalog II which occurred during flares of a given importance. Table 4.7 gives the results for all importance classes in the catalog, along with the probable error (p.e.) of each mean, the number of events (N) used to find the mean, and the minimum and maximum burst amplitudes in the catalog for each flare importance.

TABLE 4.7

MEAN E(8,12) AMPLITUDES FOR FLARE-ASSOCIATED BURSTS

(All flux values are in erg/cm^{2}sec)

Flare Importance	$\overline{\Delta E}$	p.e.	N	Minimum ΔE	Maximum ΔE
1f	.0052	.0010	11	.0000	.0149
1n	.0183	.0014	138	.0005	.2163
1b	.0345	.0028	50	.0043	.1912
2f	.0248	--	1	--	--
2n	.0423	.0127	13	.0031	.2635
2b	.0970	.0209	11	.0390	.3909
3n	.1328	--	1	--	--
3b	.8060	--	1	--	--

The table clearly shows that the average amplitude is directly related not only to the flare's area but also to its brightness. The mean burst amplitude becomes larger with an increase in either of these factors. One reason that some of the earlier investigators did not arrive at a similar conclusion is undoubtedly due to their use of unverified flare lists. But Table 4.7 suggests an even more important source of confusion: the very large range of individual values within a given flare class. For example, observed amplitudes vary by more than two orders of magnitude in the case of bursts associated with 1n flares. Thus, the relationship which does exist can be revealed only by a statistical analysis of a large number of events, as in the present study.

In order to present the relationship in a quantitative form, a crude estimate of the peak enhancement in the Hα emission-rate was obtained by means of the average flare area and maximum Hα intensity appropriate for each flare importance. Because of difficulties caused by the well known limb-darkening effect, only Hα values for the center of the solar disk were considered. These were taken from the photometric study of solar flares made by Dodson et al. (1956), and converted into flux units by the procedure derived in the Appendix of the present paper. The mean flux amplitudes for both the Hα and soft X-ray events were then used to find the emission-rate enhancements at the sun, $\overline{\Delta S}(H\alpha)$ and $\overline{\Delta S}(8,12)$, which are listed in Table 4.8. These entries are tabulated in order of increasing $\overline{\Delta S}(H\alpha)$ and include values for subflares which were measured during the construction of an earlier catalog. The latter naturally should not be given as much weight as those derived from Catalog II flares, but are included to point out that the relation found here may also extend to smaller events.

TABLE 4.8

MEAN EMISSION-RATE ENHANCEMENTS FOR Hα AND SOFT X-RAY EVENTS

(Emission-rates in 10^{25} erg/sec)

$\overline{\Delta S}$(Hα)	$\overline{\Delta S}$(8,12)	Flare Importance
5.8	1.5	1f
6.9	1.1	Sn
12	3.0	Sb
29	5.1	1n
53	10	1b
55	7	2f
110	12	2n
170	27	2b
290	37	3n
380	227	3b

The values derived in this study agree fairly well with results found by other investigators. Vaiana and Zehnpfennig (1969) estimate that the peak 3.5 - 14 Å flux during a 1n flare was about 5×10^{24} erg/sec, but they note that this was really a rather small event. For the optical flare, several observers report a peak Hα emission rate about 10^{27} erg/sec both with events of importance 2^+ (Severny, 1952; Billings and Roberts, 1953) and importance 3^+ (Teske, 1962; Ellison, 1963a).

The relation between rates of soft X-ray and Hα emission is even more clearly seen in Figure 4-7 which shows a graph of the Table 4.8 values, with a straight line indicating the best linear fit to the plotted points. Obviously, there is an excellent statistical relationship between Hα and soft X-ray enhancements which is well represented by a direct proportionality. Thus, the present study implies that the following expression holds on the average:

$$\overline{\Delta S}(8,12) = 0.16\ \overline{\Delta S}(H\alpha) \qquad (4.4)$$

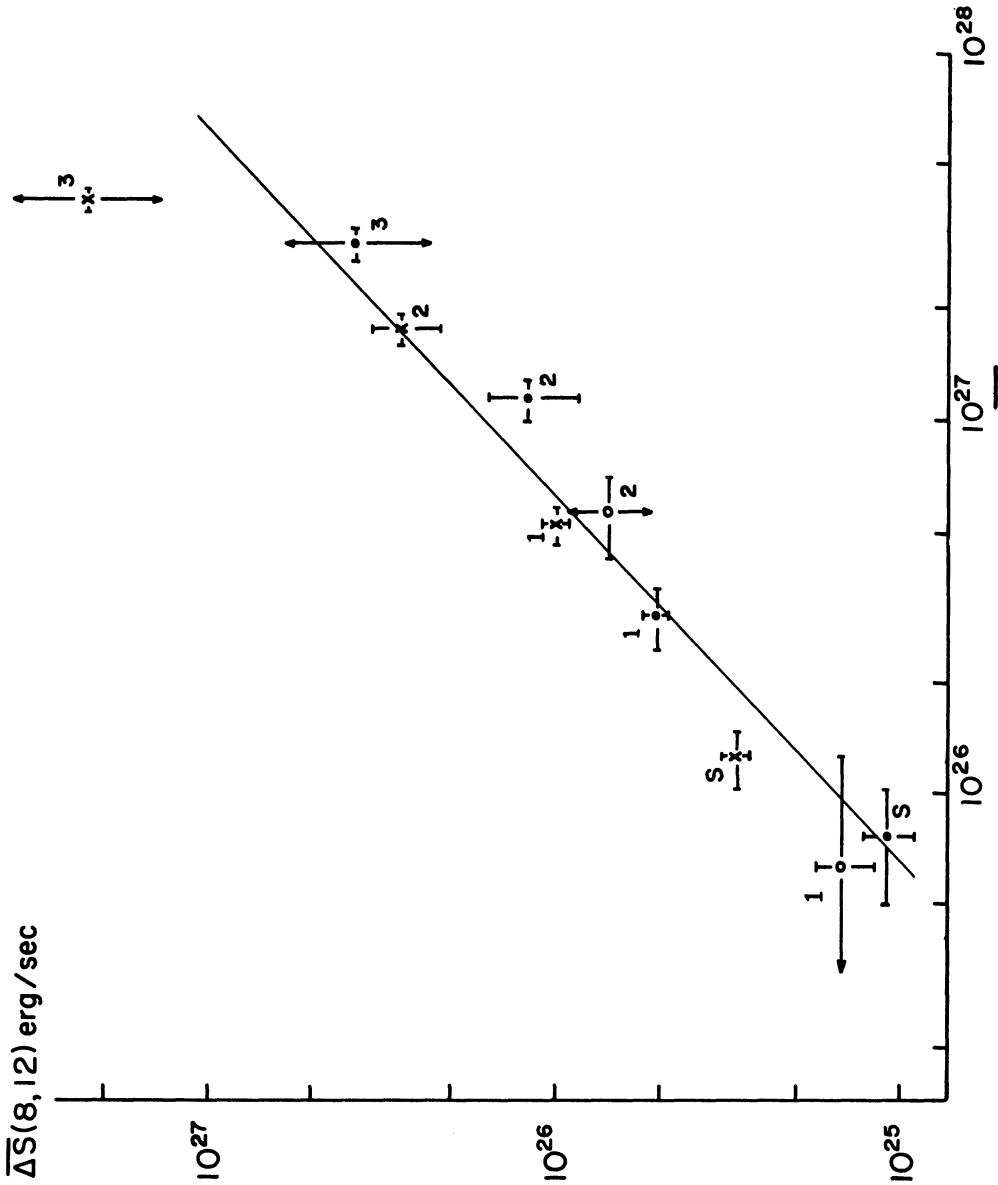

Figure 4-7. Relation between $\overline{\Delta S}(8,12)$ and estimated $\overline{\Delta S}(H\alpha)$ for various flare importance classes. Points are plotted for faint (o), normal (●), and bright (x) flares. The error bars for the mean X-ray values refer to the probable errors derived from Table 4.7. Those for the estimated Hα values result from an assumed uncertainty of ±0.1 in the flare's intensity relative to the center of the undisturbed solar disk (see the Appendix). No error can be assigned to $\Delta S(8,12)$ associated with 2f, 3n, or 3b flares since there is only one example of each type of these bursts. The straight line indicates the best fit by a linear relationship (i.e., unity slope).

It should be noted, however, that the relationship found here applies to emission rates at the maximum of the Hα flare and X-ray burst. As shown in Section IV-5c, these maxima occur at different times in general.

To obtain the relation given in (4.4), the soft X-radiation was assumed to be isotropic into 4π steradians because of the thermal nature of 8-12 Å emission (see Section IV-4b). Since the solar atmosphere is optically thin at such wavelengths (Allen, 1969), any possible effects of X-ray photon scattering were neglected. On the other hand, semi-isotropic radiation into 2π steradians was assumed for the Hα emission, following Pottasch's (1965) belief that all resonance-line photons created by collisional excitations ultimately escape from the solar surface. (See, however, the discussion by Athay, 1966.) Uncertainties caused by these assumptions also apply to the constant of proportionality in expression (4.4), of course, but the value of this constant is unreliable for an even more fundamental reason. Namely, the Hα flux is strongly overestimated by using the maximum intensity of the flare's brightest point, as in the above method, rather than some mean intensity averaged over the entire flaring region. Isophotometry of three flares (to be described in Chapter V) indicates that the correct method leads to Hα flux values which are lower by a factor of 5.

However, this difficulty is not critical for the present study since the important result here is the existence of a proportionality between mean soft X-ray and Hα enhanced emissions, rather than the exact value of the proportionality constant involved. Because the flare importance does have such a major statistical influence on the amplitude of the associated X-ray burst, the remainder of this chapter (unless otherwise noted) will only consider bursts

which accompany 1n flares, the most numerous importance class in Catalog II. The amplitudes of these bursts will be referred to by the symbol $\Delta E_{1n}(8,12)$ and the bursts themselves will be called "1n" X-ray bursts.

b. Time of Occurrence

As mentioned in Section IV-3, there is some evidence that European observatories as a whole tend to rank flares on a slightly higher importance scale than do observatories in other parts of the world (Dodson and Hedeman, 1960; C. S. Warwick, 1965). To investigate this question using the X-ray data of Catalog II, the mean E(8,12) amplitudes were determined for all "1n" bursts whose maxima occurred during "European," "American," and "Asian" observing hours: defined here as 0600-1359, 1400-2259, and 2300-0559 UT, respectively. Table 4.9 shows that "1n" bursts do have lower average amplitudes when associated with reported flares that can be attributed roughly to European observers. This is exactly the result expected if these observers did indeed rate flares as importance 1n which would have been assigned somewhat lower rankings elsewhere. This is not meant to imply in any way, of course, that the reports from some flare-patrol stations are correct while others are not. Rather, it merely indicates that world-wide ratings of solar flare importances are not made on a uniform basis at the present time. This fact undoubtedly accounts for a part of the burst amplitude variations described earlier, and points out again the advantage of studying flare characteristics by means of statistical investigations of a large number of events, which tend to average out such effects.

TABLE 4.9

MEAN $E_{ln}(8,12)$ AMPLITUDE VERSUS UNIVERSAL TIME

Time of Maximum (UT)	Observers	$\overline{\Delta E}_{ln}(8,12)$ erg/cm^{2}sec
2300 - 0559	"Asian"	.0238 $\pm$ .0034 p.e.
0600 - 1359	"European"	.0147 $\pm$ .0008
1400 - 2259	"American"	.0211 $\pm$ .0040

c. Location on the Disk

The average amplitude of "ln" X-ray bursts was also considered as a function of the position of the burst on the solar disk. This was done in two ways: (a) by dividing the sun into its various hemispheres and quadrants, and (b) by comparing limb bursts with those that occurred nearer the center of the disk. As in the relative-timing investigations described in Section IV-5a, events that occurred within 60° heliocentric of the solar disk center are called "center" bursts while those beyond 60° are "limb" bursts. Table 4.10 gives the results of these studies and shows that there are no strong statistical differences among the categories tested. The same result has been reported for similar studies using data from the effects of Sudden Ionospheric Disturbances (Giovanelli, 1938; C. S. Warwick, 1963; Reid, 1969).

TABLE 4.10

MEAN $E_{ln}(8,12)$ AMPLITUDE VERSUS LOCATION ON THE DISK

Location	$\overline{\Delta E}_{ln}(8,12)$ erg/cm^{2}sec
Northern hemisphere	.0191 ± .0015 p.e.
Southern hemisphere	.0150 .0015
Eastern hemisphere	.0174 ± .0016 p.e.
Western hemisphere	.0182 .0015
N-E quadrant	.0186 ± .0022 p.e.
N-W quadrant	.0197 .0019
S-E quadrant	.0143 .0013
S-W quadrant	.0156 .0026
Center	.0161 ± .0012 p.e.
Limb	.0218 .0024

However, there is some suggestion of a moderate center-to-limb effect since the most significant difference in Table 4.10 is between the center and limb bursts. Student's t-test implies that this difference has only a 13% probability of being due purely to chance. The variation is such that soft X-ray bursts associated with 1n flares near disk center have a slightly lower mean amplitude than those near the limb. This effect is shown even more clearly in Table 4.11, where the data are subdivided into smaller intervals of R, the distance of the flare from the center of the disk in units of solar radii. The intervals of R used here were chosen to include roughly equal numbers of events. The trend of the mean burst amplitudes is obvious, with the tabulated values increasing monotonically as the limb is approached. This result is consistent with the study by Dodson et al. (1956), which showed that SID's were larger on

the average for limb flares of a given importance. Such an effect is most likely due to the reduced visibility of Hα flares near the limb (Dodson and Hedeman, 1964) which leads to the general tendency for their importance to be underestimated (Sawyer, 1967).

TABLE 4.11

MEAN $E_{ln}(8,12)$ AMPLITUDE VERSUS DISK-CENTER DISTANCE

R solar radii	$\overline{\Delta E}_{ln}(8,12)$ erg/cm^{2}sec
.000 - .400	.0139 ± .0027 p.e.
.401 - .600	.0146 .0014
.601 - .800	.0173 .0024
.801 - .960	.0213 .0026
.961 - 1.000	.0249 .0061

As an aside, it is interesting to note that both in Tables 4.10 and 4.11, the mean amplitudes for bursts nearest the limb have the largest probable errors, which is due to the fact that they contain the widest range in individual values. This result also appears in the SID study by Dodson et al. (1956), and again is probably caused by the Hα visibility difficulties at the limb.

Another way to investigate the possible center-to-limb effect is to examine the frequency of X-ray burst occurrence as a function of disk-center distance. If there is a variation in the mean burst amplitude with position on the disk, this variation will be reflected in the frequency distribution of the observed bursts. Unfortunately, the method has been improperly applied so often by others as to require some special comment.

Many investigators, including Culhane and Phillips (1969), Drake (1969), Ohki (1969), and Pinter (1969a), have reported very strong center-to-limb differences in the frequencies of X-ray bursts. In each case, these variations have been attributed to some intrinsic property of the X-ray burst itself; for example, a "beamed" radiation field due to nonthermal emission processes. Only Drake has suggested that the effect might be influenced by the well known center-to-limb variation in the frequency of reported Hα flares (see for example DeFeiter, 1966). Yet the variation in the visibility of Hα flares is of paramount importance to these studies. Since they all utilized data from experiments with no spatial resolution, the assignment of an X-ray burst's position required a simultaneous, reported Hα flare. For example, an X-ray burst which occurred at the limb could not be identified as such if the Hα event associated with it was not seen. Thus, the correct question to ask here is: <u>given an Hα flare</u> at a particular disk-center distance, what is the probability of occurrence of a detectable X-ray burst? The present study indicates that the probability is very nearly unity, so that no "directivity effect" exists for the radiation field of soft X-ray bursts. This result is therefore consistent with the finding that soft X-radiation is thermal in character even during burst conditions (Section IV-4b) and the assumption that the burst emission is isotropic into 4π steradians (Section IV-6b). Obviously, conclusions drawn from studies which did not take the visibility function of Hα flares properly into account should be treated with caution.

d. General Solar-Activity Level

Table 4.12 gives the mean amplitudes of "ln" bursts as a function of whether they began while the Michigan detector was in its high or low sensitivity mode of operation. The table shows that "low sensitivity" X-ray bursts have a significantly higher amplitude on the average, since Student's t-test implies that the observed difference between these two categories has less than 1% probability of being due to chance. The nonburst soft X-ray flux is a valid index of the general solar-activity level (Chapter III) and, whenever this flux exceeds 0.0044 erg/cm^{2}sec, the Michigan experiment automatically switches into its low sensitivity mode (Chapter II). Thus, the above result indicates that X-ray bursts accompanying ln flares tend to have greater amplitudes on those days when the general level of solar activity is high. This agrees with the similar effect reported by Teske (1969a) for the amplitudes of E(8,12) bursts associated with subflares.

TABLE 4.12

MEAN $E_{ln}(8,12)$ AMPLITUDE VERSUS INITIAL DETECTOR MODE

Initial Operating Mode of Detector	$\overline{\Delta E}_{ln}(8,12)$ erg/cm^2 sec
High sensitivity	.0094 $\pm$ .0009 p.e.
Low sensitivity	.0212 $\pm$ .0015

The same result is derived from Table 4.13, which gives the correlation coefficients for $\Delta E_{ln}(8,12)$ versus the base flux $E_B(8,12)$ and the Zurich Sunspot number R_Z. Specifically, the latter coefficient is for the monthly mean

of the final Zurich Sunspot numbers (taken from the SGDB) versus the mean $\Delta E_{ln}(8,12)$ for all events in Catalog II which occurred during the month in question. In addition, the table indicates the probable significance P for each of these two coefficients.

TABLE 4.13

CORRELATION OF $\Delta E_{ln}(8,12)$ WITH SOLAR-ACTIVITY INDICES

Index of General Solar-Activity Level	Correlation Coefficient	P
$E_B(8,12)$	+ 0.41	> 99%
R_Z	+ 0.60	96%

The first correlation shown in Table 4.13 merely indicates that the relation found by crudely dividing the data into "high" and "low" levels of solar activity also holds when the solar-activity level is more precisely defined by $E_B(8,12)$. The relationships based on sensitivity levels and on $E_B(8,12)$ involve parameters which can be measured only by detectors above the earth's atmosphere, but the expressed purpose of this chapter was to investigate parameters accessible to ground-based observers. This is not a problem, however, since the nonburst soft X-ray level used above is known to be closely associated with the classical indices of solar activity (e.g., Teske, 1969a, 1969b). Thus, any of these indices should also correlate well with the "ln" X-ray burst amplitude. Table 4.13 shows that this is indeed the case, at least when the index R_Z is considered.

The relationship indicated by this study is probably a result of the general

density increase in the corona which accompanies a rise in the level of solar activity (see, for example, Elwert, 1963; DeJager, 1964). This possibility will be considered again in the next sub-section.

e. Characteristics of the Associated Plage

If the general level of solar activity over the entire disk is related to the amplitude of "1n" soft X-ray bursts, as shown above, then it seems reasonable to expect that a similar relationship might also exist with the specific activity level of the burst-associated plage itself. In order to test this possibility, three indices of plage activity were considered: the flare-richness of the plage, its age, and the area of its major spot group.

The frequency distribution of the active regions as a function of their flare-richness is shown in Figure 4-8, which indicates how many plages were responsible for a given number of events in Catalog II. The plages were then divided into those which produced more than 10 cataloged events and those which produced 5 or less, called "prolific" and "nonprolific" regions, respectively. The group of prolific flare-producing regions consisted of McMath #8740, 8818, 8905, 8942, and 9184. Plage regions McMath #8791, 8907, 9047, 9115, 9146, and 9204 were not included in either category, being considered as moderately flare-rich. (Note that this division is not exactly the same as the one made in Paper I because of the different flare catalogs used.) The first two entries of Table 4.14 show that the mean amplitude of "1n" bursts is significantly higher for those which are associated with prolific plage regions; there is only a 2% probability that this result could be due to chance. Such a result had

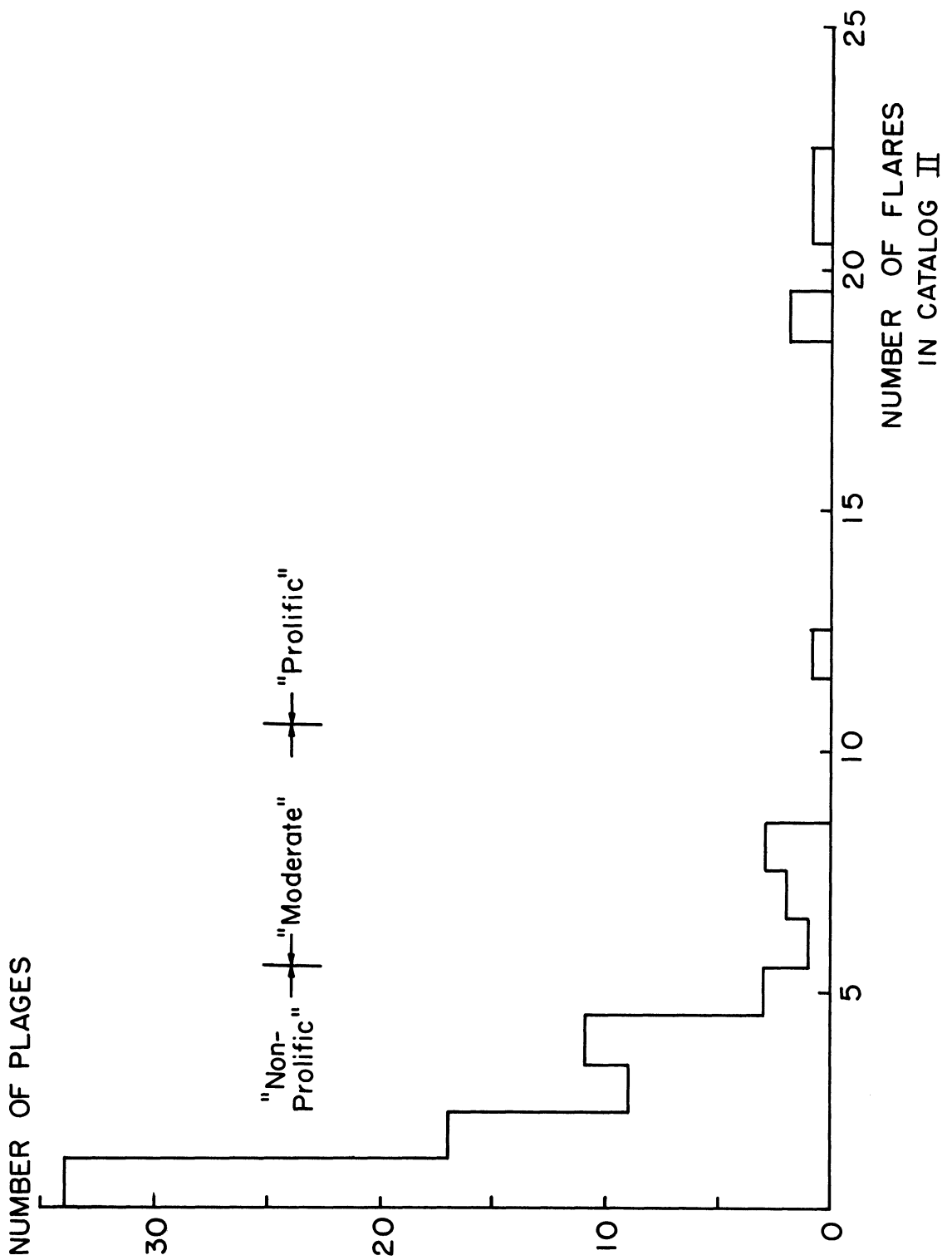

Figure 4-8. Frequency distribution of plages having a given number of events in Catalog II. Plages which produced more than 10 cataloged flares are considered "prolific." Those which produced 5 or less are defined as "nonprolific."

already been suggested in Paper I by an investigation of median burst amplitudes, although the division of plages into prolific and nonprolific categories was somewhat different in that study. Using the plage division given in Paper I, Culhane and Phillips (1969) have also found the same effect for 3-4 Å soft X-ray bursts.

TABLE 4.14

MEAN $E_{ln}(8,12)$ AMPLITUDE VERSUS PLAGE CHARACTERISTICS

Plage Characteristic		$\overline{\Delta E}_{ln}(8,12)$ erg/cm^{2}sec
Flare-richness:	prolific	.0244 ± .0025 p.e.
	nonprolific	.0155 .0014
Age (rotations):	1	.0190 ± .0023 p.e.
	2	.0181 .0013
	3	.0169 .0021
	4	.0165 .0050
	5	.0125 .0031

The second parameter considered was the age of the plage as measured by the number of solar rotations it had been visible since its formation. All cataloged bursts were used which occurred in plages with a single age given by the SGDB. (Two plages may merge together forming a single active region; if the ages of the parent regions were different, the SGDB lists both for the resulting plage.) The bottom portion of Table 4.14 shows that there is a steady decline in the mean "ln" burst amplitude as the associated plage region becomes older. Unfortunately, there were too few qualified events in these averages (especially for plage ages of 4 and 5 rotations) to make the result statis-

tically conclusive, and a much more extensive set of X-ray burst observations will be necessary to confirm this finding. But the monotonic decrease in the mean amplitude values derived here is certainly very suggestive that a region's age is somehow related to its X-ray producing capability during a flare.

A plausible, physical basis for such a relationship has been reported by Neupert (1967, 1968), who claims that the temperature and density of the condensation overlying a plage both decline as the region ages. (Also see Chapter III of the present paper.) All realistic thermal mechanisms for the production of soft X-radiation predict that the only physical conditions directly related to the X-ray emission rate are the temperature and density (as well as volume) of the radiating source. Thus Neupert's finding is completely consistent with the result of the above study if these physical conditions normally undergo the same percentage change in the X-ray source during an Hα flare of a given importance. (This requirement also seems necessary to explain the relationships described in the previous section.) Further support for this hypothesis is given by Svestka (1963), who finds that anomalously high X-ray enhancements accompanied importance 1 flares which occurred in a region with an abnormally high density according to one interpretation of its optical spectrum.

It should be noted, however, that the two effects indicated in Table 4.14 are not completely independent because flare-rich plages are usually also young. Typically the flaring frequency within a region diminishes as the plage grows older (e.g., Giovanelli, 1939; Witte, 1951).

Another semi-independent index of a region's activity level is the area of its sunspots. Since a plage may sometimes contain two (or more) sunspot groups,

we used here the total area of the group nearest the flare itself, as tabulated in the Rome Solar Phenomena Bulletin (Cimino, 1967). Whenever the identity of the proper spot group could not be established unambiguously, the event was eliminated from further consideration. Furthermore, this study examines only those bursts which accompanied 1n or 1b flares in McMath plage regions #8740, 8818, 8905, or 8942, and occurred within 72° heliocentric of the solar disk center ($R \leq 0.95$).

Figure 4-9 shows the resulting distribution of X-ray burst amplitude as a function of the related sunspot area. Clearly, no direct relationship exists between individual values. But the absence of points in the lower-right portion of the figure might be interpreted as implying that the region associated with a given size sunspot can give rise to an X-ray burst of any amplitude up to a certain limiting value, and that the amplitude limit increases with the size of the spot group. This finding is consistent with the results of the Dodson and Hedeman (1970) examination of major flares (importance 2 or larger) which occur in plages with very small or no sunspots. They report that these flares were associated with a lower than normal percentage of both great SWF's and large amplitude 2-12 Å X-ray bursts. They further note that: "These flares usually occurred during the late, flare-poor phase of a center of activity," a statement which agrees precisely with aspects of the present study described previously.

A relationship such as the one found above could be explained if the X-ray emission rate were governed by the temperature and density of the source region (as implied by the first two studies in this section), but confined to a range

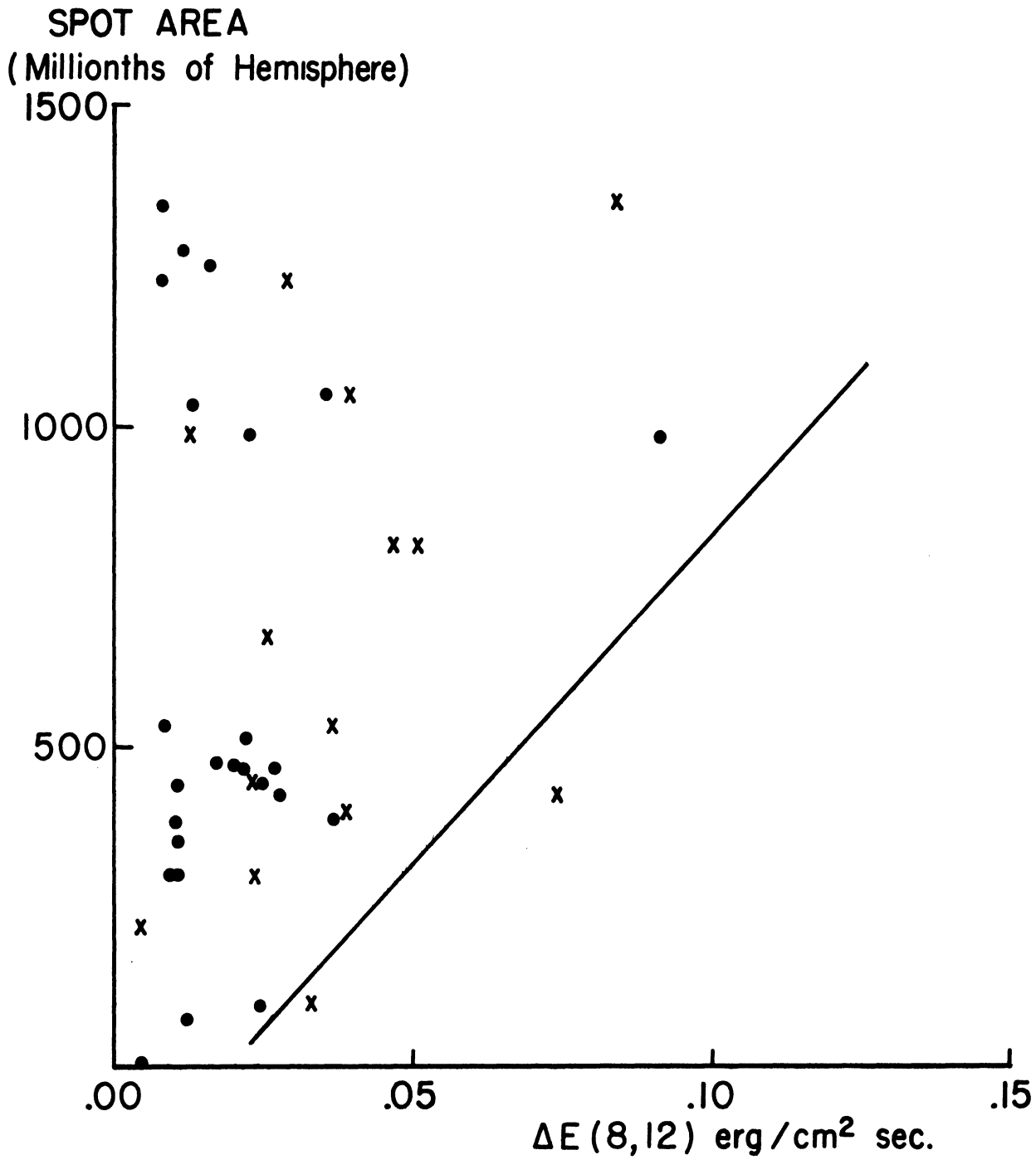

Figure 4-9. Scatter diagram of ΔE(8,12) versus total area of the related sunspot group. X-ray bursts associated with 1n flares are shown as •; those with 1b flares as x. Note the relative absence of points to the right of the line arbitrarily drawn in the figure.

given by the region's magnetic energy density (which is crudely indicated by the area of the associated sunspot group). To test this suggestion properly, one should also consider the classification of the sunspot group's complexity and measured magnetic field strength, in addition to its total area, but this will be left for future investigation.

f. Characteristics of the Associated Radio Bursts

Teske (1969a) has already reported that there is a good correlation between the amplitude of soft X-ray bursts observed by the Michigan detector and the amplitude of corresponding 2800 MHz bursts. Furthermore, Paper I showed that 2800 MHz bursts accompanying flares in "prolific" regions tend to have larger amplitudes than those associated with flares in "nonprolific" regions, an effect identical to that for X-ray bursts (see the discussion in the preceeding section). Two additional studies relating the amplitude of E(8,12) bursts to some properties of their radio counterparts will be described here.

Tandberg-Hanssen (1967) has noted that the most "active" flares so far as X-ray production is concerned are also those that produce strong Type IV radio bursts. The present study indicates that at least some X-ray enhancements do not follow this general relation. Table 4.15 lists the nine events in Catalog II which were associated with a Type IV radio burst reported in the SGDB and which had soft X-ray coverage at the time of maximum. Type IV bursts are quite rare; they occur with only about 5% of the well verified flares in Catalog II (15 cases out of 283, six of which had no amplitude data available). They also occur preferentially with very large flares; only four of these 15 cases accompanied flares

TABLE 4.15

SOFT X-RAY EVENTS ASSOCIATED WITH TYPE IV RADIO BURSTS

Catalog II Number	Hα Flare Importance	Type IV Burst Importance	ΔE(8,12) erg/cm²sec	$\Delta E/\overline{\Delta E}$
7	2b	2	.1211	1.2
8	1b	2	.0257	.7
53	2n	3	.2635	6.2
55	3b	3	.8060	-
140	1b	3	.0460	1.3
156	2b	3	.0400	.4
176	1n	3	.0083	.5
232	1b	2	.0643	1.9
259	2n	3	.0319	.8

of importance 1n or less, although the latter account for nearly 70% of all flares in the catalog (see Section IV-3). In addition, Boischot and Denisse (1957) have shown that type IV emission is most likely due to the synchrotron radiation of electrons accelerated to relativistic energies, again indicating the extraordinary magnitude of the physical process giving rise to this phenomenon.

However, flares having Type IV bursts are not invariably associated with great X-ray bursts, as can be seen in Table 4.15. Except for events #53 and 55, the E(8,12) amplitudes do not appear to be exceptionally large. This is seen even more clearly by noting the ratio of the observed burst amplitudes to the mean amplitudes for the appropriate flare importances which were determined in Section IV-6a. (The ratio was not calculated for event #55, the great 23 May 1967 flare, because this was the only example of its importance class in Catalog II. Therefore, the 23 May event will not be considered in the following discussion.) Of the 8 remaining bursts, only 4 had amplitudes larger than

the mean value for their associated flare importance. Moreover, of the remaining 5 events that accompanied "great" Type IV bursts (rated intensity 3 in the SGDB), more than half had amplitudes below the mean. While this sample is obviously too small to draw any definite conclusions about average behavior, it does seem clear that Type IV association is not restricted solely to events with exceptional soft X-ray enhancements.

The other investigation to be described here concerns the mean E(8,12) amplitude for bursts accompanying radio events with two types of spectra. Actually, the radio burst spectrum used for a given event is "synthetic" in the sense that the flux values at various frequencies were not necessarily measured simultaneously, but rather refer to the maximum flux attained at each frequency during the burst. This procedure was followed in order to utilize the standardized reports of radio events in the SGDB. With the spectral distributions derived in this manner, the radio bursts were divided into two morphological groups: Class A, characterized by spectra having the greatest reported flux at the highest frequency listed (normally about 10,000 MHz); and Class B, with spectra having the greatest reported flux at some smaller frequency. Thus, Class A bursts have stronger cm-wavelength radiation relative to those of Class B. Since a particularly complete set of radio observations is necessary to categorize these bursts properly, only 54 events were found with clearly defined spectral type and for which an X-ray burst amplitude was listed in Catalog II.

The first line of Table 4.16 shows that the mean E(8,12) amplitude for all X-ray bursts accompanying Class A radio events is higher than that for Class B, with a 96% probability (as given by Student's t-test) that this effect is real.

TABLE 4.16

MEAN E(8,12) AMPLITUDE VERSUS SPECTRAL CLASS OF RADIO BURST

	$\overline{\Delta E}(8,12)$ erg/cm^{2}sec		P
	Spectral Class A	Spectral Class B	
All events	.0983 ± .0293 p.e.	.0308 ± .0049 p.e.	96%
"1n" events	.0526 ± .0191	.0199 ± .0018	94%

But there is a tendency for the Class A bursts to be associated with the very largest Hα flares; 61% of these bursts occurred during flares of importance 1b or greater, compared to only 44% of the Class B bursts. Thus it is conceivable that the higher mean amplitude of X-ray bursts accompanying Class A radio events is accounted for by the relation found in Section IV-6a between $\overline{\Delta E}(8,12)$ and Hα flare importance. The second line of Table 4.16 shows that this is not the case, however. Here only events which occurred during 1n flares were considered, thus eliminating the influence of the flare importance effect. Yet the mean X-ray amplitude still is higher for bursts accompanied by Class A radio events, with just a 6% probability that this observed difference is due to chance. A similar result for hard X-ray bursts can be inferred from the report by Arnoldy et al. (1968a), that the probability of detecting a 0.2-1.2 Å X-ray event is negligible unless the spectrum of the associated radio burst includes cm-wavelength enhancements.

Unfortunately, the interpretation of a "synthetic" spectrum, as obtained from the peak fluxes of a radio burst at various frequencies, is by no means straightforward (cf. Kundu, 1962), so that the physical meaning of the relationship found above is not clear. Furthermore, there is a possibility that the sample of events studied here was somehow biased. Kundu (1965) finds that the peak

flux of a cm-wavelength radio burst usually increases with increasing frequency, while only 33% of the events in the present investigation showed that property. In any case, the relation indicated here between the X-ray burst amplitude and the spectral type of the associated cm-wavelength event needs to be confirmed by a more refined analysis. Although such a refined analysis would require a great deal of effort, a careful comparison of the simultaneous X-ray, visible, and radio aspects of the total flare phenomenon should lead to new insights concerning the physical processes involved.

7. TOTAL X-RAY BURST ENERGIES

It would be of considerable interest to know the total energy emitted in the X-ray band during flares of various importance. Both as absolute amounts and as amounts relative to the total emission at other wavelengths, such values would serve as helpful guides for the construction of new flare models and as stringent tests for models already proposed.

There are two ways to determine the mean X-ray burst energy as a function of flare importance using data from the Michigan experiment. The first and more accurate method is to planimeter the time-profile curve for each burst associated with a given class flare, and then average the individual energy values so derived. Unfortunately, the records for most of the X-ray bursts in Catalog II were interrupted at least once during the event's time development by one or more of the sources of data-loss (satellite night, tape recorder playback, and trapped particle interference) described in Chapter II. The statistical uncertainties in the calculated means would be quite large if just the events with complete flux curves were used. Furthermore, the results would be biased since

this method systematically discriminates against longer duration events. Thus, it is not possible to take full advantage of the potentially higher accuracy afforded by the above procedure.

Therefore, the second method was used which gives a rougher estimate of the total X-ray energy but by a much easier procedure. Here the burst's time-profile is approximated by a simple triangle, so that the time-integrated E(8,12) flux is given by one-half the burst's amplitude times its duration. Average values for the amplitude and duration of bursts associated with flares of various importance were used to simplify the procedure further. Mean E(8,12) amplitudes were taken directly from Table 4.7, and converted into the corresponding enhancement values of the solar X-ray emission rate by assuming isotropic radiation into 4π steradians with no photon scattering (see Section IV-6a). The values 2000, 4000, and 8000 seconds were used for the mean durations of bursts associated with flares of areal importance 1, 2, and 3, respectively. The mean duration for "importance 1" E(8,12) bursts was taken from the results of the study described in Section IV-4c; the other values were estimated from the author's subjective impression of the longevity of these great bursts. In all cases, the durations were deliberately chosen to be underestimates in order to compensate for the fact that approximating the burst's time-profile by a triangular area will tend to overestimate the event's total emission. This occurs because the rise and decay of soft X-ray enhancements are more nearly exponential than linear changes.

Table 4.17 shows the results found by the above procedure. The absolute values given are probably accurate to within a factor of 4; they are most likely correct within a factor of 2 relative to one another. Comparable estimates of

TABLE 4.17

TOTAL 8-12 Å EMISSION DURING Hα FLARES

Hα Flare Importance	Mean Total 8-12 Å Emission (erg)
1f	2×10^{28}
1n	5×10^{28}
1b	1×10^{29}
2f	1×10^{29}
2n	2×10^{29}
2b	5×10^{29}
3n	1×10^{30}
3b	1×10^{31}

the total flare emission at other wavelengths have been reported by many investigators and are summarized in Table 4.18. Values listed as "Visual" refer

TABLE 4.18

REPORTED VALUES OF TOTAL FLARE EMISSION

Wavelength Interval	Flare Importance	Total Energy Emission (erg)	Reference
0-1.2 Å	1b	3.0×10^{26}	Kane (1969)
3.5-12 Å	"typical"	$10^{28} - 10^{29}$	Krieger and Vaiana (1969)
3.5-12 Å	"great"	$> 10^{30}$	Krieger and Vaiana (1969)
8-12 Å	1	6.0×10^{28}	Teske (1969a)
0-14 Å	2b	1.4×10^{29}	Van Allen (1967b)
3.5-14 Å	1n	few 10^{28}	Vaiana and Giacconi (1968)
10-1030 Å	1b	6.0×10^{29}	This paper, Chapter V
Hα	1b	1.0×10^{29}	This paper, Chapter V
Hα	2	10^{31}	J. W. Warwick (1962)
Hα	2^+	3.0×10^{30}	Billings and Roberts (1953)
Hα	2^+	3.0×10^{29}	Van Griethuysen and Houtgast (1959)
Hα	3^+	10^{31}	Bruzek (1967)
Visual	2	6.0×10^{29}	Kiepenheuer (1964)
Visual	3^+	10^{32}	Kiepenheuer (1964)
Visual	3^+	10^{32}	Parker (1957)
Visual	3^+	10^{32}	Ellison (1963b)
Visual	3^+	10^{32}	Bruzek (1967)
Microwave	1b	8.0×10^{22}	This paper, Chapter V

to radiation in all emission lines and the continuum at optical wavelengths; the "Microwave" value includes emission between 2,000 and 15,000 MHz. Clearly, the amount of energy emitted as X-radiation accounts for a significant portion of the total electromagnetic energy lost during a flare event. This point will be considered again in the next chapter, which describes the individual characteristics of three selected flares.

To summarize the results of the present chapter, we have shown that all 283 of the well confirmed Hα flares observed by the Michigan experiment were accompanied by a detectable enhancement in soft X-radiation, with one possible exception. Properties of the general time-profiles for such enhancements imply that 8-12 Å X-radiation is thermal in nature even during flare-associated bursts. In addition, the times of start, maximum, and end for X-ray bursts are similar to those of the Hα flare, although the X-ray enhancement tends to start first by a few minutes on the average.

We have also shown that there is a definite correlation between the peak amplitude of the X-ray burst and the associated flare's area and intensity. For a flare of a given importance, the peak amplitude of the X-ray burst is a function of its distance from the solar limb, an effect which is most likely due to the Hα observations. The peak amplitude also depends on the general level of solar activity at the time of the burst and on the age and "flare-richness" of the associated plage. The latter effects are probably due to density variations in the X-ray emitting region itself. Furthermore, it appears that the amount of

energy emitted as 8-12 Å X-radiation accounts for a significant portion of the total electromagnetic energy lost during a flare event.

Some of the statistical relationships found above will be re-examined in the next chapter in order to determine the degree to which they can be considered valid during individual events. For that purpose, three especially well observed flares will be investigated in some detail.

CHAPTER V

THE X-RAY BURST COMPONENT: STUDIES OF INDIVIDUAL EVENTS

Numerous studies have examined the relation between the soft X-ray flux and Hα intensity during solar flares (Landini et al., 1965; Culhane and Phillips, 1969; Teske, 1969a). Others have compared the X-ray flux with the area of the associated Hα event (Valnicek, 1967; Hudson et al., 1969b). However, the relation of an area or intensity to a flux is difficult to interpret. A much more meaningful comparison would be between the X-ray flux and the corresponding Hα flux of the flare. The previous chapter described a crude approximation to such a relationship for the time of flare maximum, but this gives no information about the time development of the relation during an event. Using a method similar to that of Chapter IV (i.e., taking the total flare area times the intensity of its brightest point), Coutrez et al. (1963), have compared rough Hα flux values during a flare with the effects of solar X-radiation as observed by SEA monitors. Even this is not completely satisfactory, as the results are still just estimates based on indirect measurements.

To overcome such objections, the time-profiles of the enhanced Hα flux for three flares were determined and directly compared to their associated E(8,12) bursts as observed by the Michigan X-ray experiment. For each flare, about twenty frames of the McMath-Hulbert Observatory's Hα patrol films were analyzed by isophotometry with up to seven iso-density contours at the times of maximum intensity. (The flare patrol photographs were made with a 0.5 Å interference filter of the Lyot type.)

These measurements were then reduced to values of the solar Hα emission rates by the procedure derived in the Appendix. Using the resultant Hα emission curves for these events, the statistical relationships found in Chapter IV were then re-examined to see how closely they apply to individual flares.

1. SELECTION OF EVENTS

A flare had to satisfy the following criteria in order to qualify for this study:

(1) filtroheliograms of the flare were obtained by McMath-Hulbert Observatory's Hα flare patrol program,

(2) the filtroheliograms were of high quality,

(3) they were continuous (at least one each thirty seconds) from the flare's start to ten minutes after its maximum intensity,

(4) the Michigan experiment's record of E(8,12) covered the above interval with no interruptions,

(5) the flare was included in Catalog II (see Chapter III for a description of this catalog), and

(6) the flare occurred within 45° heliocentric of the center of the solar disk ($R < 0.7$).

These criteria insure that the event was well observed and not strongly affected by the various difficulties associated with limb flares (cf. Appendix).

Of the 283 flares in Catalog II, only three satisfied the above requirements. Each of these flares was rated importance 1b and occurred within a region undergoing its third rotation. Other data are given in Tables 5.1

and 5.2, which, with two exceptions, are taken directly from Catalog II. The exceptions are that (a) the Hα starting time is the earliest start reported by a cinematographic station; and (b) the disk-center distance R (in units of solar radii) is from the SGDB. Figures 5-1, 5-2, and 5-3 show the McMath-Hulbert flare patrol filtroheliogram near the time of maximum intensity for each flare. (Note the image of the clock impressed on these photographs. This clock was calibrated with WWV time signals three times a day to insure that each exposure could be identified to within a few seconds.)

TABLE 5.1

Hα DATA FOR THE ANALYZED FLARES

Date	Start	Max.	End	Imp.	Location	R	No.
26 March 1967	1603	1605	1619	1b	N24E08 8740	.51	13
24 March 1968	1632	1645	1735	1b	S12W02 9273	.09	280
25 March 1968	1442	1449 1507	1600	1b	S12W14 9273	.25	281

TABLE 5.2

E(8,12) DATA FOR THE ANALYZED FLARES

Date	Start	Max.	End	Base	Ampl.	No.
26 March 1967	1604.0	1608.0	1630	.0084	.0236	13
24 March 1968	1633.5	1647.0	1833	.0053	.0412	280
25 March 1968	1444.0	1452.0 1507.5	-	.0040	.0435	281

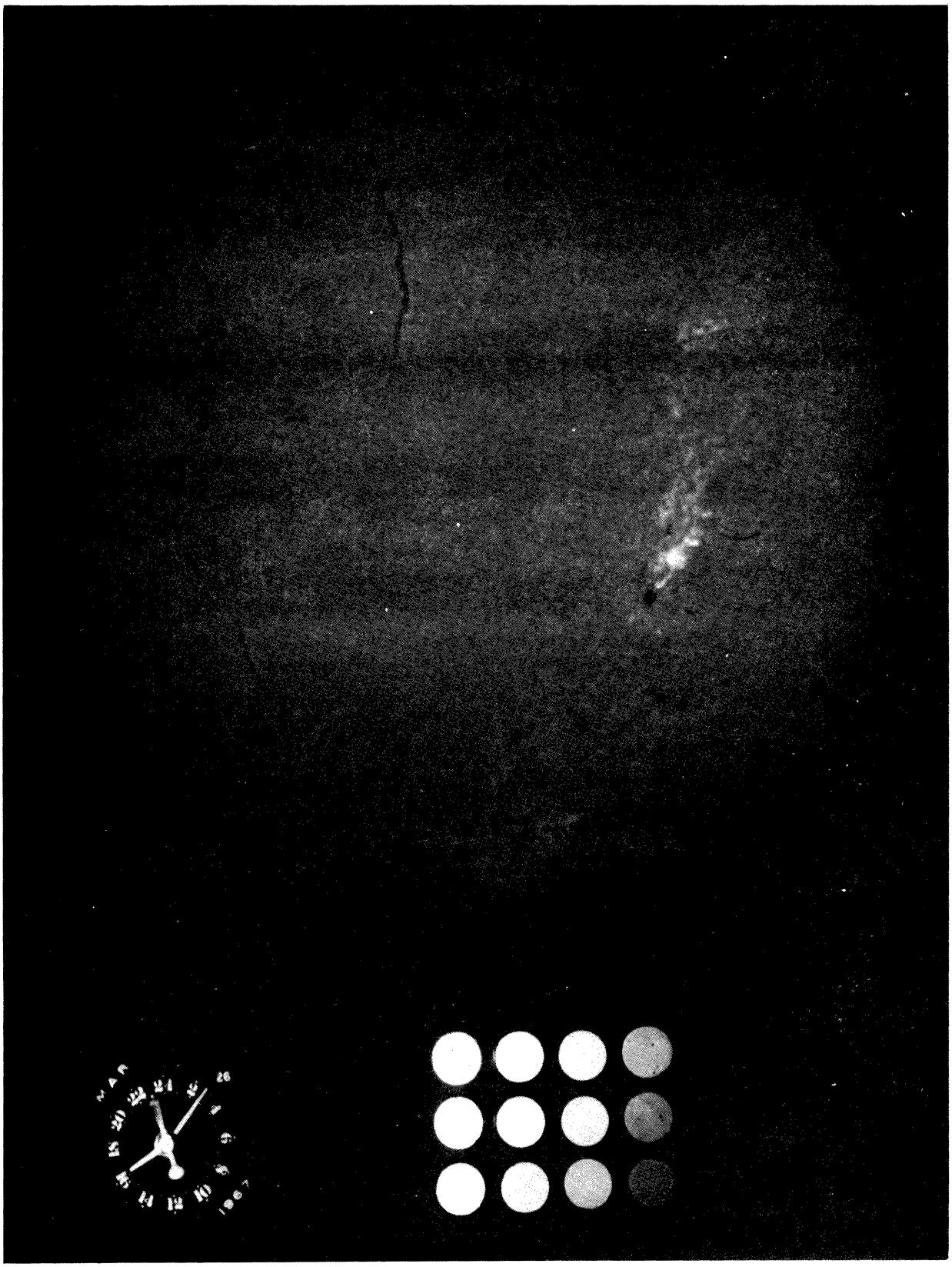

Figure 5-1. Hα filtroheliogram of 1b flare on 26 March 1967. The exposure was taken at 1608 UT, two minutes after the flare's maximum intensity. This photograph is from the McMath-Hulbert Observatory's flare-patrol records, as are the next two figures. Note the clock image and calibration spots impressed on each exposure.

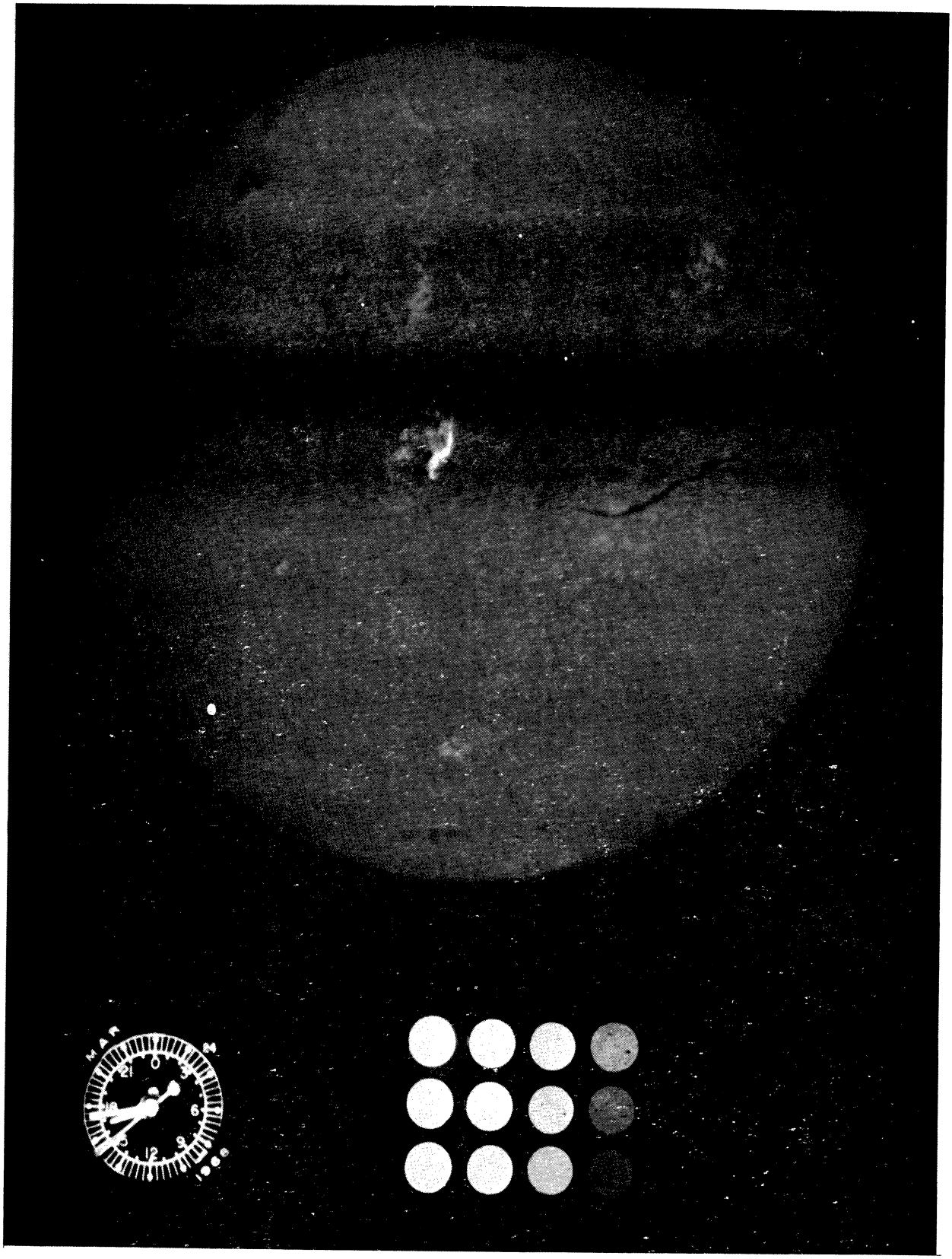

Figure 5-2. Hα filtroheliogram of 1b flare on 24 March 1968. The exposure was taken at 1644 UT, near the time of the flare's maximum intensity.

Figure 5-3. Hα filtroheliogram of 1b flare on 25 March 1968. The exposure was taken at 1506 UT, near the time of the flare's maximum intensity.

Quite by chance, two of the events selected by the above procedure are closely related to one another. Flare #281 occurred just 22 hours after flare #280 and in the same plage. As can be seen by comparing Figures 5-2 and 5-3, the flaring regions were almost identical in appearance for these two events. The existence of a class of successive flares which take place in the same region and show a common pattern of structure was first reported by Waldmeier (1938) and confirmed by Dodson and Hedeman (1949). Ellison et al. (1960), suggested the term "homologous" be used to describe this class of flares. The term can also apply to successive radio bursts which have similar characteristics (Fokker, 1968), as well as to similar X-ray bursts (Fortini, 1963). In fact Pinter (1969b) notes that the very events investigated in the present study are excellent examples of such homologous X-ray bursts. Thus, the fact that the events of 24 and 25 March 1968 belong to this special class should be kept in mind when considering the results described below.

2. Hα ISOPHOTOMETRY

Selected frames of the film record for the three flares just discussed were analyzed by the McMath-Hulbert Observatory isophotometer. An early version of the instrument used in the present study has been described by Mohler and Pierce (1957). Basically, the isophotometer has an analyzing light beam which is focused on a small portion of the film being measured. The light transmitted by that point on the film is sensed by a photoelectric cell which controls the rotation of a mechanical cam. At certain positions of the cam, it trips a micro-switch which causes a pen to mark a precise position on a sheet of paper. Thus,

a mark is made whenever the analyzing light beam encounters one of several, discrete values of photographic density on the film.

The film itself is mounted on a carriage which moves it past the analyzing beam according to a preselected routine. In order to photometer the entire area of interest on the film, this routine proceeds as follows: first the area is scanned over its full width; then the film carriage is returned by the identical path to the side on which it began; next it is displaced a small amount in the perpendicular direction and the above steps are repeated. This continues until the whole area has been covered.

A mechanical coupling causes a sheet of paper to be moved beneath the marking pen in exact synchronism with the motion of the film carriage. Thus, while the analyzing light beam is scanning the film, the pen "scans" the sheet of paper marking those points which correspond to positions on the film having certain photographic densities. The microswitch which activates the pen operates only when the film carriage is travelling in a given direction, eliminating the effects of backlash in the associated gear trains. The above procedure slowly builds a set of contours, called isophotes, which represent lines of equal density on the film being photometered. Figure 5-4 shows some examples of the isophotes derived from the 25 March 1968 flare. Also shown is the relative size of the analyzing light beam, which was selected to match the resolution of the flare image on the patrol film. This resolution is about 5 arc-sec, which is equivalent to 4×10^3 km at the center of the solar disk.

In addition to controlling the rotation of the mechanical cam, the isophotometer's photoelectric cell also drives the pen of a chart-recorder. Thus,

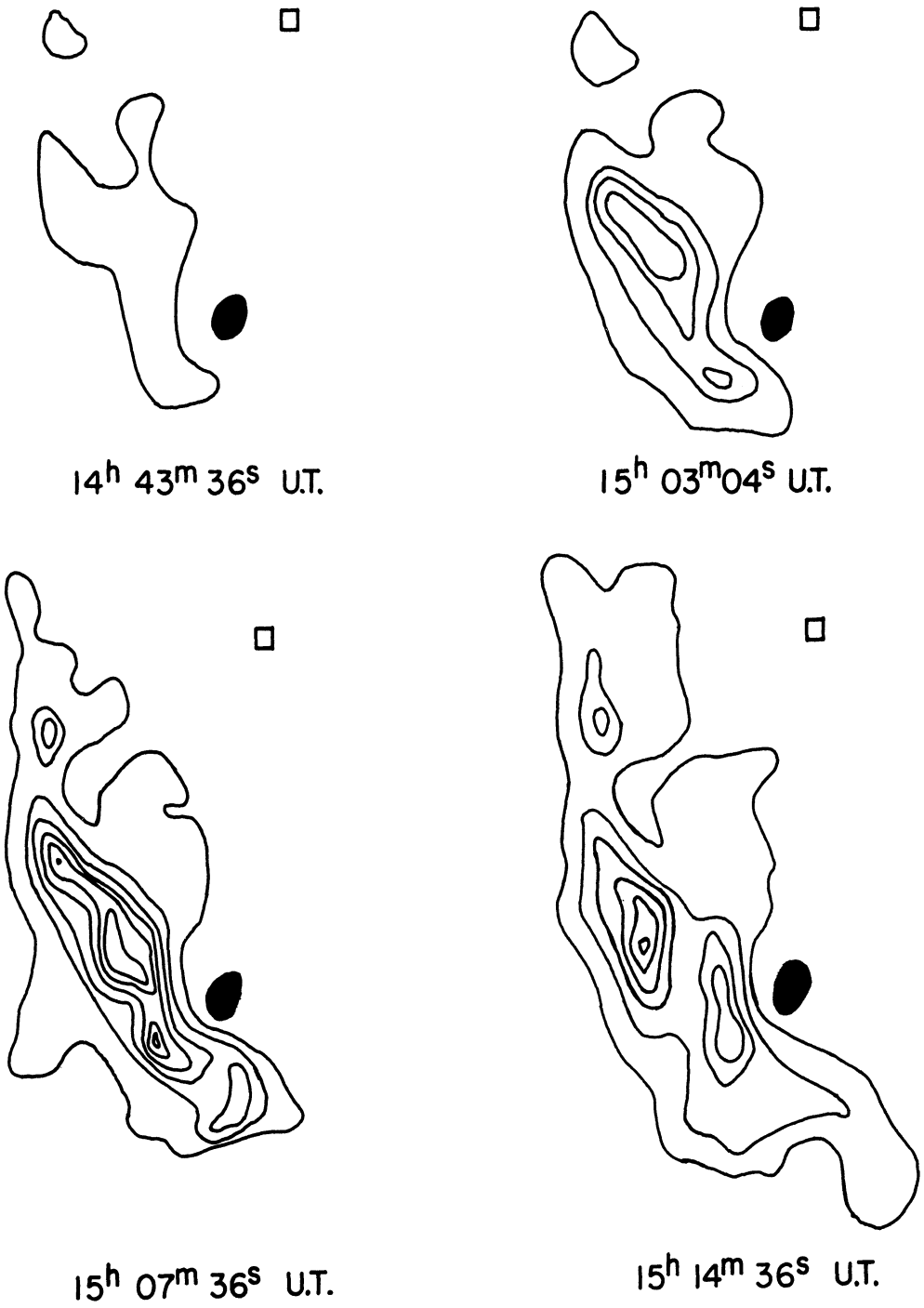

Figure 5-4. Representative Hα isophotes of the 1b flare on 25 March 1968. Each contour represents a line of constant photographic density on the filtroheliogram and thus constant intensity within the flaring region. The filled circles are the contours of the main sunspot in the plage. The small rectangle indicates the size of the isophotometer's analyzing light beam.

a given density on the film gives rise to a corresponding deflection D on the chart-recorder. It will be implicitly understood in the following that any reference to the photographic density of some feature actually refers to its measured chart-recorder deflection.

In the Appendix of this paper, it is shown that the enhancement of Hα emission during a flare can be related to the parameter R'_c which is defined as:

$$R'_c = \sum_{c}^{c(max)} (A_c - A_{c+1}) \cdot \frac{\bar{P}'_c - P_\mu}{P_o} \qquad (5.1)$$

where:

A_c is the area (actually the corresponding solid-angle in steradians) within contour c,

c(max) is the innermost contour,

P_μ and P_o are the measured, undisturbed Hα intensities at the heliocentric distance of the flare and the center of the solar disk respectively, and

$\bar{P}'_c$ is a flare intensity which falls between contours c and c+1 as defined in the Appendix.

To find the appropriate intensity values for this expression, the characteristic curve P = f(D) must be determined for the film. This was done by measuring the photographic densities for the set of calibration spots which are impressed on each filtroheliogram (see Figure 5-1, 5-2, or 5-3) and using Teske's measurements of the relative intensities of these spots (personal communication). As mentioned in the Appendix, we have found that the derived value of R'_c is very sensitive to slight changes in the characteristic curve used. Therefore, we

have determined it individually for each exposure analyzed in the present study. Once the characteristic curve is known and the photographic densities of the various contours D_c and undisturbed disk center D_o are measured, the intensity ratios $\bar{P}'_c/P_o$ necessary for equation (5.1) can be found by means of the relations given in the Appendix.

The area values A_c were measured by planimetering the appropriate contours in each isophote. To improve the accuracy of these measurements and eliminate one source of systematic error, each area was planimetered four times in one direction and an equal number in the other direction. The mean of these eight values was then taken to be the area within the contour in question.

The intensity ratio P_μ/P_o which appears in equation (5.1) is the same for all filtroheliograms of a given flare. The ratios used for the three flares investigated here were taken from the limb-darkening study by O. R. White (1962) and are listed in Table 5.3.

TABLE 5.3

DATA FOR THE REDUCTION OF THE ANALYZED FLARES

Date	μ	$W_\mu(H\alpha)/W_o(H\alpha)$	P_μ/P_o	P_*/P_μ	φ	z
26 March 1967	.858	0.88	0.96	1.24	1.36	3.3
24 March 1968	.995	1.00	1.00	1.25	1.27	3.3
25 March 1968	.967	0.97	0.99	1.24	1.12	3.3

Also listed are the appropriate values of the following parameters:

μ, the flare's heliocentric distance ($\cos\theta$);

$W_\mu(H\alpha)/W_o(H\alpha)$, the ratio of the undisturbed Hα equivalent width at μ to that at the center of the solar disk (derived from David, 1961);

P_*/P_μ, the relative intensity to which all measurements of a given flare were standardized;

φ, the conversion factor between the total relative flux and the relative flux standardized to P_*/P_μ;

z, the figure of merit for the filtroheliograph (kindly supplied by Dr. Dodson-Prince, personal communication).

(A more comprehensive definition of these parameters can be found in the Appendix.)

The above values are needed in order to convert the relative flux values R'_c, given by (5.1), into the total enhancement of Hα emission during the flare $\Delta S(H\alpha,t)$. This is done in two steps. First the standardized relative flux R'_* is derived from values of R'_c for a given isophote by one of the relations (A.27 or A.29) given in the Appendix. Then $\Delta S(H\alpha,t)$ can be found from R'_* by the following expression:

$$\Delta S(H\alpha,t) = 7.2 \times 10^{33} \frac{W_\mu(H\alpha)}{W_o(H\alpha)} \varphi R'_*(t) \text{ erg/sec} \qquad (5.2)$$

which is derived from equation (A.30) of the Appendix.

It is difficult to know the relative error in $\Delta S(H\alpha,t)$ resulting from the above reduction procedure. However, we have investigated the internal consistency of the isophote planimetry and the effects of reasonable inaccuracies in the determination of photographic densities and the films' characteristic curves for measurements made in the present study. From this analysis, we have estimated

the relative error for the March 1968 flares to be about 6%. Because the film record for the March 1967 flare was somewhat lower in quality, we have assigned a 10% uncertainty to its values.

The enhanced Hα emission curves for these three flares are presented in the next section.

3. GENERAL COMPARISON OF THE SOFT X-RAY AND Hα EVENTS

For the 24 March 1968 flare, Figure 5-5 shows the time development of the 8-12 Å emission rate $\Delta S(8,12;t)$ observed by the Michigan soft X-ray detector, the Hα emission rate $\Delta S(H\alpha,t)$ derived in the previous section, and the intensity of the flare's brightest point I_{max}/I_o as found by the method described in the Appendix. To the author's knowledge, this is the first direct comparison of the absolute rates of X-ray and Hα emission during a flare. The X-ray emission remained enhanced until about 1834 UT, so measurements made at 1738 and 1834 UT are also indicated on the figure.

Although it may not be obvious by casual inspection, the X-ray emission curve follows more closely the total Hα emission curve than it does the Hα intensity curve. For example, the emission curves peak simultaneously, while the intensity reaches its maximum about three minutes earlier. In addition, the intensity falls to its pre-flare level before 1738 UT, while the total Hα emission remains enhanced after that time, as does the X-ray emission. However, it should be noted that by 1834 UT the X-ray burst has ended, yet the Hα emission still remains high due to a great post-flare increase in the size of the associated plage. Another similarity in the two emission rate curves is

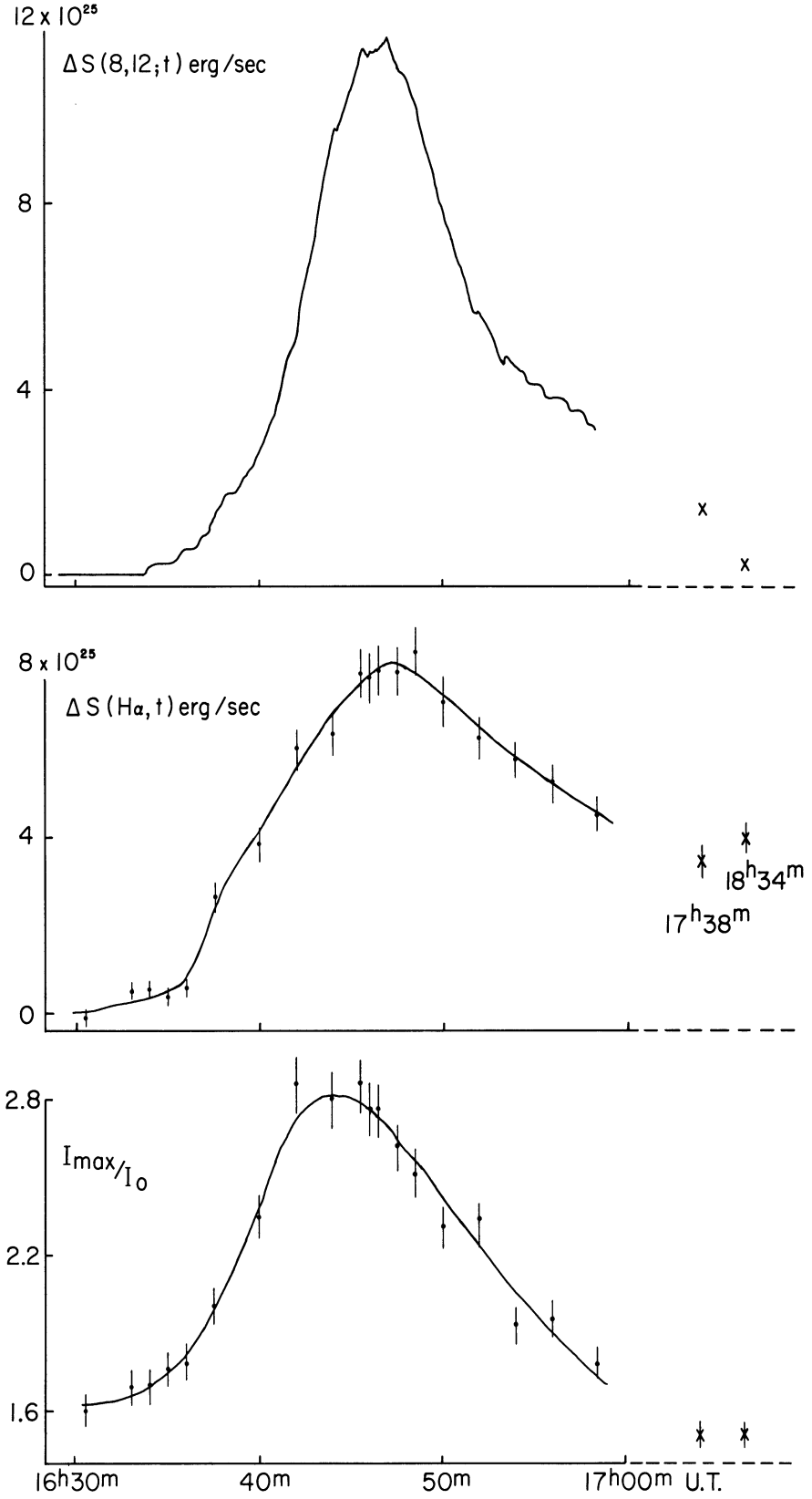

Figure 5-5. Comparison of the 8-12 Å emission rate (top), Hα emission rate (middle), and Hα intensity (bottom) during the 1b flare on 24 March 1968. Additional values at 1738 UT and 1834 UT are indicated by x. The relative error for measurements of the total Hα emission rate is 6%, while that for the intensity is 4%.

the "bump" at about 1638 UT. But the existence of this feature is somewhat doubtful in Hα since it is defined by only one measured point.

Figure 5-6 shows the corresponding curves for the 25 March 1968 flare. Here each of the three features in the Hα emission curve is definitely established and each has a clear counterpart in the associated X-ray burst. This excellent correspondence implies a very close relation indeed between the energetics of the Hα and soft X-ray events.

The Michigan detector was in its operating mode of high sensitivity for the first few minutes of this burst (indicated by the short, elevated segment in the $\Delta S(8,12;t)$ figure). When this portion of the event is plotted on the same vertical scale as the rest of the burst (shown in the main curve of the figure), it becomes apparent what a subtle enhancement this initial rise represents. It is evident that this initial, very gradual rise would not have been detected if the Michigan instrument had been in its low sensitivity mode, which agrees with the statistical results discussed in Chapter IV. But even considering the high sensitivity data, the Hα enhancement starts before the X-ray enhancement in the present case; indeed, this is true for all three of the features in the emission curves for the 25 March 1968 flare. In fact, for all three of the flares investigated here, the Hα event starts before its associated soft X-ray burst. This is atypical, but by no means rare, for soft X-ray bursts which accompany Hα flares in general, as demonstrated in Chapter IV.

Figure 5-6 shows that the 25 March 1968 flare consisted of two main phases, one at roughtly 1450 UT and another at 1505 UT. The ratio of the amplitudes of these two peaks is less than 2:1 for the Hα intensities, nearly 3:1 for the Hα

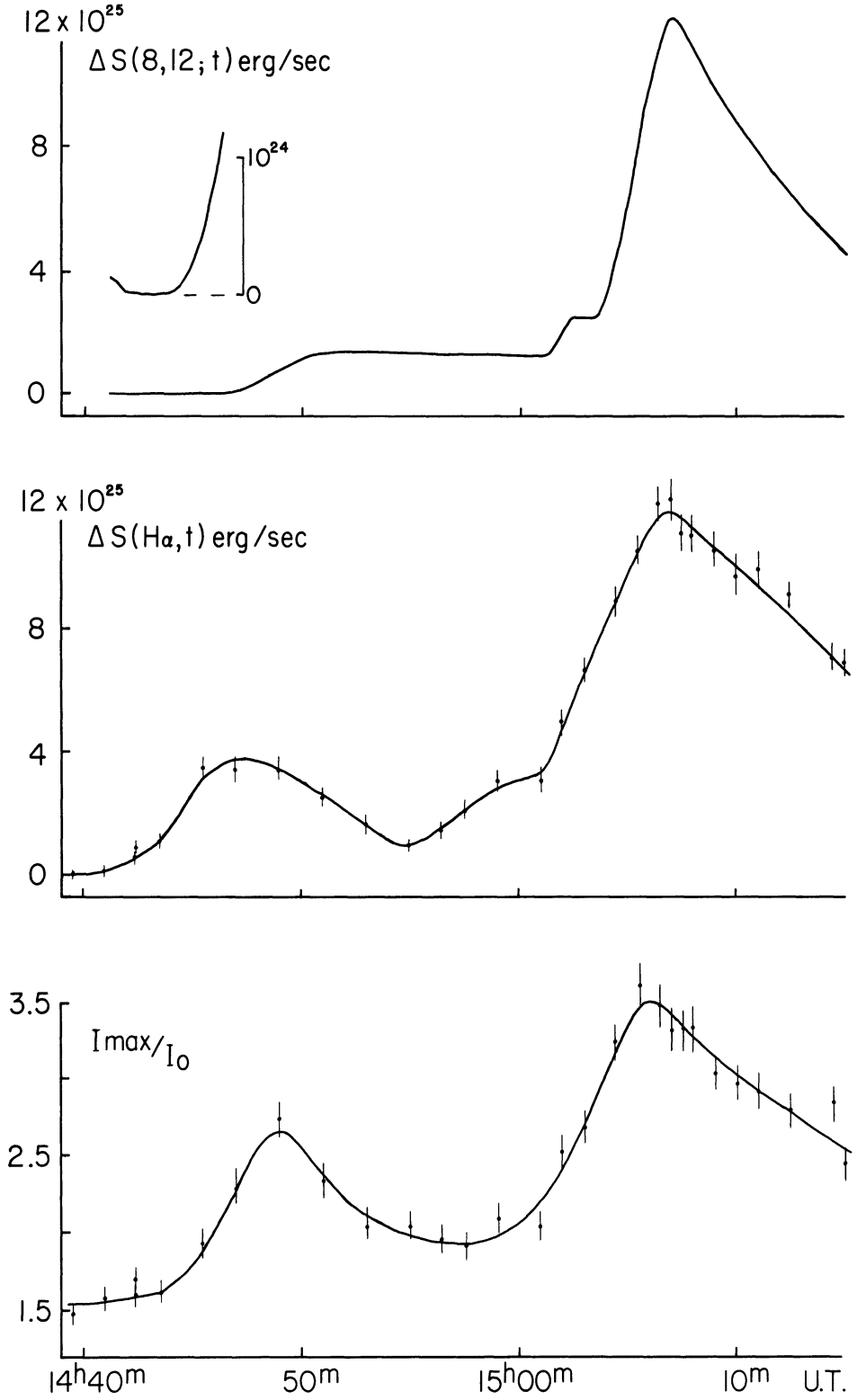

Figure 5-6. Comparison of the 8-12 Å emission rate (top), Hα emission rate (middle), and Hα intensity (bottom) during the 1b flare on 25 March 1968. The short, raised segment in the graph at top shows X-ray data obtained by the Michigan detector while in its high sensitivity mode of operation. This segment is plotted on a magnified ordinate scale. The relative error for measurements of the total Hα emission rate is 6%, while that for the intensity is 4%.

emission rates, but almost 10:1 for the emission rates of the 8-12 Å radiation. This implies that during the flare (a) the X-ray producing mechanism is much more sensitive than the Hα mechanism to changes in the physical conditions of the emitting region, (b) the physical characteristics of the X-ray emitting region undergo much stronger variations than those of the region emitting Hα radiation, or (c) some combination of the above. It is also interesting to note that the Hα emission rate peaks before the intensity curve during the first phase of this flare but after it during the second phase. Both Hα curves peak well before the first X-ray maximum, while the Hα and X-ray emission rates peak simultaneously at the second maximum.

Although there are many minor differences, the main impression given by the comparisons just described is the notable similarity in the time profiles of the soft X-ray and Hα emission rates. This is all the more remarkable considering the great differences that must exist in the physical conditions of the two emitting regions. For example, a typical temperature derived from observations of soft X-ray bursts is on the order of a few 10^6 K (see Table 2.2 of Chapter II). Hydrogen would be virtually 100% ionized at such a temperature and thus any Hα emission would be completely negligible. Actually, the temperature appropriate for the Hα emitting region during a flare is roughly 10^4 K (e.g., DeJager, 1959; DeFeiter, 1966). In addition, the densities of the two regions are far different. For the Hα flare, densities of a few 10^{13} cm^{-3} are normally found (DeJager, 1959; Fritzova-Svestkova and Svestka, 1967) while the source of the X-ray burst seems to have a density no greater than 10^{11} cm^{-3} (Vaiana and Giacconi, 1968; Culhane and Phillips, 1969; Friedman and Hamberger,

1969; Hudson et al., 1969a). It is a clear challenge for theoreticians to account for the fact that two emissions arising from such distinct sources can show the remarkable degree of time correlation which is observed in the flares just discussed.

However, the 26 March 1967 flare shows that the relation between the Hα and soft X-ray emission rates is not always a simple one. This flare took place in a relatively small portion of a very large, fragmented region. In that respect, it is different from the two flares previously described, which involved nearly all of the smaller, more compact region in which they occurred. The time development of the X-ray emission rate, total Hα emission rate, and Hα intensity displayed in Figure 5-7 are not at all similar to one another. (To check the reliability of the Hα measurements, eight of the nineteen exposures analyzed for this flare were completely isophotometered a second time. Very good agreement resulted for each pair of values thus obtained.) The disparities among these curves include the differing times of start and maximum as well as the fact that the X-ray burst is a simple one while the Hα event shows two definite components.

These peculiarities also appear in Figure 5-8, which plots the total Hα and soft X-ray emission rates at one-minute intervals during the time development of the three analyzed flares. Times of maximum Hα intensity are indicated by circles in the figure. Although the 26 March 1967 event has such an irregular trace, at least the general slopes of the rising portions for all three flares are nearly the same. In addition, the relation between the Hα and X-ray emission rates on the rising segment of the curve is almost identical

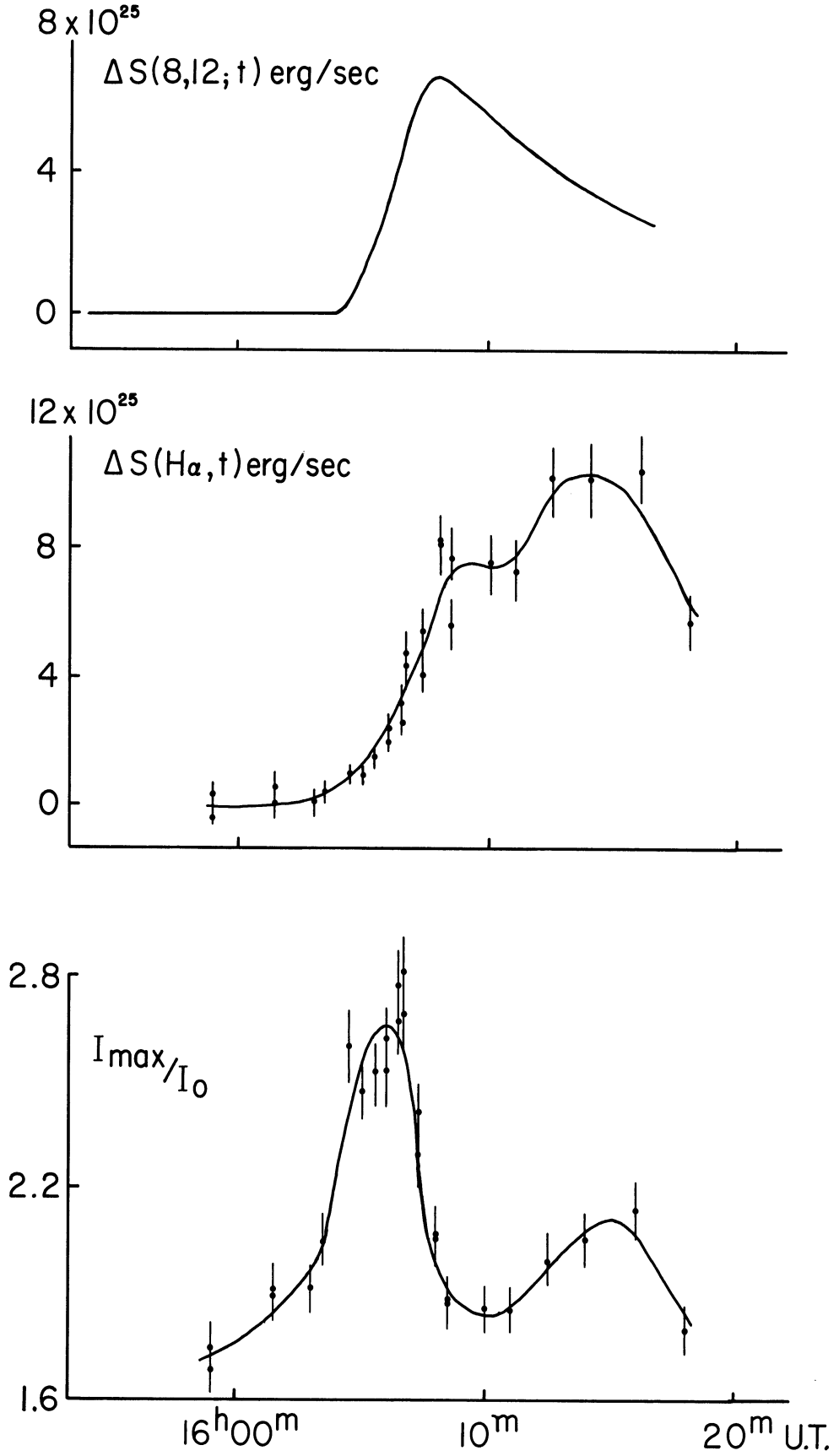

Figure 5-7. Comparison of the 8-12 Å emission rate (top), Hα emission rate (middle), and Hα intensity (bottom) during the 1b flare on 26 March 1967. The relative error for measurements of the total Hα emission rate is 10%, while that for the intensity is 4%.

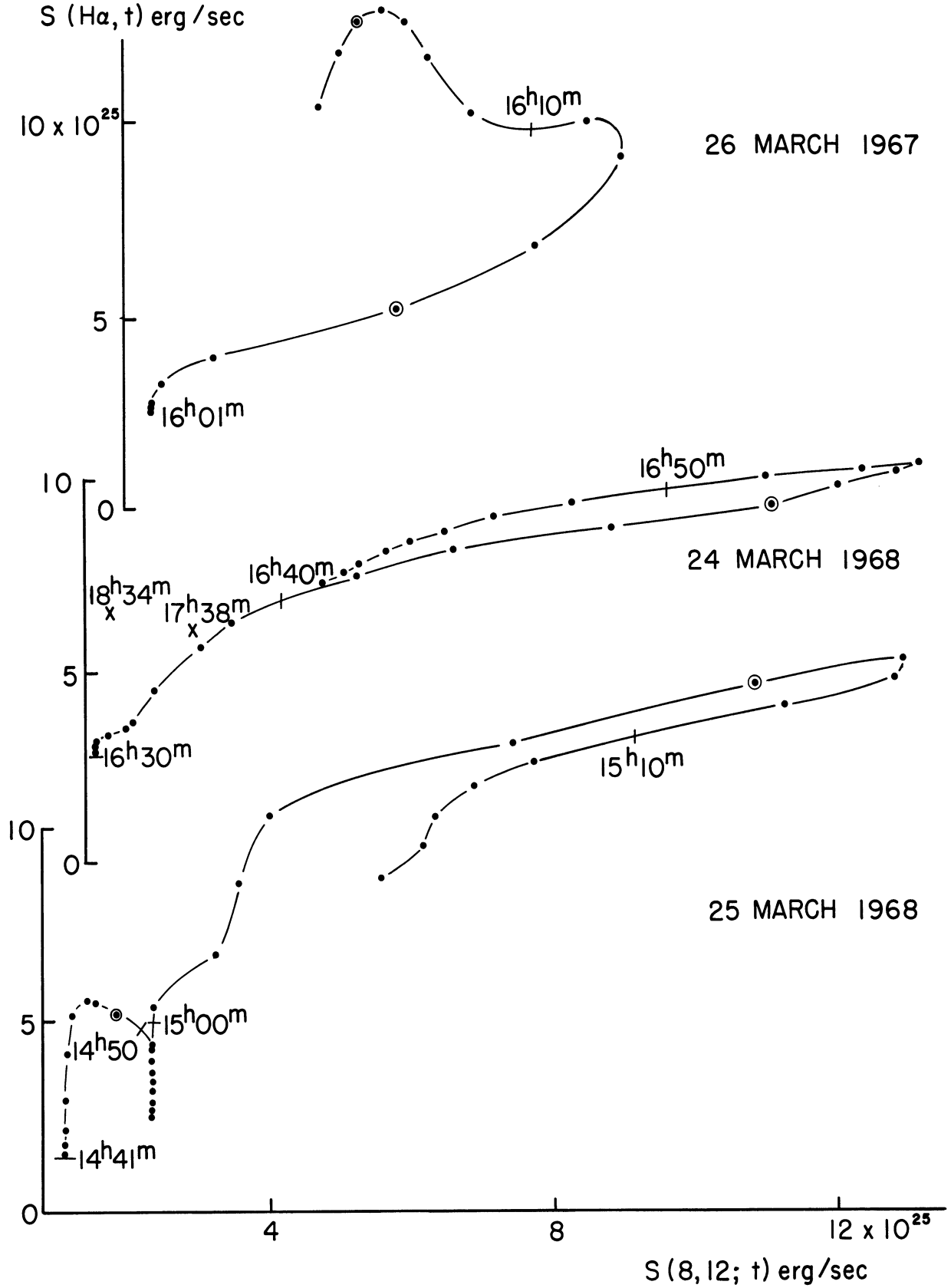

Figure 5-8. Comparison of the Hα and 8-12 Å emission rates for the 1b flares on 26 March 1967 (top), 24 March 1968 (middle), and 25 March 1968 (bottom). Values are plotted at one-minute intervals. Circled points refer to times of maximum Hα intensity.

to that on its falling portion for both 1968 events. The slope that best fits the linear part of these curves shows that near maximum the 8-12 Å emission rate varies roughly 3 times as rapidly as the flare's Hα emission rate. Thus soft X-radiation is a much more sensitive indicator of changes in the flaring region, as had also been implied by the comparison of the two phases of the 25 March 1968 event described earlier.

4. COMPARISON WITH THE RESULTS OF CHAPTER IV

In the previous chapter, several statistical relationships were found between various aspects of an Hα flare and its associated X-ray burst. It would be of interest to investigate the degree to which these relationships hold during individual events, and this has been done for the three flares just discussed.

Unfortunately, the pre-flare levels of the Hα emission rates for these events were not determined well enough to assign a definite photometric starting time to the flares. However, we have already noted that in each case the enhancement in the Hα emission rate was clearly established at the time of the first increase in X-radiation, which is an atypical (but by no means rare) occurrence for flares in general.

The photometric times of the principal maxima for the three flares are listed in Table 5.4.

TABLE 5.4

PHOTOMETRIC TIMES OF MAXIMUM
(All times are in UT)

Date	Hα Intensity	Hα Emission Rate	8-12 Å Emission Rate
26 March 1967	1606	1614	1608
24 March 1968	1644	1647	1647
25 March 1968	1449	1447	1452
	1506	1507	1507

The times of maximum Hα intensity found here all agree nicely (plus or minus one minute) with the flare maximum times for these events listed in the Quarterly Bulletin, and shown in Table 5.1 of this paper. Thus, for flares with well defined maxima, visual inspection of patrol filtroheliograms seems to be a reasonably accurate method for determining the time of a flare's peak intensity; and so studies utilizing these reported maximum times can be regarded with some confidence.

In each of the four cases considered here, the X-ray emission rate peaks after the intensity maximum of the Hα flare, typically by a few minutes. This is precisely the result found by the statistical analysis in Chapter IV. However, (if the average of just four cases is meaningful) the total X-ray and Hα emission rates both reach maximum simultaneously. This is yet another indication of the very close correlation shown by these two components of the flare phenomenon.

All three flares investigated in this chapter are rated 1b, and the photometric analysis described above shows that they have areas and peak

intensities which are typical for that importance. Thus, we cannot consider here the relation between the peak enhancements in soft X-ray and Hα emission rates, ΔS(8,12) and ΔS(Hα), as a function of flare importance. But we can see how closely the peak emission rates for these individual flares match the rates found for 1b flares in general. Table 5.5 lists the values resulting from this study along with the emission rates appropriate for 1b flares as derived from the statistical study in Chapter IV.

TABLE 5.5

PEAK ENHANCEMENTS IN EMISSION RATES
(All emission rates are in 10^{25} erg/sec)

Date	ΔS(Hα)	ΔS(8,12)
26 March 1967	10	7
24 March 1968	8	12
25 March 1968	12	12
"Average" 1b	53	10

Note that the rough approximation method of Chapter IV does indeed result in an overestimate of ΔS(Hα), as had been suggested in that chapter. Apparently, the method predicts values which are about a factor of 5 too high. On the other hand, the individual values of ΔS(8,12) are exactly in line with the "average" amplitude of bursts associated with 1b flares.

The most important result given by this comparison is that, at least for these three flares, the peak enhancement in 8-12 Å radiation is virtually identical to that in Hα. The absolute value of each measurement may be in error by

as much as a factor of 2 (see Chapter II), but even in the worst case, the peak Hα and soft X-ray emission rates would be equal within an order of magnitude.

Finally, we have investigated the time-integrated Hα and soft X-ray energies which were emitted during these flares. Since none of the events was traced continuously to its conclusion, the Hα and X-ray curves for each event were extrapolated down to their pre-flare levels. These extrapolations were made with care but, of course, are little more than well-intentioned guesses. However, in each case the majority of the emission occurred during periods which were covered by observations, so that these extrapolations should not give rise to significant errors.

The results of this study are shown in Table 5.6, along with the appropriate X-ray value found by the statistical study in Chapter IV. The total amounts of 8-12 Å energy emitted during the three flares seem to be quite typical for bursts accompanying 1b flares. But the most important result here is once again the striking similarity in the values of the total energy emitted as Hα radiation and as 8-12 Å X-radiation by these flares. Even considering the possiblity of errors in the absolute calibrations of the above measurements, one must conclude that emission in Hα and in soft X-radiation both contribute very nearly identical amounts to the energy losses of these flares.

TABLE 5.6

TOTAL FLARE EMISSION IN Hα AND 8-12 Å
(All emission values are in 10^{28} erg)

Date	Total Hα Emission	Total 8-12 Å Emission
26 March 1967	9	6
24 March 1968	10	10
25 March 1968	11	13
"Average" 1b	-	10

5. OBSERVATIONS AT OTHER WAVELENGTHS

Observations of the hard X-ray, EUV (Extreme Ultraviolet), and microwave bursts which accompanied the 24 March 1968 flare were also compared to the Hα and soft X-ray events. The data for the hard X-ray burst were supplied by S. R. Kane (personal communication) and refer to the total emission between 0-1.2 Å. The EUV data were derived from SFD observations by R. F. Donnelly (personal communication) using an ionospheric electron-loss rate of $\tau = 20$ seconds. These latter data refer to the emission at 10-1030 Å and should be correct to within a factor of 4. In each case, the measurements were in the form of a time-profile for the burst. These profiles were then planimetered to obtain the time-integrated energies within the appropriate wavelength intervals. For the microwave burst, the peak emission rates and durations at individual frequencies were taken from the reports listed in the SGDB. The emission values which resulted were then integrated between 2000 and 15000 MHz to find the total energy emitted in the microwave burst.

Table 5.7 summarizes the values of the energy involved in each wavelength interval considered for the 24 March event. Hard X-ray emission and microwave radiation, at opposite ends of the spectrum, account for the smallest amounts of energy. In addition, these latter spectral intervals show a very high correlation in their time variations, even with regard to the detailed fine structure of the bursts (e.g., Arnoldy et al., 1967, 1968b; Parks and Winckler, 1969). A much larger amount of energy is released in the form of 8-12 Å X-radiation and Hα emission, which likewise display notable similarities in their time variations as shown by the present study. Of the wavelength intervals considered here, the major source of energy loss in this flare seems to be EUV radiation. The time profile of this emission is often closely related to those of hard X-ray and microwave bursts (Neupert, 1964; Donnelly, 1969a) but also shows characteristics which are comparable to those of soft X-ray and Hα events (Donnelly, personal communication).

TABLE 5.7

TOTAL ENERGY EMISSION DURING THE 24 MARCH 1968 FLARE

	Wavelength Interval	Total Energy Emission (erg)
Hard X-ray	0-1.2 Å	3×10^{26}
Soft X-ray	8-12 Å	1×10^{29}
EUV	10-1030 Å	6×10^{29}
Hα	6563 Å	1×10^{29}
Microwave	2-15 cm	8×10^{22}

The explanation of these relationships among such diverse radiations offers a challenging problem indeed for any potential model of the total flare phenomenon.

CHAPTER VI

SUMMARY

All known mechanisms that may be important for the production of soft solar X-radiation imply that the X-ray emission rate depends mainly upon three characteristics of the emitting region, namely its temperature T, density N, and volume V (Acton, 1964). The relevant temperature and density are normally the electron temperature T_e and the electron density N_e, although this is not always the case (e.g., Boldt and Serlemitsos, 1969). Other parameters, such as the magnetic field strength, may also affect the emission rate, but only by their influence on the region's temperature, density, and volume.

Unfortunately, it is not possible to derive, unambiguously, values for all three of these characteristics from the observations made by the Michigan X-ray experiment because it has no spatial or spectral resolution. Thus, a rigorous model of the X-ray emitting source cannot be constructed by means of the Michigan data alone, but these data can be used to place general constraints on some aspects of such a model. We will discuss here very briefly several of these general considerations based on the results of studies described in previous chapters.

1. THE SLOWLY VARYING COMPONENT

The investigations discussed in Chapter III of this paper point out the close relation between calcium plages and the source of the slowly varying component of solar soft X-radiation. Even without spatial resolution, the data

indicate that the X-ray emitting regions are physically connected with these plages. Their areas, if not identical, are at least closely associated, as shown by the correlation of $E_b(8,12)$ and ΣA. The fact that $E_b(8,12)$ forms an even better correlation with Σ A x I implies that the variations in the temperature and density enhancements which determine the plage's intensity also relate to the X-ray emitting region. The major part of the soft X-radiation apparently originates from a source whose thickness does not depend strongly on its area, since the correlation of $E_b(8,12)$ with $\Sigma A^{3/2}$ x I is no better than that with Σ A x I. A study of individual values within the latter relation gives some evidence that the temperature and/or density of the X-ray emitting region declines as it ages and that emission of soft X-radiation can occur at significant heights above the chromosphere.

The existence of X-radiation from such elevated sources requires localized regions of enhanced temperatures and/or densities within the cooler ambient corona. Comparisons of X-ray observations at several wavelength intervals show that these condensations cannot be isothermal, but apparently consist of a small core at a very high temperature surrounded by more extensive regions of material which becomes cooler with distance from the core. Furthermore, these comparisons indicate that at least some of the condensations which exist during periods when the general level of solar activity is high must be substantially hotter than those observed when the activity-level is low. Perhaps the same basic mechanism which is responsible for increased levels of solar activity also gives rise to further enhancements in the temperatures of the X-ray sources overlying chromospheric plages.

2. THE BURST COMPONENT

The present investigation considered only those X-ray bursts which accompanied well verified Hα flares of importance 1 or greater. In addition, all bursts associated with "sympathetic" flares were eliminated. Thus, the results described here may not apply to all X-ray bursts in general.

The total flare phenomenon almost invariably includes a significant enhancement in soft X-radiation. Some cases of a relatively weak, impulsive component in 8-12 Å bursts have been observed which might be due to nonthermal processes. However, the properties of the general time-profiles for flare-associated enhancements, as well as their frequency of occurrence from center to limb, imply that they are predominantly thermal in nature.

There are three possible mechanisms for this radiation, viz. thermal bremsstrahlumg (free-free), recombination (free-bound), and line emission (bound-bound).

The standard expression for thermal bremsstrahlung indicates that the flux between 8-12 Å from this mechanism is given by:

$$E(8,12) = 5 \times 10^{-52} T_6^{1/2}(e^{-12/T_6} - e^{-18/T_6}) EM \text{ erg/cm}^2\text{sec} \qquad (6.1)$$

where T_6 is the temperature in millions of degrees Kelvin and EM is the radiating region's emission measure in units of cm^{-3}, as defined by:

$$EM = \int N_e^2 \, dV \qquad (6.2)$$

To obtain (6.1), a Gaunt factor of unity was assumed and the emitting plasma was taken to be pure hydrogen. As found in Chapter IV, the average peak en-

hancement in the 8-12 Å radiation accompanying a 1n flare is 0.0183 erg/cm^2 sec, which represents only a moderate-sized burst. Table 6.1 gives the emission measure which would be necessary at various temperatures to account for this peak X-ray enhancement if it were due solely to thermal bremsstrahlung emission.

TABLE 6.1

"1n" X-RAY EMISSION MEASURES DUE TO THERMAL BREMSSTRAHLUNG

Temperature (10^6 K)	Emission Measure (cm^{-3})
1	6.0×10^{54}
2	1.1×10^{52}
5	2.6×10^{50}
10	8.5×10^{49}
20	5.8×10^{49}
50	5.8×10^{49}
100	7.1×10^{49}

The smallest value listed is still more than two orders of magnitude greater than most emission measures reported for any burst observed with detectors having either spatial or spectral resolution (Vaiana and Giacconi, 1968; Beigman et al., 1969; Culhane and Phillips, 1969; Hudson et al., 1969a). Furthermore, of the experiments just cited, the two which most closely match the Michigan detector's response gave rise to determinations of emission measures which were much less than those found at shorter wavelengths. In addition, the smallest value given in Table 6.1 exceeds the emission measure for the entire quiet corona (Mandel'shtam, 1965a)! Therefore, it seems clear that thermal bremsstrahlung radiation is completely negligible at 8-12 Å during flare associated bursts. The dominant mechanisms at these times are therefore recombination and line emission.

The above result is supported by several theoretical calculations of the soft X-ray spectrum. We have already indicated that temperatures in excess of 10 x 10^6 K have not been observed for X-ray bursts near 10 Å (see Chapter II). Culhane (1969) finds that at temperatures less than that value, free-bound radiation dominates all other sources of continuous emission. (He does not explicitly treat line emission.) In addition, Kawabata (1960) reports that for 2-8 Å radiation, free-bound and/or line emission is greater than thermal bremsstrahlung up to temperatures of 30 x 10^6 K. Similar results are also found by Cox and Tucker (1969).

The amplitude of the soft X-ray burst depends in a statistical sense on the area of the Hα flare which it accompanies. Thus, the sizes of these emitting volumes are presumably somehow related. In addition, larger X-ray bursts are associated with flares of a given size which are exceptionally bright. Using measurements of the halfwidth of high Balmer lines during flares, Svestka and Fritzova-Svestkova (1967) have found that such intensity variations in the case of Hα radiation are due to changes in the density of the flaring region. Therefore, these same density variations quite likely also extend into the region of the X-ray burst's emission.

Soft X-ray bursts tend to have larger amplitudes when the general level of solar activity is high, or when the burst accompanies a flare which occurs in a young, flare-rich plage. This fact can again be explained by the effect of additional density enhancements in the X-ray emitting source under these conditions. Furthermore, there is some evidence that a region associated with a sunspot group of a given area can give rise to X-ray bursts no greater than a

certain limiting value in amplitude, and that this amplitude limit increases with the size of the spot group. Thus, it is possible that the X-ray emission rate is governed by the temperature and density of the source region, but confined to a range given by the region's magnetic energy density.

Bursts of soft X-radiation also tend to have larger amplitudes when accompanied by radio bursts which have strong cm-wavelength enhancements. Unfortunately, the physical interpretation of this observation is not at all clear from the Michigan experiment.

The time-profile of the soft X-ray burst is quite similar to that of its associated Hα flare. This is true when the Hα intensity of the flare is considered; but the time-correlation is even more striking when the X-ray and Hα flux curves are compared. It is not obvious how to account for such a close correlation between these two emissions since they originate from regions having completely different physical characteristics.

One possibility is that the time variation of each emission process is governed by the energy source term rather than the decay term as is normally assumed (cf. Acton, 1964; Hudson et al., 1969a; Takakura, 1969). Thus the temperature and/or density enhancements which give rise to the Hα and X-ray events must be continuously maintained by the flare's source of energy (commonly believed to be the reconnection of magnetic field lines). By this hypothesis, the decay time-scale of the temperature-density enhancement in the absence of such a supporting mechanism would be small compared to the time scale of the flare itself. Furthermore, the mechanism which causes this temperature-density enhancement would have to affect both the Hα and X-ray emitting sources at the

same time and by proportionate amounts. Such a hypothesis is not totally new since many workers have found it necessary to suggest that a continuous supply of energy must be involved even during the flare's decline (Kawabata, 1966b; Oster and Sabatino, 1966; Holt and Ramaty, 1969; Zirin et al., 1969).

X-ray observations are important to our knowledge of the flare phenomenon because they refer to the hottest portions of the event. But they are of even greater interest since an enhancement in the soft X-ray emission appears to be the very first manifestation of a solar flare, at least on the average. Thus, such observations give information about the earliest phases of the event and may eventually lead to an understanding of the conditions which cause a flare to occur. This would be a strong step toward the very desirable ability to predict accurately the onset of a solar flare well in advance.

Yet there is another, more fundamental, reason for the importance of soft X-ray observations. Emission in the form of soft X-radiation accounts for a significant portion of the total electromagnetic energy released by a solar flare. The amount is nearly identical to that emitted as Hα radiation, which has historically been considered as "the" flare phenomenon. Indeed the energy released in just the four-Ångstrom interval between 8-12 Å may actually comprise about one-tenth of the flare's total emission over the entire electromagnetic spectrum!

Obviously, the present studies, described at such great length above, have by no means answered all of the questions that can be posed concerning flare-associated soft X-radiation. In fact, they undoubtedly have raised more questions than they have answered. But if the problem of solar flares has not yet been solved, it has not been through lack of effort. Indeed, these phenomena have been the object of countless observational and theoretical investigations since 1859, when the first recorded observations of a solar flare were reported independently by Carrington (1859) and Hodgson (1859). In spite of this enormous amount of work, many aspects of the flare's mechanism(s) remain obscure.

Perhaps the problem is too difficult. As Parker (1964) has cautioned:

> "We should be aware that we are observing an extremely complex phenomenon. There is always the chance—which we don't want to think about yet—that we will not succeed in unraveling the basic nature of the flare process."

However, the present author is more optimistic. With the advent of observations made from space vehicles, measurements of the flare's emission throughout the entire electromagnetic spectrum are now becoming available for the first time. Such measurements will provide a vast amount of new information to aid in the explanation of the flare phenomenon and its cause. We believe that much of this information will come from observations of the sun's soft X-radiation. Future investigations of this spectral region will undoubtedly greatly enhance our knowledge of the energetic processes associated with solar flares and, in turn, will lead to a better understanding of the sun itself.

REFERENCES

Aarons, J., (1963), "Radio Astronomical and Satellite Studies of the Atmosphere," North-Holland Press: Amsterdam.

Acton, L. W., (1964), Doctoral Thesis, University of Colorado.

_____, (1968), Ap.J. 152, 305.

Acton, L. W., Chubb, T. A., Kreplin, R. W., and Meekins, J. F., (1963), J.G.R. 68, 3335.

Allen, C. W., (1965), Space Science Rev. 4, 91.

_____, (1969), Solar Phys. 8, 72.

Angle, K. L., (1968), A.J. 73, 553 (Abstract).

Arnoldy, R. L., Kane, S. R., and Winckler, J. R., (1967), Solar Phys. 2, 171.

_____, (1968a), Ap.J. 151, 711.

_____, (1968b), I.A.U. Symposium 35, 490.

Athay, R. G., (1966), Ap.J. 146, 223.

Becker, U., (1958), Zs.f.Ap. 44, 243.

Behr, A., and Siedentopf, H., (1952), Zs.f.Ap. 30, 177.

Beigman, I. L., and Vainshtein, L. A., (1969), Kosmich. Issled. (In press.)

_____, Grineva, Yu. I., Mandel'shtam, S. L., Vainshtein, L. A., and Zhitnik, I. A., (1969), Solar Phys. 9, 160.

Billings, D. E., (1959), Ap.J. 130, 961.

_____, and Roberts, W. O., (1953), Ap.J. 118, 429.

Blake, R. L., Chubb, T. A., Friedman, H., and Unzicker, A. E., (1963a), Space Research 4, 785.

_____, (1963b), Ap.J. 137, 3.

_____, (1965a), Ap.J. 142, 1.

REFERENCES (Continued)

Blake, R. L., Chubb, T. A., Friedman, H., and Unzicker, A. E., (1965b), Ann. d'Ap. 28, 583.

Boischot, A., and Denisse, J. F., (1957), Compt. rend. 245, 2199.

Boldt, E., and Serlemitsos, P., (1969), Ap.J. 157, 557.

Bowen, P. J., Norman, K., Pounds, K. A., Sanford, P. W., and Willmore, A. P., (1964), Proc. Royal Soc. London (A) 281, 538.

Boyd, R. L. F., (1965), Space Science Rev. 4, 35.

Brandt, J. C., (1969), Solar Phys. 6, 171.

Broadfoot, A. L., (1967), Ap.J. 149, 675.

Bruzek, A., (1967), "Physics of Solar Flares: the Energy and Mass Problem" in "Solar Physics" (ed. J. N. Xanthakis), Interscience: New York, p. 399.

Burnight, T. R., (1949), Phys. Rev. 76 (series 2), 165.

Carrington, R. C., (1859), M.N.R.A.S. 20, 13.

Castelli, J. P., Aarons, J., and Michael, G. A., (1968a), I.A.U. Symposium 35, 601.

_____, (1968b), Ap.J. 153, 267

Chambe, G., and Sain, M., (1969), Astron. and Astrophys. 2, 133.

Chitnis, E. V., and Kale, P., (1966), Space Research 7, 1394.

Chubb, T. A., Friedman, H., Kreplin, R. W., and Kupperian, J. E. Jr., (1957), J.G.R. 62, 389.

_____, Friedman, H., and Kreplin, R. W., (1960), J.G.R. 65, 1831.

Cimino, M., (1967), "Solar Phenomena," Osservatorio Astronomico di Roma, No. 111-116.

Cline, T. L., Holt, S. S., and Hones, E. W. Jr., (1968), J.G.R. 73, 434.

REFERENCES (Continued)

Comper, W., (1959), Sz.f.Ap. 47, 34.

Conner, J. P., Evans, W. D., Montgomery, M. D., Singer, S., and Stogsdill, E. E., (1964), Space Research 5, 546.

Cooke, B. A., Pounds, K. A., Russell, P. C., and Stewardson, E. A., (1962), Proc. Phys. Soc. London 79, 883.

Coutrez, R., Gouze, R., Koeckelenbergh, A., Pourbaix, E., and Roquigny, R., (1963), "Contribution to the Study of SEA's and Associated Events" in "Radio Astronomical and Satellite Studies of the Atmosphere" (ed. J. Aarons), North-Holland Press: Amsterdam, p. 476.

Covington, A. E., (1959), "Paris Symposium on Radio Astronomy" (ed. R. N. Bracewell), Stanford University Press, p. 159.

_____, and Harvey, G. A., (1958), J. Royal Astron. Soc. Canada 52, 161.

Cox, D. P., and Tucker, W. H., (1969), Ap.J. 157, 1157.

Culhane, J. L., Personal Communication.

_____, (1969), M.N.R.A.S. 144, 375.

_____, and Phillips, K. J. H., (1969), "Solar X-ray Bursts at Energies Less than 10 kev Observed with OSO-IV," Preprint: Mullard Space Science Laboratory, Department of Physics, University College London.

_____, Willmore, A. P., Pounds, K. A., and Sanford, P. W., (1963), Space Research 4, 741.

_____, Sanford, P. W., Shaw, M. L., Pounds, K. A., and Smith, D. G., (1968) AAS Special Meeting on Solar Astron., Tucson, Arizona, February 1968.

_____, Sanford, P. W., Shaw, M. L., Phillips, K. J. H., Willmore, A. P., Bowen, P. J., Pounds, K. A., and Smith, D. G., (1969), M.N.R.A.S. 145, 435.

David, K. H., (1961), Zs.f.Ap. 53, 37.

DeFeiter, L. D., (1966), "Analysis of the Balmer Spectrum of Solar Flares," Recherches Astronomiques de l'Observatoire d'Utrecht, XVIII (2).

REFERENCES (Continued)

DeJager, C., (1952), Rech. Astron. Obs. Utrecht 13, Part 1.

_____, (1959), Handbuch der Physik, Vol. LII, p. 80.

_____, (1964), "Research in Geophysics," Vol. 1, M.I.T. Press: Cambridge (Mass.).

_____, (1965a), I.A.U. Symposium 23, 45.

_____, (1965b), Ann. d'Ap. 28, 125.

DeMastus, H. L., and Stover, R. R., (1967), P.A.S.P. 79, 523.

Dickerman, P. J., and Thornton, E., (1966), "Solar Physics 1958-1964," NASA SP-100.

Dodson-Prince, H. W., Personal Communication.

Dodson, H. W., and Hedeman, E. R., (1949), Ap.J. 110, 242.

_____, (1960), J.G.R. 65, 123.

_____, (1964), Planetary Space Science 12, 393.

_____, (1968), World Data Center A: ESSA Research Laboratory Report UAG-2, August.

_____, (1969a), "Description and Evaluation of the Major Hα Flare, May 23, 1967," World Data Center A: ESSA Research Laboratory Report UAG-5, p. 7, February.

_____, (1969b), "The History and Morphology of Solar Activity 1964-1965" in Annals of the IQSY, Vol. 4, M.I.T. Press, p. 3.

_____, (1969c), Nobel Symposium 9, 37.

_____, (1970), Solar Phys. (In press.)

_____, Hedeman, E. R., and McMath, R. R., (1956), Ap.J. Supp. 2, 241.

Donnelly, R. F., Personal Communication.

_____, (1968a), Solar Phys. 5, 123.

REFERENCES (Continued)

Donnelly, R. F., (1968b), "Early Detection of a Solar Flare: A Study of X-ray, Extreme Ultraviolet, H-alpha, and Solar Radio Emission from Solar Flares," ESSA Technical Report ERL 81-SDL 2, July.

_____, (1969a), Ap.J. 158, L165.

_____, (1969b), "Contribution of X-ray and Extreme Ultraviolet Radiation of Solar Flares to Sudden Frequency Deviations," ESSA Technical Report ERL 95-SDL 7, February.

Drake, J. F., Personal Communication.

_____, (1969), "Characteristics of 2-12 Å Solar X-ray Flares," University of Iowa Report No. 69-41, August.

Ellison, M. A., (1943), M.N.R.A.S. 103, 3.

_____, (1949), M.N.R.A.S. 109, 3.

_____, (1952), Publ. Royal Obs. Edinburgh 1, 75.

_____, (1957), Vistas in Astron. 2, 799.

_____, (1963a), Planetary Space Science 11, 597.

_____, (1963b), Quart. J. Royal Astron. Soc. (London) 4, 62.

_____, McKenna, S. M. P., and Reid, J. H., (1960), Dunsink Obs. Publ. 1, No. 1.

Elwert, G., (1956), Zs.f.Ap. 41, 67.

_____, (1963), Proc. Intern'l Conf. Ionosphere, July 1962, p. 57.

_____, (1964), AAS-NASA Symposium on the Physics of Solar Flares, NASA SP-50, p. 365.

_____, (1968), I.A.U. Symposium 35, 439.

Evans, J. W., Dunn, R. B., Firor, J. W., Goldberg, L., Neupert, W. M. Newkirk, G. A., Pierce, A. K., Reeves, E. M., and Glaser, H., (1969), "Position Paper of the Astronomy Missions Board," NASA SP-213.

Evans, K., and Pounds, K. A., (1968), Ap.J. 152, 319.

REFERENCES (Continued)

Falciani, R., Landini, M., Righini, A., and Rigutti, M., (1968), I.A.U. Symposium 35, 451.

Fokker, A. D., (1968), I.A.U. Symposium 35, 553.

Fortini, T., (1963), Ap.J. 138, 278.

Friedman, H., (1962), Rep. Prog. Phys. 25, 163.

_____, (1963a), I.A.U. Symposium 16, 45.

_____, (1963b), Ann. Rev. Astron. Ap. 1, 59.

_____, (1964), AAS-NASA Symposium on the Physics of Solar Flares, NASA SP-50, p. 147.

Friedman, M., and Hamberger, S. M., (1969), Solar Phys. 8, 104.

Fritz, G., Kreplin, R. W., Meekins, J F., Unzicker, A. E., and Friedman, H., (1967), Ap.J. 148, L133.

Fritzova-Svestkova, L., and Svestka, Z., (1967), Solar Phys. 2, 87.

Garcia, J. D., and Mack, J. E., (1965), J. Opt. Soc. Amer. 55, 654.

Giacconi, R., Gursky, H., and VanSpeybroeck, L. P., (1968), Ann Rev. Astron. Ap. 6, 373.

Giovanelli, R. G., (1938), Ap.J. 88, 204.

_____, (1939), Ap.J. 89, 555.

_____, (1940), Ap.J. 91, 334.

Goldberg, L., (1967), Ann. Rev. Astron. Ap. 5, 279.

Hallam, K. L., (1964), AAS-NASA Symposium on the Physics of Solar Flares, NASA SP-50, p. 63.

Hinteregger, H. E., (1965), Space Science Rev. 4, 461.

Hodgson, R., (1859), M.N.R.A.S. 20, 15.

Holt, S. S., and Cline, T. L., (1968), Ap.J. 154, 1027.

REFERENCES (Continued)

Holt, S. S., and Ramaty, R., (1969), Solar Phys. 8, 119.

Horan, D. M., Personal Communication.

Hudson, H. S., Peterson, L. E., and Schwartz, D. A., (1969a), Ap.J. 157, 389.

Hudson, H., McKenzie, D., Zirin, H., and Ingham, W., (1969b), Bull. Amer. Astron. Soc. 1, 280 (Abstract).

Hulburt, E. O., (1938), Phys. Rev. 53, 344.

Jones, B. B., Freeman, F. F., and Wilson, R., (1968), Nature 219, 252.

Kane, S. R., Personal Communication.

_____, (1969), Ap.J. 157, L139.

_____, and Winckler, J. R., (1969), Solar Phys. 6, 304.

Kawabata, K., (1960), Rep. Ionos. Space Res. Japan 14, 405.

_____, (1963), I.A.U. Symposium 16, 143.

_____, (1966a), Rep. Ionos. Space Res. Japan 20, 118.

_____, (1966b), Rep. Ionos. Space Res. Japan 20, 107.

Kiepenheuer, K. O., (1964), AAS-NASA Symposium on the Physics of Solar Flares, NASA SP-50, p. 323.

Kreplin, R. W., (1961), Ann. de Geophys. 17, 151.

_____, and Gregory, B. N., (1965), Space Research 6, 1011.

_____, Chubb, T. A., and Friedman, H., (1962), J.G.R. 67, 2231.

Krieger, A. S., and Vaiana, G. S., (1969), Bull. Amer. Astron. Soc. 1, 283 (Abstract).

Kundu, M. R., (1962), J.G.R. 67, 2695.

_____, (1963), Space Science Rev. 2, 438.

_____, (1964), AAS-NASA Symposium on the Physics of Solar Flares, NASA SP-50, p. 335.

REFERENCES (Continued)

Kundu, M. R., (1965), "Solar Radio Astronomy," Interscience Press: New York.

Landini, M., (1967), Solar Phys. 2, 106.

_____, Russo, D., and Tagliaferri, G. L., (1965), Space Research 6, 1041.

Lincoln, J. V., Personal Communication.

Lindsay, J. C., (1964), Planetary Space Science 12, 379.

_____, (1965), Ann. d'Ap. 28, 586.

_____, Neupert, W. M., and Stone, R. G., (1965), "Introduction to Space Science," (ed. W. N. Hess), Gordon and Breach Science Press: New York, p. 605.

LoPresto, J. C., Personal Communication.

Mandel'shtam, S. L., (1965a), Space Science Rev. 4, 587.

_____, (1965b), Ann. d'Ap. 28, 614.

_____, (1967), Appl. Optics 6, 1834.

_____, Tindo, I. P., Voron'ko, Yu., Shurygin, A. I., and Vasiljev, B. N., (1961), Phys. Inst. Acad. Sci. USSR: A108, A109, A110, A133.

_____, Vasiljev, B. N., Voron'ko, Yu., Tindo, I. P., and Shurygin, A. I., (1962), Space Research 3, 822.

Martyn, D. F., Munro, G. H., Higgs, A. J., and Williams, S. E., (1937), Nature 140, 603.

Maunder, A., (1907), M.N.R.A.S. 67, 451.

McIntosh, P. S., (1967), included in "White-Light Solar Flare and the May 25th Aurora," Sky and Telescope 34, 57.

Meekins, J. F., Kreplin, R. W., Chubb, T. A., and Friedman, H., (1968), Science 162, 891.

Meisel, D. D., (1968), Solar Phys. 5, 575.

Michard, R., and Ribes, M. E., (1968), I.A.U. Symposium 35, 420.

REFERENCES (Continued)

Mitra, A. P., (1965), Space Research 6, 558.

Mohler, O. C., and Pierce, A. K., (1957), Ap.J. 125, 285.

Moore, C. E., Minnaert, M. G. J., and Houtgast, J., (1966), "Second Revision of Rowland's Preliminary Table of Solar Spectrum Wavelengths," National Bureau of Standards Monograph 61.

Mount, G. H., Personal Communication.

Muney, W. S., and Underwood, J. H., (1968), A. J. 73, S72 (Abstract).

Negus, C. R., and Glencross, W. M., (1968), Nature 220, 48.

Neupert, W. M., Personal Communication.

_____, (1964), AAS-NASA Symposium on the Physics of Solar Flares, NASA SP-50, p. 49.

_____, (1967), Solar Phys. 2, 294.

_____, (1968), I.A.U. Symposium 35, 404.

_____, (1969), Ann. Rev. Astron. Ap. 7, 121.

_____, White, W. A., Gates, W. J., Swartz, M., and Young, R. M., (1969), Solar Phys. 6, 183.

Newton, H. W., and Barton, H. J., (1937), M.N.R.A.S. 97, 605.

Noci, G., and Russo, D., (1964), Space Research 5, 517.

Ohki, K., (1969), Solar Phys. 7, 260.

Oster, L., and Sabatino, S., (1966), Ap.J. 143, 944.

Paolini, F. R., Giacconi, R., Manley, O., Reidy, W. P., Vaiana, G. S., and Zehnpfennig, T., (1968), A.J. 73, S73 (Abstract).

Parker, E. N., (1957), Phys. Rev. 107, 830.

_____, (1964), AAS-NASA Symposium on the Physics of Solar Flares, NASA SP-50, p. 417.

REFERENCES (Continued)

Parks, G. K., and Winckler, J. R., (1969), Ap.J. 155, L117.

Peterson, L. E., and Winckler, J. R., (1958), Phys. Rev. Letters 1, 205.

_____, (1959), J.G.R. 64, 697.

Pinter, S., (1969a), Solar Phys. 8, 142.

_____, (1969b), Solar Phys. 8, 149.

Pottasch, S. R., (1965), B.A.N. 18, 7.

Pounds, K. A., (1965a), I.A.U. Symposium 23, 61.

_____, (1965b), Ann. d'Ap. 28, 132.

_____, (1970), Ann. de Geophys. (In press.)

_____, and Russell, P. C., (1966), Space Research 6, 34.

_____, and Sanford, P. W., (1963), Proc. Intern'l Conf. Ionosphere, July 1962, p. 50.

_____, and Willmore, A. P., (1963), Proc. Intern'l Conf. Ionosphere, July 1962, p. 513.

_____, Evans, K., and Russell, P. C., (1968), I.A.U. Symposium 35, 431.

Quarterly Bulletin on Solar Activity, (1968), I.A.U. Publication, Zurich, No. 157-161.

Ramsay, J. V., Norton, D. G., and Mugridge, E. G. V., (1968), Solar Phys. 4, 476.

Reid, J. H., (1969), J. Atmos. Terr. Phys. 31, 859.

Reidy, W. P., and Vaiana, G. S., (1966), Space Research 7, 1247.

_____, Vaiana, G. S., Zehnpfennig, T., and Giacconi, R., (1968), Ap.J. 151, 333.

Richardson, R. S., (1951), Ap.J. 114, 356.

REFERENCES (Continued)

Rugge, H. R., Personal Communication.

_____, and Walker, A. B. C. Jr., (1967), Space Research 8, 439.

Sawyer, C., (1967), Ap.J. 147, 1135.

Severny, A. B., (1952), Izvestia Krymsk. Astron. Obs. 9, 3.

Smith, H. J., (1962), "Some Synoptic Flare Data, 1937-1960," GRD Research Note: AFCRL-62-827.

_____, and Smith, E. v. P., (1963), "Solar Flares," Macmillan Press: New York.

Solar Geophysical Data Bulletin, (1967-1968), issued by the Institute for Environmental Research, U.S. Department of Commerce, No. 272-289.

Stock, J., and Williams, A. D., (1962), "Photographic Photometry" in "Astronomical Techniques" (ed. W. A. Hiltner), University of Chicago Press, p. 374.

Svestka, Z., (1963), Space Research 4, 768.

_____, and Fritzova-Svestkova, L., (1967), Solar Phys. 2, 75.

_____, Kopecky, M., and Blaha, M., (1961), Bull. Astron. Inst. Czech. 12, 229.

Takakura, T., (1969), Solar Phys. 6, 133.

_____, and Kai, K., (1961), P.A.S.J. 13, 94.

_____, (1966), P.A.S.J. 18, 57.

Takao, K., (1967), Rep. Ionos. Space Res. Japan 21, 125.

Tandberg-Hanssen, E., (1967), "Solar Activity," Blaisdell Press: Waltham (Mass.).

Teske, R. G., Personal Communication.

_____, (1962), Ap.J. 136, 534.

_____, (1967), A.J. 72, 832 (Abstract).

REFERENCES (Continued)

Teske, R. G., (1969a), Solar Phys. 6, 193.

_____, (1969b), OSO Workshop, Boulder, Colorado, August 1969.

_____, and Thomas, R. J., (1969), Solar Phys. 8, 348.

Tindo, I. P., and Shurygin, A. I., (1965), Kosmich. Issled. 3, 262.

Underwood, J. H., (1968), Science 159, 383.

_____, and Muney, W. S., (1967), Solar Phys. 1, 129.

Vaiana, G. S., and Giacconi, R., (1968), Proc. Conf. Plasma Instabilities in Astrophysics, Asilomar, October 1968.

_____, and Zehnpfennig, T., (1969), Bull. Amer. Astron. Soc. 1, 294 (Abstract).

_____, Reidy, W. P., Zehnpfennig, T., VanSpeybroeck, L., and Giacconi, R., (1968), Science 161, 564.

Valnicek, B., (1967), Astron. Inst. Czech. 18, 249.

Van Allen, J. A., (1967a), J.G.R. 72, 5903.

_____, (1967b), A.J. 72, 833 (Abstract).

_____, (1968), Ap.J. 152, L85.

Van Griethuysen, I. G., and Houtgast, J., (1959), B.A.N. 14, 279.

Vegard, L., (1938), Geofysiske Publikasjoner 12, 5.

Victoreen, J. A., (1949), J. Appl. Phys. 20, 1141.

Waldmeier, M., (1938), Zs.f.Ap. 16, 276.

_____, (1940), Zs.f.Ap. 20, 46.

_____, (1947), J. Terr. Mag. Atmos. Elect. 52, 333.

_____, and Bachmann, H., (1959), Zs.f.Ap. 47, 81.

REFERENCES (Concluded)

Walker, A. B. C. Jr., Rugge, H. R., Chater, W. T., and Howey, C. K., (1967), Trans. Amer. Geophys. Union 48, 151.

Warwick, C. S., (1963), "The Sudden Ionospheric Disturbance" in "Radio Astronomical and Satellite Studies of the Atmosphere" (ed. J. Aarons), North-Holland Press: Amsterdam, p. 457.

_____, (1965), Ap.J. 142, 767.

Warwick, C., and Wood, M., (1959), Ap.J. 129, 801.

Warwick, J. W., (1962), P.A.S.P. 74, 302.

Wende, C. D., (1969), J.G.R. 74, 4649.

White, O. R., (1962), Ap.J. Supp. 7, 333.

White, W. A., (1963), Space Research 4, 771.

_____, (1964), AAS-NASA Symposium on the Physics of Solar Flares, NASA SP-50, p. 131.

Winckler, J. R., (1964), AAS-NASA Symposium on the Physics of Solar Flares, NASA SP-50, p. 117.

Witte, B., (1951), "A Contribution to the Study of the Relation Between Solar Flares and Sunspot Groups," HAO Solar Research Memorandum.

Yefremov, A. I., Podmoshensky, A. L., Yefimov, O. N., and Lebedev, A. A., (1962), Space Research 3, 843.

Zhitnik, I. A., Krutov, V. V., Maljavkin, L. P., Mandel'shtam, S. L., and Cheremukhin, G. S., (1966), Space Research 7, 1263.

_____, (1967), Kosmich. Issled. 5, 274.

Zirin, H., Ingham, W., Hudson, H., and McKenzie, D., (1969), Solar Physics 9, 269.

APPENDIX

TWO METHODS FOR THE DETERMINATION OF FLARE EMISSION IN Hα

It is by no means a simple task to interpret flare filtroheliograms in terms of the quantitative enhancement of the flaring region's Hα emission rate. To the author's knowledge, a complete, detailed description of the necessary reduction procedures does not seem to exist in the standard literature. Therefore, the two methods used in the present paper will be derived here.

1. GENERAL FORMULATION

The exact shape of the Hα line's profile depends upon heliocentric position (μ) for undisturbed areas of the solar disk, and also upon time (t) for regions which are flaring. Thus the following set of conventions has been adopted for the present derivation:

$I\mu(C)$: Continuum intensity (near Hα) at heliocentric distance μ;

$I\mu(\lambda)$: Intensity within undisturbed Hα profile at μ;

$I\dot{\mu}(\lambda,t)$: Intensity within the flare's Hα profile at time t and position μ.

In addition, the following relations have been defined:

$$r(\lambda) = I\mu(\lambda)/I\mu(C) \qquad (A.1)$$

$$r'(\lambda,t) = I\dot{\mu}(\lambda,t)/I\mu(C) \qquad (A.2)$$

Other conventions used are:

(a) any value measured at the center of the solar disk is designated by subscript o, e.g. $I_o(C)$;

(b) any symbol pertaining to the Hα flare is indicated by superscript ', e.g. $r'(\lambda,t)$.

The enhancement in Hα flux observed at the earth during a flare is then given by:

$$\Delta E(H\alpha, t) = \int_A dA \int_{H\alpha} [r'(\lambda,t)-r(\lambda)]I\mu(C)d\lambda \qquad (A.3)$$

where A is the flare's area in steradians as seen from the earth. Note that, in general, the Hα line profile also varies as a function of position within the flaring region. Assuming that the profile is filled uniformly during the flare's development, we can write:

$$r'(\lambda,t) = r(\lambda) + \rho(t)\,[1-r(\lambda)] \qquad (A.4)$$

(The validity of this assumption will be discussed later.) Thus (A.3) becomes:

$$\Delta E(H\alpha,t) = I\mu(C) \int_A \rho(t)dA \int_{H\alpha} [1-r(\lambda)]d\lambda \qquad (A.5)$$

By definition, the equivalent width of Hα is:

$$W\mu(H\alpha) = \int_{H\alpha} [1-r(\lambda)]d\lambda \qquad (A.6)$$

Substituting (A.6) into (A.5), we have:

$$\Delta E(H\alpha,t) = W\mu(H\alpha)I\mu(C) \int_A \rho(t)dA \qquad (A.7)$$

Then, with the assumption that the flare's Hα radiation is semi-isotropic into 2π steradians (see the discussion in Section IV-6a), the enhanced Hα emission at the sun can be written as:

$$\Delta S(H\alpha,t) = 2\pi d^2 W\mu(H\alpha)\, I\mu(C) \int_A \rho(t)dA \qquad (A.8)$$

where $d = 1.50 \times 10^{13}$ cm is the distance between the sun and the earth. The value of the equivalent width for Hα at the center of the disk is $W_o(H\alpha) = 4.02$ Å (Moore et al., 1966). The disk-center continuum intensity at 6563 Å is taken to be $I_o(C) = 2.93 \times 10^6$ erg/(cm^{2}sec Å sterad). (This is the intensity of a black body with a brightness temperature of 6200 K.) Expression (A.8) thus becomes:

$$\Delta S(H\alpha,t) = 1.66 \times 10^{34} \frac{W\mu(H\alpha)}{W_o(H\alpha)} \frac{I\mu(C)}{I_o(C)} \int_A \rho(t)dA \text{ erg/sec} \qquad (A.9)$$

if $\int_A \rho(t)dA$ is determined in units of steradians.

We now consider how this equation can be put into a form which contains only measurable parameters. Observing techniques normally used do not directly measure the intensity of the Hα line center. Instead, they record the line's intensity as folded into the detector's instrumental transmission profile $T(\lambda)$, which may also include the effects of scattered light. Such intensity measurements will be indicated here by the symbol P, with some of the same auxilliary notations as given for the "pure" intensities I. For example, an instrumental measurement of the Hα intensity for a flare occurring at heliocentric distance μ is:

$$P'\mu(H\alpha, t) = \int_o^\infty T(\lambda) I'\mu(\lambda,t)d\lambda \qquad (A.10)$$

Thus, the measurement of a flare's intensity relative to the nearby undis-

turbed Hα background would be equivalent to:

$$\frac{P'_\mu(H\alpha,\, t)}{P_\mu(H\alpha)} = \frac{\int_0^\infty T(\lambda) I'_\mu(\lambda,t)\,d\lambda}{\int_0^\infty T(\lambda) I_\mu(\lambda)\,d\lambda} = \frac{\int_0^\infty T(\lambda) r'(\lambda,t)\,d\lambda}{\int_0^\infty T(\lambda) r(\lambda)\,d\lambda} \qquad (A.11)$$

Substituting the expression for $r'(\lambda,t)$ given by (A.4) into (A.11), one can show:

$$\frac{P'_\mu(H\alpha,\, t)}{P_\mu(H\alpha)} = 1 + \rho(t)\left[\frac{\int_0^\infty T(\lambda)\,d\lambda}{\int_0^\infty T(\lambda) r(\lambda)\,d\lambda} - 1\right] \qquad (A.12)$$

Now we define a parameter z:

$$z = \frac{\int_0^\infty T(\lambda)\,d\lambda}{\int_0^\infty T(\lambda) r(\lambda)\,d\lambda} \qquad (A.13)$$

This may be considered as a "figure of merit" for the monochrometer because it measures how much contrast the instrument can provide between observations made at the center of the absorption line and those made in the continuum. The highest value of z possible is 1/r(center), which for Hα is 6.3 (LoPresto, personal communication). Note that it is not at all necessary (as Van Griethuysen and Houtgast (1959) had mistakenly assumed) to know the instrumental transmission $T(\lambda)$ in detail to find the appropriate figure of merit for a given monochrometer. One need only measure the ratio of the continuum intensity to the Hα intensity at some μ, since:

$$\frac{P\mu(C)}{P\mu(H\alpha)} = \frac{\int_o^\infty T(\lambda)I\mu(C)d\lambda}{\int_o^\infty T(\lambda)I\mu(\lambda)d\lambda} = \frac{\int_o^\infty T(\lambda)d\lambda}{\int_o^\infty T(\lambda)r(\lambda)d\lambda} = z \qquad (A.14)$$

Furthermore, the measurement can be made at any heliocentric distance, because this ratio remains constant over the entire solar disk (DeJager, 1952; Dodson et al., 1956).

Expressions (A.12) and (A.13) can be combined to give:

$$\rho(t) = \left[\frac{P'\mu(H\alpha, t)}{P\mu(H\alpha)} - 1\right] \Big/ (z-1) \qquad (A.15)$$

Note that it is just this quantity, integrated over the solid angle of the flare's area, which gives the enhanced Hα flux by means of (A.9). Now, if we define R'(t) as:

$$R'(t) = \int_A \frac{P'\mu(H\alpha,t)-P\mu(H\alpha)}{P_o(H\alpha)}\, dA \text{ steradians} \qquad (A.16)$$

and take advantage of the fact that:

$$\frac{I\mu(C)}{I_o(C)} \cdot \frac{P_o(H\alpha)}{P\mu(H\alpha)} = 1 \qquad (A.17)$$

equation (A.9) becomes:

$$\Delta S(H\alpha,t) = \frac{1.66 \times 10^{34}}{(z-1)} \frac{W\mu(H\alpha)}{W_o(H\alpha)} R'(t) \text{ erg/sec} \qquad (A.18)$$

The next two sections will describe the specific methods which were used

to integrate $\rho(t)$ over the area of the flare. But first some comment should be made concerning the validity of the formulation to this point. In particular, we will discuss the effects of two potential sources of error; (a) misadjustment of the monochrometer, and (b) deviations from even-filling of the flare Hα profile.

Most flare-patrol stations now observe with some type of commercial "filter-optics" monochrometer, such as the Lyot filter. (This includes the McMath-Hulbert Observatory, at which the film examined in the present study was secured.) Ramsay et al. (1968), claim that most Lyot filters may be in poor adjustment when delivered from the manufacturer, perhaps even with a transmission-profile minimum near Hα center! But the above analysis shows that no systematic error will result from such a misadjustment as long as the measured ratio of continuum to Hα intensity z is greater than unity. This is true whether the manufacturer is at fault or the observer merely sets the filter's line-shifter improperly. The only effect of some misadjustment will be to make the measurements less sensitive to subtle changes in the Hα emission, and thus lower the precision which can be attained.

We must also examine the assumption that the Hα line fills uniformly during a flare (equation (A.4)). Dodson and Hedeman (1969c) have found that spectra of flares near the central part of the solar disk consistently have exhibited little or no evidence for major Doppler shifts. This eliminates one possible cause of an emission-line asymmetry, at least for events far from the limb. Van Griethuysen and Houtgast (1959) state that the even filling of the Hα line is a good approximation for faint and medium flares; but Ellison (1952, 1957) and Teske (1962)

have observed Hα emission profiles with strong central reversals for very large, bright flares. However, such reversals may be relatively rare, since many investigators (e.g., Ellison, 1949, 1963a; Comper, 1959; DeJager, 1959) have published spectra taken during the time-development of 3 and 3^+ flares which show Hα emission profiles that quite closely approximate the shape predicted by equation (A.4). Svestka et al. (1961), present some evidence that the number of flares with strong self-reversal increases toward the limb, which again suggests that the formulation derived above may be more appropriate for events near the center of the disk. Therefore, it is difficult to estimate the error introduced by line-profile irregularities in general. Ironically, an instrument with a narrower band-pass, and thus a higher potential precision, is affected even more strongly by this type of error.

Smith and Smith (1963) have noted yet another possible source of uncertainty which cannot be taken quantitatively into account. They point out that flares, particularly large ones, may change the physical conditions of the chromosphere's deeper layers. Moreover, although flares appear to be thin, surface phenomena, it is not known at what depths they originate. Therefore, it may be rather naive to assume simply that the line profile of the region below the flare is identical to that of the undisturbed disk. However, it does not seem advantageous to alter the present formulation for that reason alone without any positive evidence to suggest a more accurate assumption. Thus we will hold to the "naive" viewpoint until such evidence is available.

The "uniform-filling" hypothesis of equation (A.4) predicts that the flare's pure emission profile (total intensity minus pre-flare intensity) is just a

scaled version of the normal Hα profile, and thus has a constant half-width. Therefore, taken at face value, the well known time-variation of the flare's Hα emission line-width (first reported by Giovanelli (1940) and Waldmeier (1940)) would seem to indicate that the line profile is not filled uniformly during the flare. But these line width measurements actually refer to an "effective half-width" (also called the visibility range) which is defined as that distance from the Hα line-center where the flare is just visible by contrast with its surroundings (Ellison, 1943). Ellison (1949) has found that the Hα "effective half-width" is roughly proportional to the flare's central intensity up to a certain value, and then increases more rapidly. One can easily show that this is exactly the effect predicted by the "uniform-filling" hypothesis (equation (A.4)) if the eye can only discriminate intensity differences of some limiting value (or percentage).

Therefore, it appears that equation (A.4) is indeed a close approximation to the flare's emission profile, except perhaps for limb flares or for some (hopefully rare) cases of very large and bright disk events.

2. METHOD A: "TYPICAL" TOTAL AREA AND PEAK INTENSITY

A crude estimate of the Hα emission can be made by means of "typical" values for the total area $\bar{A}$ and measured peak intensity $\bar{P}'(H\alpha)$ appropriate for each flare class. Because of difficulties caused by the well known limb-darkening effect, only values for the center of the solar disk are considered here. Thus, (A.18) becomes:

$$\Delta S(H\alpha) = \frac{1.66 \times 10^{34}}{(z-1)} \cdot R' \text{ erg/sec} \qquad (A.19)$$

(The time-variable has been eliminated since all values in this section will refer to the time of flare maximum.) Now, R' can be roughly approximated as:

$$\bar{R}' = \bar{A} \cdot \left[\frac{\bar{P}_o'(H\alpha)}{P_o(H\alpha)} - 1 \right] \qquad (A.20)$$

where $\bar{A}$ is in units of steradians. The flare area used was the middle value of the range defined by the I.A.U. for each importance class (see Table 4.2 in Chapter IV). This may be slightly higher than the actual area for a typical flare of that class, since flare frequency decreases rapidly with increasing peak area. But a correction for such an effect would be unnecessarily precise for the rather crude level of accuracy attainable by the present overall method.

Measurements of the flare's peak intensity were taken from the Dodson, Hedeman, and McMath (1956) paper "Photometry of Solar Flares." Specifically, this paper lists measurements of the peak Hα intensity relative to the continuum at the center of the disk, i.e. $P_o'(H\alpha)/P_o(C)$. In order to convert these into the proper form for equation (A.20), they must be multiplied by $P_o(C)/P_o(H\alpha)$ (which expression (A.14) shows is nothing more than the value z). The instrument used by Dodson et al., was characterized by z = 3.1, so that equation (A.19) can be written as:

$$\overline{\Delta S}(H\alpha) = 7.9 \times 10^{33} \bar{A} \cdot \left[3.1 \frac{\bar{P}_o'(H\alpha)}{P_o(C)} - 1 \right] \qquad (A.21)$$

The values of area and measured intensity which were used in the present study are given in Table A.1. The enhanced Hα emission rates which then result by means of equation (A.21) are listed in Table 4.8 of Chapter IV. They are also plotted in Figure 4-7 relative to the enhanced emission rates of the associated soft X-radiation.

TABLE A.1

"TYPICAL" AREAS AND PEAK INTENSITIES FOR Hα FLARES

Flare Importance	$\bar{A}$ (steradians)	$\bar{P}'_o(H\alpha)/P_o(C)$ (Dodson et al., 1956)
Sn	9.9×10^{-9}	0.6 ± 0.1
Sb	9.9×10^{-9}	0.8 ± 0.1
1f	2.4×10^{-8}	0.4 ± 0.1
1n	2.4×10^{-8}	0.8 ± 0.1
1b	2.4×10^{-8}	1.2 ± 0.1
2f	5.8×10^{-8}	0.7 ± 0.1
2n	5.8×10^{-8}	1.1 ± 0.1
2b	5.8×10^{-8}	1.5 ± 0.1
3n	1.2×10^{-7}	1.3 ± 0.1
3b	1.2×10^{-7}	1.6 ± 0.1

3. METHOD B: ISOPHOTOMETRY

In order to accommodate further notation complexities, some simplification of the previously used conventions will be made here:

(1) the heliocentric distance μ will not be explicitly noted for values that refer to the flare itself (values marked by superscript '),

(2) the time dependency of all values will be implicitly understood,

(3) unless otherwise indicated, all measurements will be made at the center of the Hα line.

Basically, the technique of isophotometry involves the construction of constant-intensity contours within the outline of a flaring region from film records of the flare. This can be done either by purely photographic methods (Falciani et al., 1968) or by means of a photometric isophotometer (Stock and Williams, 1962). If the film has been properly calibrated, the intensity of each contour relative to the center of the solar disk can be determined. Then, knowing the area enclosed by each curve, one can calculate the enhanced emission being radiated between these contours and thus, by summing over the entire set, find the whole flare's Hα emission. Measurements of many filtroheliogram frames made during the development of the flare then give the time-history of the event's enhanced Hα emission.

However, the quantity actually measured at a given point on the film is not the relative intensity P/P_s (where P_s is some arbitrary value), but rather the photographic density D. These quantities are related by a logarithmic expression, normally called the characteristic curve, which can be written as:

$$\log \frac{P}{P_s} = f(D) \qquad (A.22)$$

For any quantitative study, this relation must be known for the film being photometered. In fact, we have found that the procedure described here is very sensitive to slight changes in the characteristic curve. Therefore it is necessary to exercise great care in measuring this relation and advisable to determine it individually for each frame considered.

To find some feature's intensity relative to the undisturbed Hα intensity

at the disk's center P/P_o the following expression is used:

$$\log \frac{P}{P_o} = \log \frac{P}{P_s} - \log \frac{P_o}{P_s} = f(D) - f(D_o) \qquad (A.23)$$

where D_o is the photographic density of the undisturbed region. Now, if D_c is the density at contour c, we can define a mean relative intensity $\bar{P}'_c/P_o$ for the flare emission between contours c and c + 1 as:

$$\log \frac{\bar{P}'_c}{P_o} = f\left(\frac{D_c + D_{c+1}}{2}\right) - f(D_o) \qquad (A.24)$$

Then, following equation (A.16), the relative flux R'_c emitted within contour c is approximately:

$$R'_c = \sum_{c}^{c(max)} (A_c - A_{c+1}) \cdot \left(\frac{\bar{P}'_c - P\mu}{P_o}\right) \qquad (A.25)$$

where c(max) is the innermost contour measured, and A_c is the area (in steradians) within contour c.

One slight modification of the above procedure is desirable. It has been found that the relative flux between the outermost two contours, 1 and 2, is better represented by a mean intensity defined as:

$$\log \frac{\bar{P}'_1}{P_o} = f\left(\frac{2D_1 + D_2}{3}\right) - f(D_o) \qquad (A.26)$$

Therefore, the mean intensity given by expression (A.24) is used only for $c > 1$.

Isophotometry also allows an accurate measurement of the flare's peak intensity P'_{max}/P_o, in addition to the relative flux emitted within each contour c. (Note that P'_{max} is not necessarily the intensity of the innermost contour $P_{c(max)}$.) This can be done most precisely by plotting R'_c as a function of the intensity of contour c, and extrapolating the curve to the point where the value of the relative flux vanishes. The intensity value at that point is then P'_{max}/P_o. However, this procedure is useful only when enough contours are measured to make the above extrapolation reliable. In other cases, a subjective estimate based on the area within the innermost contour is reasonably accurate. Of course, the higher the figure of merit z for the monochrometer used to make these measurements, the closer they will be to the "true" peak intensity values.

Unfortunately, the method described above for the determination of relative fluxes must be refined further. This is necessary since the outermost contour does not in general fall at the same intensity level from one exposure to another. Thus, in order to compare fluxes measured for a series of filtrograms (such as for a study of the flare's time development), all values must be standardized relative to some uniform level P_*/P_o. Flux values converted to such a standard intensity level will be referred to as R'_*. The present study utilized one of the following three interpolation methods for this standardization, depending on the circumstances involved:

(1) if only two values of R'_c were known (including the value zero at P'_{max}/P_o), a linear interpolation in log (P/P_o) was used, i.e.:

$$R'_* = R'_{c2} + (R'_{c1} - R'_{c2}) \frac{Y_* - Y_2}{Y_1 - Y_2} \qquad (A.27)$$

where $Y_* = \log (P_*/P_o)$ and $Y_j = \log (P_{cj}/P_o)$;

(2) if only three values of R'_c were known and

$$\log \frac{P'_{max}}{P_o} - \log \frac{P_{c(max)}}{P_o} < 0.04 \ , \qquad (A.28)$$

a linear interpolation was again used;

(3) otherwise, a parabola was fitted through the three values of R'_c nearest to P_*/P_o by the following relation:

$$\begin{aligned} R'_* = {} & R'_{c1} \frac{(Y_* - Y_2)(Y_* - Y_3)}{(Y_1 - Y_2)(Y_1 - Y_3)} \\ & + R'_{c2} \frac{(Y_* - Y_1)(Y_* - Y_3)}{(Y_2 - Y_1)(Y_2 - Y_3)} \\ & + R'_{c3} \frac{(Y_* - Y_1)(Y_* - Y_2)}{(Y_3 - Y_1)(Y_3 - Y_2)} \end{aligned} \qquad (A.29)$$

At this point in the analysis, we can determine the relative enhanced flux of the plage plus flare Hα radiation which is emitted at intensity levels above $P_*/P\mu$. But there is no way to measure directly the flux emitted at intensities $P/P\mu$ between unity (the adjacent undisturbed intensity) and the intensity of the outermost isophote-contour. (A contour at $P_c/P\mu = 1$ is not possible.) One method of estimating the total flux R' is to plot the measured values of R'_c as a function of $P_c/P\mu$ and extrapolate this curve to a relative intensity of unity.

But this is practicable only if three or more contours have been measured. Therefore, in the present study, we have made such an extrapolation only for times near flare maximum (when up to seven contours were recorded). Then the mean ratio for these times R'/R'_* was applied to all the measured frames of the flare in question. Finally, if this ratio is called φ, equation (A.18) can be written:

$$\Delta S(H\alpha, t) = \frac{1.66 \times 10^{34}}{(z-1)} \frac{W\mu(H\alpha)}{W_o(H\alpha)} \varphi R'_*(t) \text{ erg/sec} \qquad (A.30)$$